

COOPERATIVE SPECTRUM SENSING USING SWARM INTELLIGENCE AND DOUBLE THRESHOLDS

BY
FAHHAM MOHAMMED

A Thesis Presented to the
DEANSHIP OF GRADUATE STUDIES
KING FAHD UNIVERSITY OF PETROLEUM & MINERALS
DHAHRAN, SAUDI ARABIA

In Partial Fulfillment of the
Requirements for the Degree of

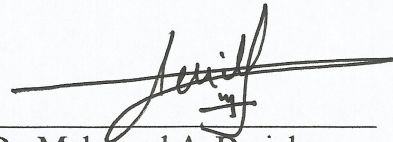
MASTER OF SCIENCE

In
ELECTRICAL ENGINEERING

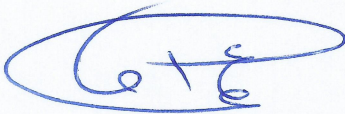
MARCH 2013

KING FAHD UNIVERSITY OF PETROLEUM & MINERALS
DHAHRAN- 31261, SAUDI ARABIA
DEANSHIP OF GRADUATE STUDIES

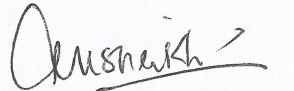
This thesis, written by **FAHHAM MOHAMMED** under the direction of his thesis advisor and approved by his thesis committee, has been presented and accepted by the Dean of Graduate Studies, in partial fulfillment of the requirements for the degree of **MASTER OF SCIENCE IN ELECTRICAL ENGINEERING**



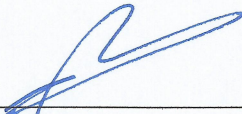
Dr. Mohamed A. Deriche
(Advisor)



Dr. Ali Ahmad Al-Shaikhi
Department Chairman



Dr. Asrar U. H. Sheikh
(Member)



Dr. Salam A. Zummo
Dean of Graduate Studies



Dr. Azzedine Zerguine
(Member)

28/5/13

Date

© Fahham Mohammed
2013

*This thesis is dedicated to my loving parents, sisters, and brother for their immense love
and continuous support.*

ACKNOWLEDGMENTS

All the praises be to Allah (SWT), and His peace and blessings be upon the prophet Muhammad (PBUH), his family, his companions and his followers.

It is with immense gratitude that I acknowledge the guidance and continuous support of my thesis advisor, Dr. Mohamed A. Deriche, whose expertise, motivation, enthusiasm, and patience has helped me in achieving the research goals.

I would also like to sincerely thank my thesis committee members, Dr. Asrar U. H. Sheikh and Dr. Azzedine Zerguine, for their encouragement, insightful comments, and thought provoking questions, to improve the quality of my research work.

I would specially like to thank my graduate advisor, Dr. Maan A. Kousa, whom I hold in high regard, for his valuable guidance throughout my graduate program.

I owe my deepest gratitude to my parents, who unconditionally supported me throughout my years of education. Special thanks to my sisters Tasneem and Almas Fatima, and my dear friend Ashfaq Mohammed, who have always stood by me, motivated me, and believed in me.

I am extremely grateful and indebted to my colleague Raza Umar for his constant guidance, encouragement and support during the course of my research work.

Finally, I would like to thank my friends Amer Bin Ziyad, Syed Abdul Baqi, Humayun Khalid and Sameer Arastu for all the help, motivation and moral support all through my graduate studies.

TABLE OF CONTENTS

ACKNOWLEDGMENTS.....	V
TABLE OF CONTENTS.....	VI
LIST OF FIGURES.....	IX
LIST OF TABLES.....	XII
LIST OF ABBREVIATIONS.....	XIII
ABSTRACT.....	XV
CHAPTER 1. INTRODUCTION.....	1
1.1 Motivation.....	1
1.2 Problem Statement.....	3
1.3 Thesis Objectives	3
1.4 Contributions.....	4
1.5 Thesis Outline	4
CHAPTER 2. LITERATURE REVIEW.....	5
2.1 Cognitive Radio	5
2.2 Classification of Spectrum Sensing Techniques	9
2.3 Transmitter Detection.....	12
2.3.1 Energy Detection	14
2.3.2 Wavelet based Spectrum Sensing	20
2.3.3 Compressed Sensing for Wideband Spectrum.....	22
2.3.4 Cyclostationary based Detection	23

2.3.5	Matched Filter Detection	25
2.3.6	Waveform based Sensing.....	26
2.3.7	Covariance based Detection	27
2.3.8	Issues with Non-Cooperative Spectrum Sensing	29
2.4	Cooperative Spectrum Sensing	30
2.4.1	Classification of Cooperative Spectrum Sensing.....	32
2.4.2	The Cooperative Spectrum Sensing Framework	37
2.4.3	Cooperative Spectrum Sensing using Decision Fusion	39
2.4.4	Cooperative Spectrum Sensing using Data Fusion	42
2.5	Simulation Results	48
2.5.1	Non-cooperative Spectrum Sensing	48
2.5.2	Cooperative Spectrum Sensing	56
2.6	Summary	62
CHAPTER 3. COOPERATIVE SPECTRUM SENSING USING PARTICLE SWARM OPTIMIZATION.....		63
3.1	Introduction.....	63
3.2	Particle Swarm Optimization	64
3.3	Applications of PSO in Communication Systems	69
3.3.1	Conventional Data Fusion using PSO.....	70
3.4	Simulation Results	78
3.5	Summary	83
CHAPTER 4. A NEW HYBRID DOUBLE THRESHOLD COOPERATIVE SPECTRUM SENSING ALGORITHM USING SWARM INTELLIGENCE.....		85
4.1	Introduction.....	85
4.2	The System Model	86
4.3	Performance Analysis of the Proposed Algorithm	89
4.4	Bit Savings over the Reporting Channel for the proposed algorithm	96

4.5	Simulation Results	100
4.5.1	Simulation Results under AWGN	101
4.5.2	Simulation Results under Rayleigh Fading	108
4.5.3	Simulation Results for Bit Savings over the Reporting Channel.....	115
4.6	Summary of Simulation Results	120
CHAPTER 5. CONCLUSION AND FUTURE WORK.....		122
5.1	Conclusion	122
5.2	Proposed Future Research Directives.....	123
5.2.1	Maximum Eigenvalue Based Detection for Fuzzy CRs	123
5.2.2	Cluster-Based Two-Threshold Cooperative Spectrum Sensing	123
PUBLICATIONS		125
REFERENCES.....		126
VITAE.....		135

LIST OF FIGURES

Figure 1.1: Measurement of 0-6 GHz Spectrum Utilization at BWRC [2]	2
Figure 2.1: Spectrum Hole Concept [8]	6
Figure 2.2: Cognitive Cycle [8]	7
Figure 2.3: Classification of Spectrum Sensing Techniques	9
Figure 2.4: Transmitter detection problems [14]	10
Figure 2.5: Block Diagram of the Energy Detector	15
Figure 2.6: Energy Detection using single threshold	17
Figure 2.7: PSD of each sub band in wideband spectrum [27]	21
Figure 2.8: Sensitivity improvement with cooperation	31
Figure 2.9: Classification of cooperative sensing: (a) Centralized, (b) Distributed, and (c) Relay-assisted [52]	32
Figure 2.10: Framework of centralized cooperative spectrum sensing [52]	37
Figure 2.11: ROC for Conventional Energy Detector (SNR = 5 dB, AWGN Case)	49
Figure 2.12: C-ROC for Conventional Energy Detector (SNR = 5 dB, AWGN Case) ...	50
Figure 2.13: ROC for Conventional Energy Detector (SNR = 10 dB, AWGN Case)	51
Figure 2.14: C-ROC for Conventional Energy Detector (SNR = 10 dB, AWGN Case) .	52
Figure 2.15: ROC for Conventional Energy Detector (Avg. SNR = 5 dB, Rayleigh Fading)	53
Figure 2.16: C-ROC for Conventional Energy Detector (Avg. SNR = 5 dB, Rayleigh Fading)	54
Figure 2.17: ROC for Conventional Energy Detector (Avg. SNR = 10 dB, Rayleigh Fading)	55
Figure 2.18: C-ROC for Conventional Energy Detector (Avg. SNR = 10 dB, Rayleigh Fading)	56
Figure 2.19: ROC – Comparison of Data and Decision Fusion (10 CRs, SNR = 3 dB, AWGN Case)	57
Figure 2.20: ROC – Comparison of Data and Decision Fusion (10 CRs, SNR = 6 dB, AWGN Case)	58

Figure 2.21: ROC – Comparison of Data and Decision Fusion (10 CRs, SNR = 4 dB, Rayleigh Fading)	59
Figure 2.22: ROC – Comparison of Data and Decision Fusion (10 CRs, SNR = 7 dB, Rayleigh Fading)	60
Figure 2.23: Normalized avg. number of bits/user \bar{B} vs. Q_f (10 CRs, SNR = 3 dB, AWGN Case).....	61
Figure 3.1: Flowchart for basic PSO algorithm	68
Figure 3.2: Cooperative Spectrum Sensing Framework using PSO	71
Figure 3.3: ROC – Data Fusion, EGC versus PSO (10 CRs, Avg. SNR = 4 dB, AWGN Case)	79
Figure 3.4: ROC – Data Fusion, EGC versus PSO (10 CRs, Avg. SNR = 6 dB, AWGN Case)	80
Figure 3.5: ROC – Data Fusion, EGC versus PSO (10 CRs, Avg. SNR = 5 dB, Rayleigh Fading).....	81
Figure 3.6: ROC – Data Fusion, EGC versus PSO (10 CRs, Avg. SNR = 7 dB, Rayleigh Fading).....	82
Figure 4.1: Double Threshold Energy Detector	86
Figure 4.2: Framework for the proposed Hybrid PSO-OR algorithm	87
Figure 4.3: ROC – Proposed Hybrid PSO-OR algorithm (10 CRs, Avg. SNR = 4 dB, AWGN Case).....	101
Figure 4.4: ROC – Hybrid EGC-OR algorithm (10 CRs, Avg. SNR = 4 dB, AWGN Case)	102
Figure 4.5: ROC – Comparison of proposed Hybrid PSO-OR algorithm with existing techniques (10 CRs, Avg. SNR = 4 dB, AWGN Case).....	103
Figure 4.6: C-ROC – Comparison of proposed Hybrid PSO-OR algorithm with existing techniques (10 CRs, Avg. SNR = 4 dB, AWGN Case).....	104
Figure 4.7: ROC – Proposed Hybrid PSO-OR algorithm (10 CRs, Avg. SNR = 6 dB, AWGN Case).....	105
Figure 4.8: ROC – Hybrid EGC-OR algorithm (10 CRs, Avg. SNR = 6 dB, AWGN Case)	106

Figure 4.9: ROC – Comparison of proposed Hybrid PSO-OR algorithm with existing techniques (10 CRs, Avg. SNR = 6 dB, AWGN Case).....	107
Figure 4.10: ROC – Proposed Hybrid PSO-OR algorithm (10 CRs, Avg. SNR = 5 dB, Rayleigh Fading)	108
Figure 4.11: ROC – Hybrid EGC-OR algorithm (10 CRs, Avg. SNR = 5 dB, Rayleigh Fading).....	109
Figure 4.12: ROC – Comparison of proposed Hybrid PSO-OR algorithm with existing techniques (10 CRs, Avg. SNR = 5 dB, Rayleigh Fading)	110
Figure 4.13: C-ROC – Comparison of proposed Hybrid PSO-OR algorithm with existing techniques (10 CRs, Avg. SNR = 5 dB, Rayleigh Fading)	111
Figure 4.14: ROC – Proposed Hybrid PSO-OR algorithm (10 CRs, Avg. SNR = 7 dB, Rayleigh Fading)	112
Figure 4.15: ROC – Hybrid EGC-OR algorithm (10 CRs, Avg. SNR = 7 dB, Rayleigh Fading).....	113
Figure 4.16: ROC – Comparison of proposed Hybrid PSO-OR algorithm with existing techniques (10 CRs, Avg. SNR = 7 dB, Rayleigh Fading)	114
Figure 4.17: Normalized avg. number of bits/user \bar{B} vs. Q_f (10 CRs, Avg. SNR = 4 dB, AWGN Case).....	115
Figure 4.18: Normalized avg. number of bits/user \bar{B} vs. Q_f (10 CRs, Avg. SNR = 6 dB, AWGN Case).....	117
Figure 4.19: Normalized avg. number of bits/user \bar{B} vs. Q_f (10 CRs, Avg. SNR = 5 dB, Rayleigh Fading)	118
Figure 4.20: Normalized avg. number of bits/user \bar{B} vs. Q_f (10 CRs, Avg. SNR = 7 dB, Rayleigh Fading)	119

LIST OF TABLES

Table 4.1:	Performance analysis summary of the proposed Hybrid PSO-OR algorithm under AWGN.....	120
Table 4.2:	Performance analysis summary of the proposed Hybrid PSO-OR algorithm under Rayleigh Fading.....	120

LIST OF ABBREVIATIONS

AWGN	: Additive White Gaussian Noise
BPF	: Band Pass Filter
CDF	: Cumulative Distribution Function
CDR	: Constant Detection Rate
CFAR	: Constant False Alarm Rate
CR	: Cognitive Radio
C-ROC	: Complementary Receiver Operating Characteristics
CROWN	: Cognitive Radio Oriented Wireless Network
CSS	: Cooperative Spectrum Sensing
ED	: Energy Detector
EGC	: Equal Gain Combining
FCC	: Federal Communications Commission
FC	: Fusion Centre
IID	: Independent and Identically Distributed
MDC	: Modified Deflection Coefficient
MRC	: Maximal Ratio Combining

PDF	: Probability Density Function
PU	: Primary User
PSD	: Power Spectral Density
PSO	: Particle Swarm Optimization
ROC	: Receiver Operating Characteristics
SS	: Spectrum Sensing
SNR	: Signal-to-Noise Ratio
WRAN	: Wireless Regional Area Network

ABSTRACT

Full Name : Fahham Mohammed

Thesis Title : COOPERATIVE SPECTRUM SENSING USING SWARM
INTELLIGENCE AND DOUBLE THRESHOLDS

Major Field : Signal Processing and Communications

Date of Degree : March 2013

In recent years, we have witnessed a rapid development in wireless communications, and as a result, there is an ever growing demand for radio spectrum. With the increasing demand for higher data rates and emergence of new applications, the demand to access the spectrum will only grow more with time. The present static frequency allocation cannot accommodate this demand as most of the spectrum is assigned to licensed (primary) users. Moreover, certain licensed users do not utilize continuously the allocated frequency band which results in inefficient spectrum usage.

Cognitive Radio (CR) has emerged as an exciting and efficient technology to solve the inefficiency of spectrum usage by opportunistically accessing the under-utilized frequency bands without interfering with the licensed users. Cognitive Radio senses the spectrum by adapting itself with the environment changes and modifying its parameters accordingly. However, individual cognitive radio may not be able to reliably detect the presence of a primary user due to effects of channel fading and/or shadowing and noise. Cooperative spectrum sensing improves the sensing reliability.

In this thesis, Cooperative Spectrum Sensing is performed in time domain using Energy Detection. Both Single Threshold and Double Threshold Energy Detectors are discussed along with their advantages and disadvantages.

This thesis proposes to approach the spectrum sensing problem with a new hybrid algorithm, Double Threshold Energy Detector using Particle Swarm Optimization (PSO), wherein the decision fusion and the data fusion schemes are combined. The mathematical equations are derived for the proposed algorithm. The proposed algorithm is compared with other existing techniques such as the Double Threshold Energy Detection using Equal Gain Combining, Single Threshold Cooperative Spectrum Sensing using PSO and Conventional OR-rule techniques. This thesis shows the power of the proposed algorithm in its ability to achieve excellent performance with a very low bandwidth usage over the reporting channel.

مُلخَص الرسالة

الاسم الكامل: فهم محمد

عنوان الرسالة: استشعار الطيف التعاوني باستخدام السرب الذكائي والعنابات المزدوجة

التخصص: اتصالات ومعالجة اشارة

تاريخ الدرجة العلمية: مارس 2013 – (جمادى الأول 1434 هـ)

في السنوات الأخيرة، شهدنا تطوراً سريعاً في عالم الاتصالات اللاسلكية، نتيجة لذلك زاد الطلب على الطيف الراديوي، بالإضافة إلى الطلب المتزايد على سرعات أعلى لنقل البيانات وظهور تطبيقات جديدة. وما زال الطلب للوصول إلى الطيف ينمو أكثر فأكثر مع مرور الوقت. تخصيص مجال ترددي ثابت لكل تطبيق لا يمكن أن يستوعب هذا الطلب، حيث قد تم تخصيص معظم الطيف لمستخدمين مرخصين وأساسيين. علاوة على ذلك، بعض المستخدمين المرخصين لا يستخدموا نطاقاتهم الراديوية باستمرار مما ينتج عنه استخدام غير فعال للطيف الراديوي .

حديثاً برزت تقنية الراديو الإدراكي (CR) وتم اعتبارها تكنولوجيا مثيرة وفعالة لحل عدم كفاءة استعمال الطيف عن طريق الاستغلال اللحظي لنطاقات الترددات غير المستخدمة دون التداخل مع المستخدمين المرخص لهم. تقنية الراديو الإدراكي تقوم بفحص الطيف من خلال تكييف نفسها مع تغيرات البيئة وتعديل معاملاتها وفقاً لذلك. ومع ذلك، فتقنية الراديو الإدراكي قد لا تكون قادرة على الكشف بشكل موثوق عن وجود مستخدم رئيسي نظراً لوجود التشويش وتأثيرات التلاشي في القنوات اللاسلكية. الاستشعار التعاوني للطيف يحسن موثوقية الاستشعار.

في هذه الأطروحة، يتم تنفيذ استشعار الطيف التعاوني في المجال الزمني باستخدام كشف الطاقة. وتناقش طريقة العتبية المفردة ، والعتبة المزدوجة للكشف عن الطاقة، جنباً إلى جنب كلا مع مزاياها وعيوبها.

هذه الأطروحة تقترح حلولاً لمعالجة مشكلة استشعار الطيف باستخدام خوارزمية جديدة. كشف الطاقة مزدوج العتبة يستخدم سرب الجسيمات المُحسّن (PSO) ، حيث يتم جمع مخططات اندماجية القرار ومخططات دمج البيانات. وهنا يتم اشتقاق المعادلات الرياضية للخوارزمية المقترحة. وتتم مقارنة الخوارزمية المقترحة مع التقنيات الأخرى القائمة مثل العتبة المزدوجة لكشف الطاقة باستخدام تكافؤ الجمع، والعتبة الوحيدة لاستشعار الطيف التعاوني باستخدام سرب الجسيمات المُحسّن، وبعض التقنيات التقليدية. تظهر هذه الأطروحة قوة الخوارزمية المقترحة في قدرتها على تحقيق أداء ممتاز مع استخدام عرض النطاق الترددي المنخفض جداً عبر القناة المقررة.

CHAPTER 1

INTRODUCTION

1.1 Motivation

Wireless networks have been characterized by the traditional policy of fixed spectrum allocation. Each service provider is given a license to operate within a particular frequency band in one geographical location. Non-licensed users are barred from accessing the commercial spectrum. Wireless communication has gone through a lot of technical advancements with the deployment of 3G and 4G technologies. With the focus shifting to new multimedia services, demand for additional bandwidth allocation has increased. As the radio spectrum is limited, the present scenario does not allow the wireless systems to adapt to fast changing demands. The FCC published a report by the Spectrum Policy Task Force (STPF) which states that spectrum utilization varies from 15% to 85% in the range of 0-6 GHz. This report shows that efficient usage of licensed spectrum is a far bigger challenge than the problem of spectrum scarcity [1]. Certain licensed bands are used most of the time while others are heavily used as shown in Figure 1.1, taken from the survey conducted at Berkeley Wireless Research Centre (BWRC) [2].

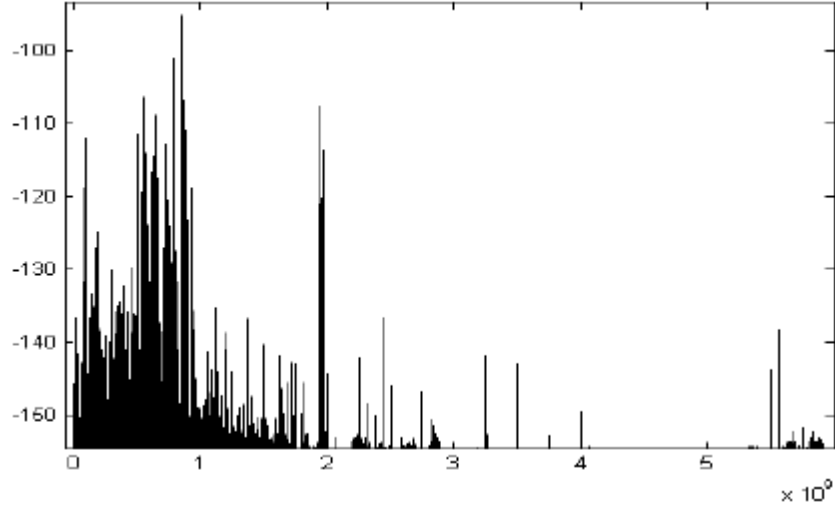


Figure 1.1: Measurement of 0-6 GHz Spectrum Utilization at BWRC [2]

The Spectrum inefficiency problem can be alleviated if a non-licensed (secondary) user is given access to a licensed frequency band temporarily whenever the licensed (primary) user is not accessing the band. Cognitive Radio (CR), which was first discussed by Mitola in [3] is seen as an important technology to improve the spectrum usage. This resulted in IEEE 802.22, a standard for practical use of cognitive radio for Wireless Regional Area Network (WRAN) [4]. The IEEE has formed a working group IEEE 802.22 WG to develop a standard for non-licensed TV spectrum access without interference [5].

Cognitive Radio is defined in [6] by Simon Haykin as “*Cognitive Radio is an intelligent wireless communication system that is aware of its surrounding environment (i.e. outside world), and uses the methodology of understanding-by-building to learn from the environment and adapt its internal states to statistical variations in the incoming RF stimuli by making corresponding changes in certain operating parameters (e.g., transmit-*

power, carrier-frequency, and modulation strategy) in real-time, with two primary objectives in mind:

- *Highly reliable communications whenever and wherever needed;*
- *Efficient utilization of the radio spectrum.”*

1.2 Problem Statement

If a cognitive radio does not have a prior knowledge about the primary user's signal characteristics, spectrum sensing becomes very challenging. It gets even more difficult due to fading/shadowing because of the obstacles in the environment. As a result, in a Cognitive Radio Network (CRN), sensing decisions from certain cognitive radios may be unreliable. In this thesis, the focus is to develop a Cooperative Spectrum Sensing technique which first identifies the CRs that are unreliable. The thesis discusses how to use the sensing information from such unreliable CRs using Particle Swarm Optimization technique, to optimize the overall sensing performance of the network.

1.3 Thesis Objectives

The main objectives of the thesis are as follows:

- Development of a robust Double Threshold Cooperative Spectrum Sensing algorithm using Particle Swarm Optimization.
- Performance analysis in terms of probability of detection and average bit rate over the reporting channel.

- Intensive testing of the new algorithm.
- Comparisons with different existing techniques.

1.4 Contributions

The main contributions achieved in this thesis are as follows:

- A new hybrid double threshold energy detector based cooperative spectrum sensing algorithm using PSO to improve the overall sensing performance and to reduce the communication overhead of the reporting channels.
- Derivation of the expressions for the probability of detection, missed detection and false alarm, and the normalized average number of reporting bits for the proposed algorithm.

1.5 Thesis Outline

The rest of the thesis is organized in the following manner. In Chapter 2, the background of the problem is discussed along with a detailed literature survey of different spectrum sensing techniques. Chapter 3 discusses the framework of cooperative spectrum sensing using Particle Swarm Optimization in detail, with its performance analysis. In Chapter 4, the proposed hybrid cooperative spectrum sensing algorithm using Particle Swarm Optimization is discussed with mathematical derivations and simulation results. Finally, Chapter 5 gives a summary of the thesis, along with some potential future research directives.

CHAPTER 2

LITERATURE REVIEW

2.1 Cognitive Radio

Cognitive Radio is an exciting technology; an extension of software defined radio, which has the ability to sense the communication environment, and adapts itself accordingly by dynamically changing its operating parameters in real time [3]. According to the definition of CR in [6], we can say that cognitive capability and reconfigurability are its two main characteristics [6], [7] and [8].

- *Cognitive Capability* is the radio's ability to sense the dynamic radio environment. In order to sense the variations, advanced techniques are required along with monitoring the frequency band of interest. This helps in identifying the best unused spectrum at a given time and geographical location.
- *Reconfigurability* allows the radio to program itself dynamically as per the environment changes. In other words, CR can be programmed to exchange information over a range of frequencies and can use various access technologies which its hardware can support [9]. Operating frequency, modulation, transmitter power and communication technology are some of the reconfigurable parameters in the CR.

With these characteristics, a CR can achieve the optimum spectrum usage which is its fundamental objective.

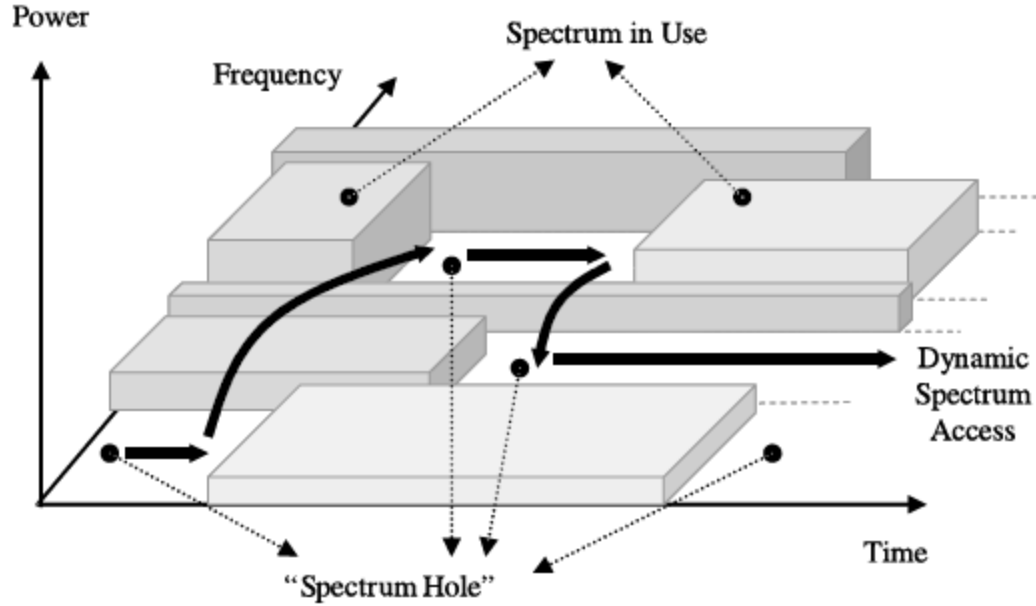


Figure 2.1: Spectrum Hole Concept [8]

Figure 2.1 [8] illustrates the pattern of spectrum usage under the static frequency allocation scheme. We clearly note that most of the licensed spectrum is under-utilized as the licensed users remain active sporadically for a certain time period. The free temporal slots across different frequency bands displayed are termed as *spectrum holes* or *white spaces* [6]. Spectrum efficiency can be achieved if a CR can sense the spectrum holes and dynamically accesses these as they become available. While accessing a particular spectrum hole if a primary user becomes active, the CR must quickly switch to another spectrum hole or modify some of its reconfigurable parameters by staying in the same band to avoid interference [8].

According to some observations in FCC publication of 2003 [10], there are two types of spectrum holes:

- *Temporal Spectral Hole*: If the primary transmission is not detected for a decent amount of time in a target frequency band, it is considered as available for access during that time slot. Here, a CR is positioned inside the coverage region of the primary user.
- *Spatial Spectral Hole*: If the primary transmission is restricted to a particular location, the target frequency band is said to be available outside the coverage region of primary user to avoid any interference with it, but the band can be accessed in the same time slot [11].

The various tasks performed by a cognitive radio are summarized in the state diagram cycle called as the cognitive cycle shown in Figure 2.2 [8].

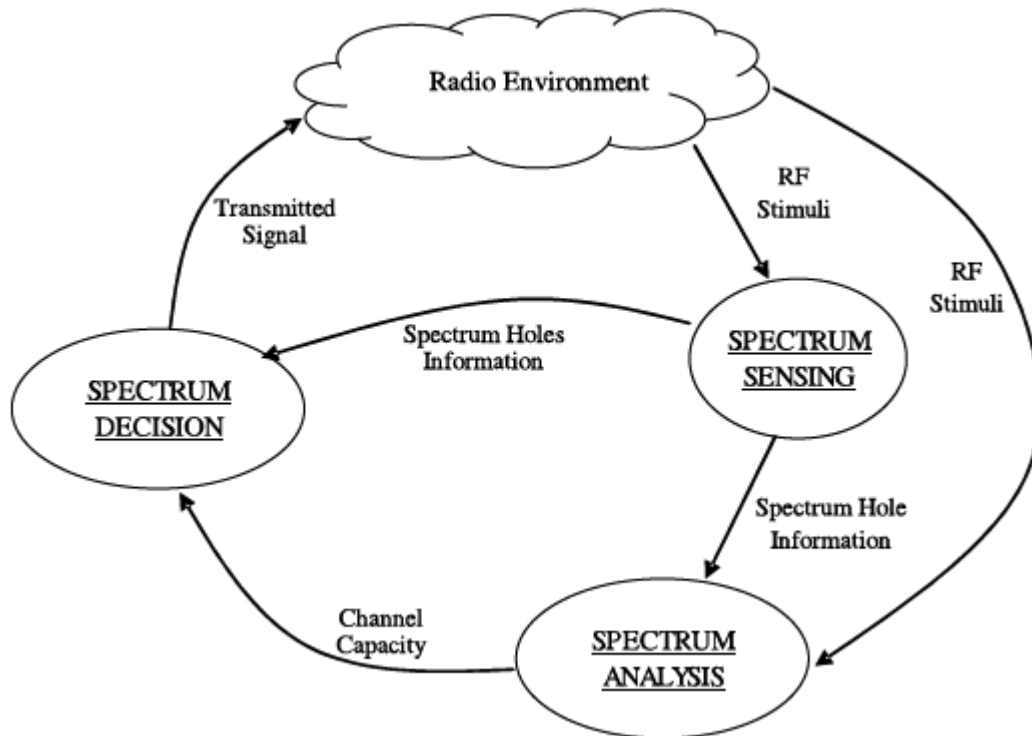


Figure 2.2: Cognitive Cycle [8]

The three major operations of a cognitive cycle are outlined as follows:

1. *Spectrum Sensing*: In order to find the spectrum holes, a CR continuously monitors various frequency bands in the spectrum and records the useful information. The process of sensing has to be very fast and precise so as to scan a large part of the spectrum.
2. *Spectrum Analysis*: The spectrum holes detected through sensing are characterized, and channel conditions are estimated across these holes.
3. *Spectrum Decision*: As per the cognitive user requirements such as the transmission bandwidth, mode of transmission, data rates etc., the CR selects the best available spectrum hole for secondary user transmission.

Even after the communication link has been set up, the CR has to continuously monitor the changes in the environment such as reappearance of a primary user or some traffic variations. Any such change would trigger the CR to perform *Spectrum Mobility* wherein it hops from the current frequency band to another available spectrum hole. This process is equivalent to handoff process in cellular networks and hence is referred to as spectrum handoff by Akyildiz in [8]. If multiple CRs are present at a particular location, *Spectrum Sharing* operation is performed wherein a CR, after identifying the best available frequency band, coordinates the access to this band with other CRs.

It is obvious from the cognitive cycle that spectrum sensing is the first and most important step in this cycle. In order to accurately monitor the continuous environment changes in time, space, frequency, code and phase domain, very efficient sensing techniques need to be employed keeping in mind the user's requirements.

2.2 Classification of Spectrum Sensing Techniques

Spectrum sensing techniques are broadly classified into two main categories: transmitter detection and interference based detection [8]. Actually, the simplest approach for identifying opportunistic spectrum access would be primary receiver detection within the coverage region of the CR. But as the CR cannot locate the primary receiver, this is not practically possible [12]. Transmitter detection is the most sought after technique by researchers due to its simplicity. Figure 2.3 shows the broad classification of different spectrum sensing techniques based on primary transmitter detection.

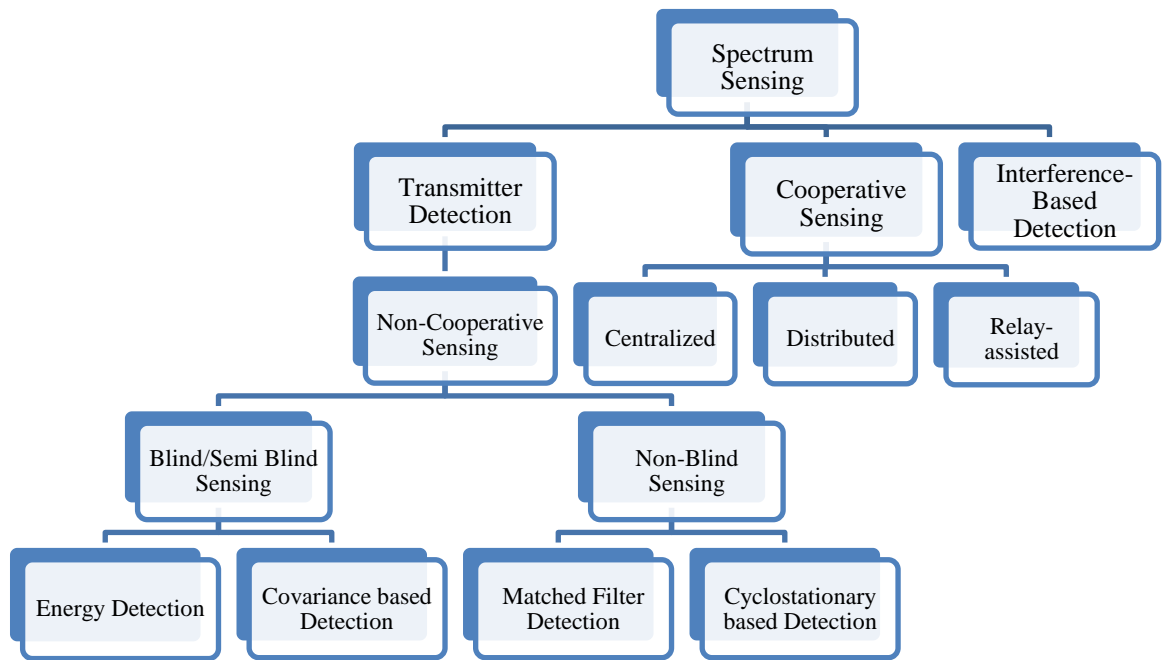


Figure 2.3: Classification of Spectrum Sensing Techniques

In transmitter detection techniques, the CR detects the weak signals from the primary transmitter by locally observing it then decide on any opportunistic spectrum usage [8]. For this approach to work, the CR has to be present in the coverage range of the primary

transmitter. One of the problems with this technique is the *primary receiver uncertainty problem* wherein if the primary receiver is in the vicinity of the CR, there is unavoidable interference at the primary receiver, as shown in Figure 2.4 (a). The other problem that may arise is when the CR is located in the range of the primary transmitter and suffers deep fading/shadowing; this is referred to as *hidden primary transmitter problem* as shown in Figure 2.4 (b) [8], [13], [14].

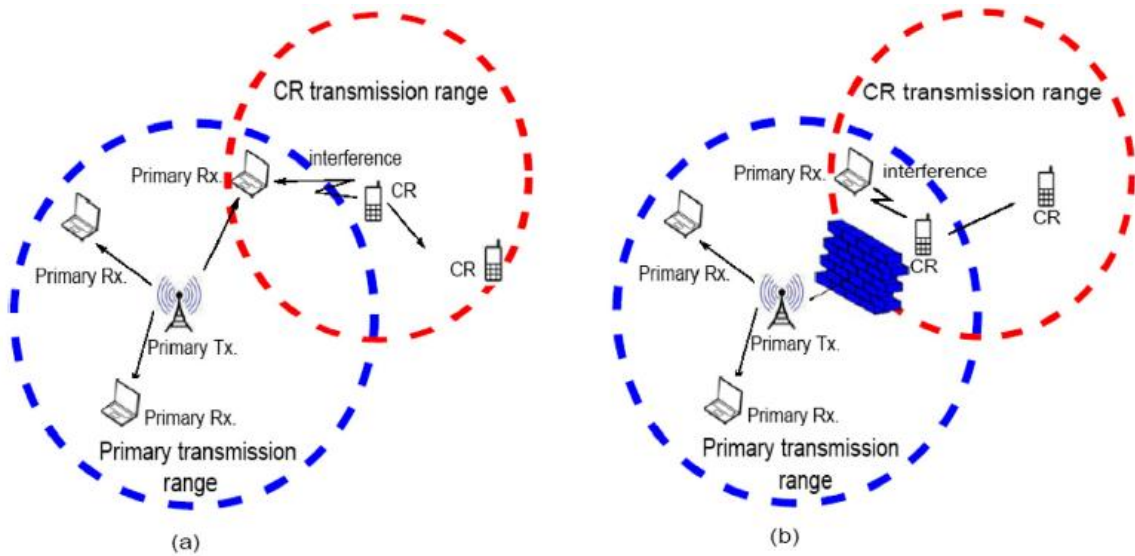


Figure 2.4: Transmitter detection problems [14]

When a lone CR independently performs transmitter detection, it is referred to as non-cooperative spectrum sensing. *Cooperative spectrum sensing* on the other hand is performed by multiple CRs, sensing a particular band in cooperation with each other to decide on any access opportunity [8], [13]. Cooperation among CRs can be achieved in a centralized or a distributed manner or with the help of external sensing [13]. In *Cognitive Radio Oriented Wireless Networks (CROWN)*, cooperating CRs can locally employ any spectrum sensing method under

transmitter detection approach (see Figure 2.3). Using non-cooperative or cooperative sensing, the CRs make use of the licensed band and transmit only when the primary users are not active. Hence, these techniques are referred as *spectrum overlay* techniques [14].

Transmitter detection techniques can be classified into *Blind/Semi-blind* and *Non-blind* spectrum sensing [14].

- *Blind/Semi-blind sensing*: With the blind sensing approach, the CR doesn't require any information about the primary user signal or noise power to perform sensing. In semi-blind sensing, an estimate of noise variance is the only thing required to carry out the sensing operation. Energy detection and covariance/other statistical based detection are the enabling algorithms under this category.
- *Non-blind sensing*: Using this technique, the CR requires information about the primary user signal as well as noise variance estimate to perform sensing. Matched filter detection and Cyclostationary based detection are the enabling algorithms under this category.

Transmitter detection techniques can also be classified as *Proactive* and *Reactive* spectrum sensing [13]:

- *Proactive sensing*: Here, the spectrum is sensed periodically and the CRs make use of past sensing information, develop predictive models regarding availability of spectrum, plan band usage in order to minimize disruptions to licensed users [15].

- *Reactive sensing*: Here, the spectrum is sensed on demand when CR has to transmit some information.

These two methods can be employed for any transmitter detection technique with or without cooperation [14].

We can also classify the spectrum sensing techniques as *Narrow band sensing* or *Wideband sensing*. As per the requirement, CR can take any of the two approaches, either sensing a single narrow band spectrum or sensing a wider spectrum [14].

Interference based detection is another spectrum sensing technique defined by a new model introduced by FCC [16], to measure the level of interference at the primary receiver. This model shows “the operative range of primary transmitter as the distance at which the received power approaches the noise floor” [12]. This technique is referred to as spectrum underlay technique as CRs can simultaneously transmit along with the primary user by avoiding interference [14]. This technique was shown to be non-implementable in practical situations [17], and hence, not discussed in this thesis.

2.3 Transmitter Detection

Spectrum sensing is a decision making problem which falls under the broad category of detection theory/decision theory. It can also be referred to as a binary hypothesis testing problem [18]. The binary hypothesis problem used to analyze spectrum sensing is given by:

$$x(t) = \begin{cases} n(t), & 0 < t \leq T \quad H_0 \\ hs(t) + n(t), & 0 < t \leq T \quad H_1 \end{cases} \quad (2.1)$$

Here, $x(t)$ is the received signal by the CR during observation time T , $n(t)$ is the Additive White Gaussian Noise (AWGN) with zero mean and variance σ^2 , $s(t)$ is the signal transmitted by the primary user, and h is the channel gain. Based on the received signal, the CR decides whether it is hypothesis H_0 , i.e. primary user is absent and only noise is received, or it hypothesis H_1 , i.e. primary user is present and target frequency band is not available for opportunistic usage. When a CR decides H_1 , it is possible that instead of the primary user occupying the target band, there is another secondary user accessing the band. Hence, spectrum sensing techniques must also identify whether the signal received under H_1 is from a primary user or not, which is by itself another challenging task [14]. The two probabilities defined to analyze the performance of any detection algorithm are:

- *Probability of Detection (P_d):* It is the probability of detecting the signal correctly in a target frequency band when it is actually present.
- *Probability of False Alarm (P_f):* It is the probability of incorrectly deciding that the signal is present in the target frequency band when it is actually absent.

We can express the two probabilities as:

$$P_d = P(\text{signal is present} | H_1) \quad (2.2)$$

$$P_f = P(\text{signal is present} | H_0) \quad (2.3)$$

The complement of P_d is the probability of missed detection (P_m), which is defined as the probability of incorrectly deciding that the signal is not present in the target frequency band when it is actually present. It is expressed as:

$$P_m = P(\text{signal is absent} | H_1) = 1 - P_d \quad (2.4)$$

The objective of robust detection algorithms is to minimize both P_f and P_m , as high P_f results in the under-utilization of spectrum holes, and high P_m results in increased interference at the primary receiver.

Various proposed spectrum sensing techniques have been discussed in the literature [13], [14] along with their advantages and disadvantages. In the following sub-sections, we will briefly discuss some of these techniques.

2.3.1 Energy Detection

Energy Detection [19], [20], also known as radiometry, is the most widely used method for signal detection due to its simplicity and low complexity. It is the most feasible approach for detection when there is no prior information available or when a CR is unable to collect enough information about the primary user signal. The energy detector measures the input signal energy over a specific time interval. Here, the input signal energy is important, and not its form. Hence, the energy detector is robust to statistical variations in the primary user signal [21]. This algorithm considers the primary user signal as noise and gives its decision based on the observed signal energy [21]. The block diagram of energy detector is shown below:

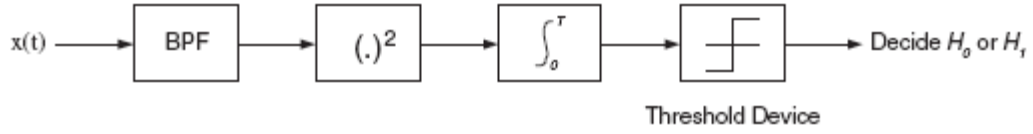


Figure 2.5: Block Diagram of the Energy Detector

The received wideband signal is passed through a band pass filter (BPF) to get it filtered for the target frequency band, which is then squared and integrated over the observation time T . The output of the integrator is the signal energy estimate which is compared to a threshold to make a decision whether the primary user is present or not. The threshold value for the energy detector depends on the noise floor [19]. The analysis of energy detector's performance is discussed in [21]. Researchers, in [22], have analyzed the performance of energy detector under fading conditions. It is very important to set a proper threshold as this algorithm decides between hypotheses H_0 and H_1 by comparing the test statistic (energy of the received signal) with the threshold. If the threshold is set to a very low value, the probability of false alarm increases, resulting in under-utilization of spectrum opportunities. Similarly, a very high threshold value will increase the missed detection probability, resulting in high interference with the primary user. Practically, we can calculate the threshold using one of the following approaches:

- *Constant False Alarm Rate (CFAR) Principle:* If a CR is expected to give a particular reuse probability of an unused spectrum, P_f is fixed to a very small value (say 5%) and P_d is maximized.

- *Constant Detection Rate (CDR) Principle:* If a CR is expected to guarantee non-interference probability, P_d is fixed to a very high value (say 95%) and P_f is minimized as much as possible.

Noise power estimate is the only variable required for energy detector to set the threshold value and hence it comes under semi-blind sensing scheme. The energy detector faces a challenge in setting the threshold value as it depends on the noise power which has to be estimated accurately, even a slight estimation error can result in substantial loss of performance [20]. In [23], the cell-averaging constant false alarm rate (CA-CFAR) strategy for finding the threshold value is analyzed and the results show that this strategy gives the desired P_f . Researchers in [24] have proposed a gradient based algorithm in which the threshold adapts in dynamic scenarios where the variances of the primary user signal and noise change with time.

In this thesis, we use energy detection for spectrum sensing, and follow the CFAR principle to calculate the threshold value. Based on whether the primary user is present (i.e. hypothesis H_1) or absent (i.e. hypothesis H_0), the received signal $x(t)$ is given by equation (2.1). The integrator output in Figure 2.5 is the energy of the received signal, which is our decision statistic (test statistic) denoted as Y . The distribution of Y is needed to analyze the performance of the energy detector. In [19], the authors show that the decision statistic Y follows the distribution mentioned below:

$$\frac{Y}{\sigma^2} \sim \begin{cases} \chi_{2TW}^2, & H_0 \\ \chi_{2TW}^2(2\gamma), & H_1 \end{cases} \quad (2.5)$$

In the above equation, γ is the received SNR at every CR, TW is the time-bandwidth product, and σ^2 is the noise variance of the received signal. Here, χ_{2TW}^2 is the central chi-square distribution with $2TW$ degrees of freedom and $\chi_{2TW}^2(2\gamma)$ is the non-central chi-square distribution with $2TW$ degrees of freedom and non-centrality parameter 2γ . We denote $u = TW$, where the values of T and W are chosen such that u is an integer.

The calculated threshold value λ divides the two decision regions H_0 and H_1 as shown below:

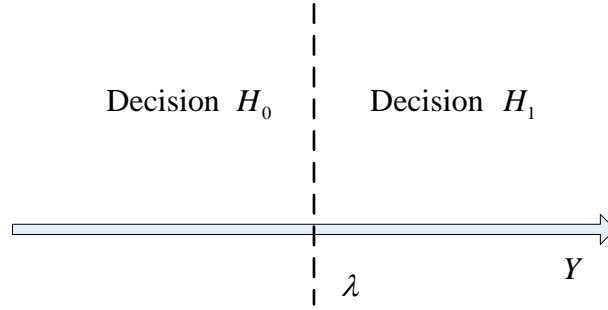


Figure 2.6: Energy Detection using single threshold

As discussed in Section 2.3, to analyze the performance of any detection algorithm, the probabilities of detection, false alarm, and missed detection are defined. Hence, for the energy detection algorithm, these probabilities can be calculated as follows:

$$P_d = P(Y > \lambda | H_1) \quad (2.6)$$

$$P_f = P(Y > \lambda | H_0) \quad (2.7)$$

$$P_m = 1 - P_d = P(Y < \lambda | H_1) \quad (2.8)$$

Here, λ is the threshold value calculated using CFAR principle. The plot of P_d vs. P_f is termed as the *Receiver Operating Characteristics (ROC) curve* and the plot of P_m vs. P_f is termed as the *Complementary Receiver Operating Characteristics (C-ROC) curve*.

For the case of AWGN channels, the channel gain h remains constant in equation (2.1). The expressions for the probabilities of detection and false alarm for such a case have been discussed in [25], and are given by:

$$P_{d \text{ AWGN}} = Q_u \left(\sqrt{2\gamma}, \sqrt{\frac{\lambda}{\sigma^2}} \right) \quad (2.9)$$

In the above equation, $Q_u(a, b)$ is the generalized Marcum Q-function [26].

$$P_f = \frac{\Gamma \left(u, \frac{\lambda}{2\sigma^2} \right)}{\Gamma(u)} \quad (2.10)$$

In the above equation, $\Gamma(.,.)$ and $\Gamma(.)$ are the incomplete and complete gamma functions respectively, given by:

$$\Gamma(a, z) = \int_z^\infty x^{a-1} e^{-x} dx \quad (2.11)$$

$$\Gamma(a) = \int_0^\infty x^{a-1} e^{-x} dx \quad (2.12)$$

For the case of Rayleigh fading, the channel gain h follows the Rayleigh distribution, hence, the SNR γ follows the exponential distribution [22]. The probability of detection for the case of Rayleigh fading is given by [25]:

$$\begin{aligned}
P_{d\ Ray} = e^{-\frac{\lambda}{2\sigma^2}} \sum_{n=0}^{u-2} \frac{1}{n!} \left(\frac{\lambda}{2}\right)^n \\
+ \left(\frac{1+\bar{\gamma}}{\bar{\gamma}}\right)^{u-1} \left[e^{-\frac{\lambda}{2\sigma^2(1+\bar{\gamma})}} \right. \\
\left. - e^{-\frac{\lambda}{2\sigma^2}} \sum_{n=0}^{u-2} \frac{1}{n!} \frac{\lambda\bar{\gamma}}{2\sigma^2(1+\bar{\gamma})} \right]
\end{aligned} \tag{2.13}$$

In the above equation, $\bar{\gamma}$ is the average received SNR. The expression for P_f is the same as in equation (2.10), i.e. without fading, as it is evaluated when the received signal is absent and hence, doesn't depend on the SNR.

Limitations of Energy Detector:

The problem with the energy detector is that it is unable to differentiate between signals of the primary user and another secondary user, resulting in increased false alarm. It is less reliable under deep fading and shadowing conditions. For the energy detector, it is assumed that the noise power is exactly known. However, such an assumption may not be valid under certain environments. Practically, the local thermal noise and the environment noise change with time [21], and the noise is approximately Gaussian with an unknown variance within a certain range [20]. Hence, such noise uncertainty degrades the energy detection performance. For a given uncertainty of x dB, there exists a threshold below which the energy detector becomes unreliable. The SNR wall is defined as the minimum SNR below which the energy detector becomes unreliable, even with infinite sensing duration [14]. The SNR wall is given by [21],

$$\gamma_w = 10^{\frac{2x}{10}} - 1 \quad (2.14)$$

Hence, for all the received SNRs below γ_w , the energy detector is unable to distinguish between H_0 and H_1 , irrespective of the number of observation samples. Even if the noise power is exactly known, energy detector is unable to detect low power primary signals such as spread spectrum signals [13].

2.3.2 Wavelet based Spectrum Sensing

The energy detector is very a good option for wide band sensing. As wideband spectrum is seen as a series of frequency sub bands, with discontinuous power levels, we can sense these sub bands simultaneously by calculating the power spectral density (PSD) of the received wideband signal, and then applying edge detection technique within the PSD of a wideband spectrum. It is assumed that PSD in each sub band is almost flat and it is discontinuous at the sub band boundaries [27]. Wavelet based sensing has been used with edge detection within the PSD of a wideband spectrum, where the edges correspond to the boundaries of sub bands. This is how sub bands are recognized, after which energy estimation is carried over each sub band to identify spectrum holes.

At a certain time burst, the PSD of the received wideband signal $r(t)$ affected by AWGN at the CR front-end is expressed as [27]:

$$S_r(f) = \sum_{n=1}^N \alpha_n^2 S_n(f) + S_w(f), \quad f \in [f_0, f_N] \quad (2.15)$$

In the above equation, α_n^2 is the PSD of n^{th} band B_n , $S_n(f)$ is the signal spectrum, and the two-sided noise PSD is simply given by $S_w(f) = N_0/2$.

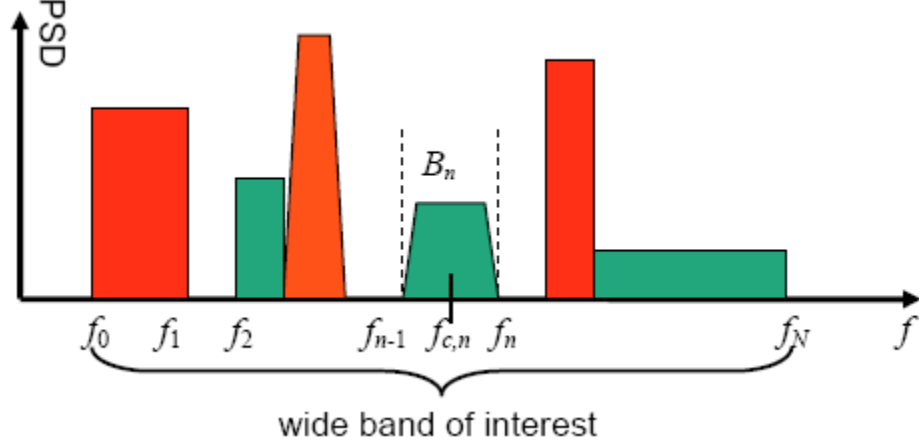


Figure 2.7: PSD of each sub band in wideband spectrum [27]

With the identification of the sub bands, the PSD in each sub band is expressed as:

$$\beta_n = \frac{1}{f_n - f_{n-1}} \int_{f_n}^{f_{n-1}} S_r(f) df \quad (2.16)$$

The noise PSD $S_w(f)$ can be measured offline, or deduced from a vacant band, say n' band, which satisfies $\alpha_{n'}^2 = 0$ and $\beta_{n'} = N_0/2$ for $f \in B_{n'}$. As the current spectrum utilization is rather low, such a vacant band always exists. Hence, $\beta_{n'} = N_0/2$ is apparently the least value among all $\{\beta_n\}$.

One problem with the above mentioned approach is the disturbance in PSD due to the noise at the receiver which is not taken into account [27]. As a result, some unwanted peaks will emerge in the wavelet transform coefficients due to the thermal noise which can be characterized as Gaussian. These unwanted peaks will hamper the correct extraction of sub band boundaries. A new technique was recently proposed in [28], which

makes use of a threshold to neglect the effect of Gaussian noise. Here, the threshold is set as the maximum noise wavelet coefficient and any coefficient value below this threshold is assumed to be zero. Thus, PSD disturbances due to receiver noise are nullified with this approach. Various mother wavelets are employed, multi-scale sum and multi-scale product are compared and their effects on detection are discussed in [28] and show that applying median filtering on wideband PSD and using single scaled wavelet transform efficiently finds the different sub band boundaries.

Wavelet based sensing is preferred over the traditional wideband sensing technique which uses a number of narrow band BPFs as it was shown to outperform the latter, has less implementation costs, and is faster in sensing wideband [27].

2.3.3 Compressed Sensing for Wideband Spectrum

Compressed sensing is a signal processing technique which makes use of the sparseness or compressibility of a signal in a particular domain, to determine the entire signal from relatively few measurements. The wavelet based sensing technique proposed in [27], was extended by the same authors in [29], where they have used sub-Nyquist sampling. The signal spectrum is sparsely populated due to the low activity of the primary users, and to capitalize on this situation, sub-Nyquist sampling is proposed to coarsely sense the wideband spectrum for finding spectrum holes. In compressed sensing, the sampling rate is calculated from the actual sparsity order of the spectrum. But as the sparsity order changes with time, sampling rate also has to change accordingly. Hence, the sampling rates in [29] are calculated from the statistical upper bound of sparsity order, resulting in

a very high sampling rate and a waste of resources. On the other hand, the authors in [30] have proposed a two-step compressed sensing algorithm to reduce the exceedingly high sampling rate. In the first step, using less number of samples, a quick estimation of the actual sparsity order is performed. Using this information, the number of samples is adjusted accordingly in the second step. This helps in adaptively changing the minimum sampling rate. The TS-CSS algorithm in [30] gives an excellent sensing performance with less number of samples and cost comparable with the conventional single-step algorithm.

2.3.4 Cyclostationary based Detection

Certain signals exhibit statistical periodicity which may occur due to modulation, coding scheme, or can also be purposely induced for synchronization like cyclic prefixes, pilot sequences. These signals are referred to as cyclostationary signals. Wireless signals also exhibit such periodicity and exploiting this feature to detect random signals in a noisy background and other modulated signals is referred to as cyclostationary detection [31],[32], [33] and [34]. Certain statistics of cyclostationary signals such as mean and correlation repeat at regular intervals, which induce spectrum redundancy in the modulated signal, resulting in correlation between widely separated frequency components. Thus, cyclostationary detection is employed using spectrum correlation function (SCF) [31] or using cyclic autocorrelation function [34].

The SCF of a received signal $x(t)$ is expressed as [31]:

$$S(f, \alpha) = \sum_{\tau=-\infty}^{\infty} R_x^a(\tau) e^{-j2\pi f t} \quad (2.17)$$

In the above equation,

$$R_x^a(\tau) = E[x(n + \tau)x^*(n - \tau)e^{j2\pi\alpha n}] \quad (2.18)$$

Here, $R_x^a(\tau)$ is the CAF, where α is the cyclic frequency. When this cyclic frequency is equal to the received signal's fundamental frequencies, the SCF achieves peak values. It is assumed that cyclic frequencies are known a priori or can be extracted [33]. In order to use cyclostationary detection for wideband spectrum, the extraction of cyclic frequencies is required as the CR may not have the knowledge about it for all the primary users. This increases the sensing time and complexity by many folds [21].

Generally the cyclostationary detection technique makes use of cyclic prefix which is induced in the cyclic autocorrelation function for OFDM signals. But if the secondary users also use OFDM with the same symbol duration, this technique cannot differentiate between primary user signal and another secondary user signal.

The cyclostationary detection technique is capable of differentiating noise from primary user signal as well as between various primary users. This is because noise is wide sense stationary and has no correlation whereas modulated signals have non negligible spectral correlation. Second order cyclostationary detection is very efficient as it is not affected by noise uncertainty, but requires complex computations and high latency. Hence, it performs better than energy detection at low SNRs. Extraction of features makes this technique non-blind, increase the sensing time and hence, spectrum holes available for short duration cannot be used reliably [14].

In order to reduce complexity and latency, but at the same time maintain reliability, the authors in [35] have used first order cyclostationary features (from trained sequences sent with actual signal) to reduce the noise uncertainty followed by energy detection, which now becomes reliable even at low SNRs. The authors have shown that this approach performs better than second order cyclostationary detection. As discussed in [36], cyclostationary detection can be implemented for fine sensing in the second stage after energy detector performs coarse sensing in the first stage.

2.3.5 Matched Filter Detection

With the knowledge of transmitted signal, Matched Filtering is the optimum approach for detecting primary users as it maximizes the received SNR [37]. Employing matched filter requires the CR to demodulate the primary user signal, i.e. it should have all the details about the received signal such as order and type of modulation, frequency, pulse shaping and frame format. To demodulate, the CR has to be coherent with the received signal, which it can achieve using preambles or pilot sequences. The output of the matched filter is compared with a threshold, which is selected to achieve a certain false alarm probability. Under AWGN, the matched filter detector output follows the distribution given as [21]:

$$f_Y(Y) \sim \begin{cases} \chi_2^2, & H_0 \\ \chi_2^2(2\gamma), & H_1 \end{cases} \quad (2.19)$$

In the above equation, γ is the received signal SNR. This assumes that the CR is synchronized with the pilot sequence of received signal. Since the CR does not know

whether the primary signal is present or absent, in practice, it may not be synchronized with received signal pilot sequence. Hence, the implementation complexity increases further, and the detection performance is also reduced.

Compared to other detection techniques, the matched filter achieves the target false alarm probability or the missed detection probability in a very short time as it requires $O(\frac{1}{SNR})$ samples for the detection [20]. The most significant disadvantage of the matched filter detection is that the CR requires a dedicated receiver for each type of primary user signal. Implementation of the system gets more and more complex [38] and power consumption becomes very high as each receiver type will need a different algorithm to be performed.

2.3.6 Waveform based Sensing

As discussed in the previous sections, wireless signals employ certain signal patterns such as pilot sequences, preambles, mid-ambles or other spread sequences to synchronize. If a CR knows the pattern, the primary user signal can be detected by correlating the received signal with its own known copy. Such a technique is referred as waveform based sensing, which can only work if the signal patterns are known apriori. Waveform based sensing performs better, is more reliable and converges faster than the energy detector [39]. Increasing the length of known pattern enhances the performance of the algorithm. Waveform based sensing metric is expressed as follows [39]:

$$M = Re \left[\sum_{n=1}^N x(n)s^*(n) \right] \quad (2.20)$$

In the above equation, $x(n)$ is the received signal. Under hypothesis H_0 and H_1 , the metric changes as follows:

$$M = \text{Re} \left[\sum_{n=1}^N w(n)s^*(n) \right] \text{ under } H_0 \quad (2.21)$$

$$M = \sum_{n=1}^N |s(n)|^2 + \text{Re} \left[\sum_{n=1}^N w(n)s^*(n) \right] \text{ under } H_1 \quad (2.22)$$

The output of the correlation is compared with set thresholds to arrive to a decision about spectrum usage. Compared with matched filter, waveform based sensing is less complex, but is very sensitive to synchronization error [39].

Matched filters and waveform based detection are the main techniques for coherent sensing. These techniques have less complexity compared to cyclostationary based detection. On the other hand, their detection performance goes down considerably if there is any synchronization error or if the primary user signal information is inaccurate.

2.3.7 Covariance based Detection

The received primary user signal is generally correlated due to channel dispersion, over sampling or due to multiple antennas at the receiver [40]. This correlation can be exploited to distinguish between the primary user signal and noise. Generally the covariance of signal and noise are different. The covariance matrix captures the correlation between the received signal samples. Hence, in covariance based detection, spectrum usage decision depends on the covariance matrix of the received signal. Certain

test statistics are generated based on received signal's sample covariance matrix. In [41], the ratio of maximum eigenvalue to minimum eigenvalue is used as one test statistic and the ratio of average eigenvalue to minimum eigenvalue is the another one. In [42], maximum eigenvalue is used and in [43], the ratio of diagonal elements to non-diagonal elements is used as the test statistic.

The sample covariance matrix can be estimated using the received signal samples and hence, covariance based detection needs no information about the received signal. Here the threshold value depends on the number of samples and the false alarm probability. Therefore, it doesn't require the estimation of noise power. For correlated signals, covariance detection gives better performance than energy detector. But for independent and identically distributed (IID) signals, the performance is same as energy detection.

Two-stage Spectrum Sensing:

Instead of using a single stage sensing, a two stage spectrum sensing algorithm was proposed, wherein the total spectrum is divided into a number of contiguous coarse sensing blocks (CSB) of equal bandwidth [44]. In the coarse sensing stage, the coarse sensing block with idle channels (CSBW) is selected. In the second stage, fine resolution sensing is performed serially within the CSBW to detect the idle channel. Whereas in [36], the first stage uses a simple energy detector to serially search for probable spectrum holes, and for the second stage, advanced sensing approaches such as feature detection are used over the probable spectrum holes from the first stage, to make a final decision about spectrum occupancy. The results show that at low SNR, where energy detector is unreliable, two-stage sensing algorithm achieves improved detection performance [36].

2.3.8 Issues with Non-Cooperative Spectrum Sensing

Practically, non-cooperative detection faces certain issues which hinder the CR users to achieve the expected performance. These issues are discussed below [14]:

- Due to multipath fading/shadowing in the environment, the received signal power at the CR is very low. If the CR is not sensitive enough, it will result in the increase of missed detection probability which in turn will cause interference to the primary user.
- Based on the location of the secondary user, the primary receiver uncertainty problem and/or hidden primary transmitter problem can arise as shown in Figure 2.4. To overcome hidden primary transmitter problem, CR's sensitivity should be much more than the primary receiver. Practically, this sensitivity should be higher by 30-40 dB [38], which is a real challenge in itself.
- In a multiuser environment, CRs are present along with other secondary networks searching for the same frequency band. In this scenario, a CR can detect another secondary user signal as the primary user signal, or the primary signal can be masked by another secondary user. As a result, CRs performance degrades considerably.
- Practically, the local thermal noise and the environment noise change with time, and the noise is approximately Gaussian with an unknown variance within a certain range. Such noise variance uncertainty makes the non-cooperative detection unreliable.

2.4 Cooperative Spectrum Sensing

It is very clear from the discussion in the previous section that non-cooperative spectrum sensing can be seriously affected due to multipath fading/shadowing, noise uncertainty and hidden primary user problem. When a CR experiences deep fading/shadowing over the sensing channel, the observed energy during a fixed sensing time is not sufficient enough to decide that a PU is present. One way to address this problem is to use more sophisticated sensing approaches such as cyclostationary based detection or matched filter detection (refer to sub-sections 2.3.4 and 2.3.5), but these require primary user signal information. In our case, using energy detection, we can increase the sensing time, thus, increasing the time-bandwidth product (TW), where W is the bandwidth of the primary user signal. Even the sensing time can be increased only up to a certain level, as it has to take care of sensing periodicity requirements [45]. Hence, using energy detection for non-cooperative detection, it is highly unlikely to maximize the detection probability and minimize the false alarm probability simultaneously [22].

The above mentioned problems can be addressed if we can exploit the spatial diversity by allowing multiple CRs to cooperate. Multipath fading varies considerably with a quarter wavelength displacement [46]. Hence, it is very unlikely that all the spatially distributed CRs in a CRN will simultaneously experience deep fading/shadowing. In a typical CRN, certain CRs receive a strong PU signal, while others suffer from deep fading/shadowing or the hidden PU problem. Thus, if these spatially distributed CRs cooperate, and combine their sensing information, such cooperation will greatly reduce the effect of deep fading/shadowing, and the problem of hidden primary user. Researchers proposed to

use cooperative spectrum sensing as it was shown to improve sensing performance [22], [47], [48], with little requirement changes at each CR [46]. Cooperative sensing also decreases the overall sensing time [49]. Cooperative sensing is also referred to as collaborative spectrum sensing [50], [51].

The improvement in performance as a result of cooperation is referred to as *cooperative gain* [52]. Cooperative gain is not only about the improvement in detection performance, it can also be seen in terms of sensing hardware. The received SNR can be very low due to fading/shadowing, which makes non-cooperative detection of PU extremely difficult. In such cases, a receiver should have very high sensitivity, which would increase hardware complexity. Moreover, if the received SNR falls below a particular level referred as SNR wall, increasing the sensitivity will not improve detection performance [53]. Cooperative sensing provides relief in sensitivity requirements, as the threshold value can be kept around the value of nominal path loss [46] as shown in Figure 2.8.

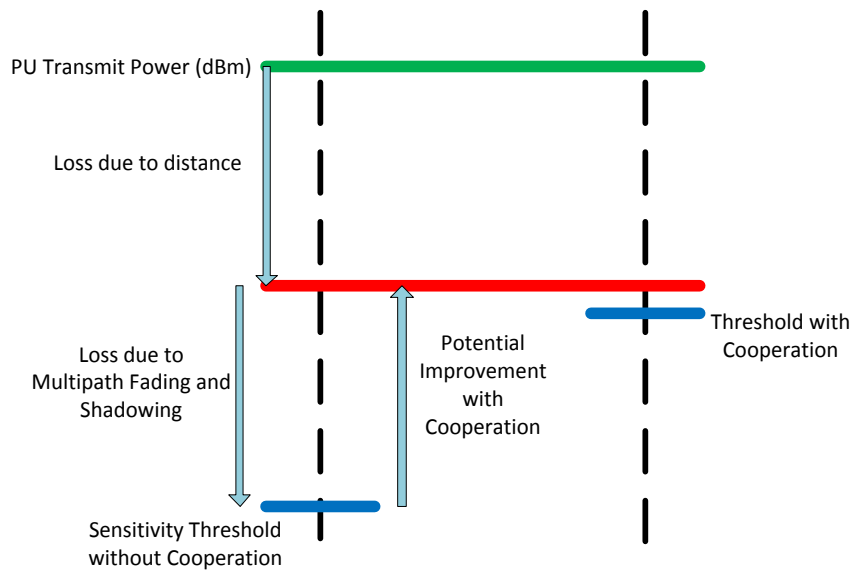


Figure 2.8: Sensitivity improvement with cooperation

If the sensing time is reduced due to cooperation, the receivers' throughput improves as they have more time for data transmission. In such cases, improved throughput also contributes to the cooperative gain [52]. Certain factors can limit the amount of cooperative gain achieved. If some of the cooperating CRs are under spatially correlated shadowing, their sensing observations are correlated. Cooperation among more spatially correlated CRs affects negatively the detection performance [46], [50]. Apart from this, cooperative sensing can introduce cooperation overhead such as delay, and operations dedicated for cooperation, which doesn't occur in non-cooperative sensing [52].

2.4.1 Classification of Cooperative Spectrum Sensing

Depending upon how the cooperating CRs share their sensing information in a CRN, cooperative spectrum sensing is classified as centralized, distributed and relay-assisted as shown in Figure 2.9 [52].

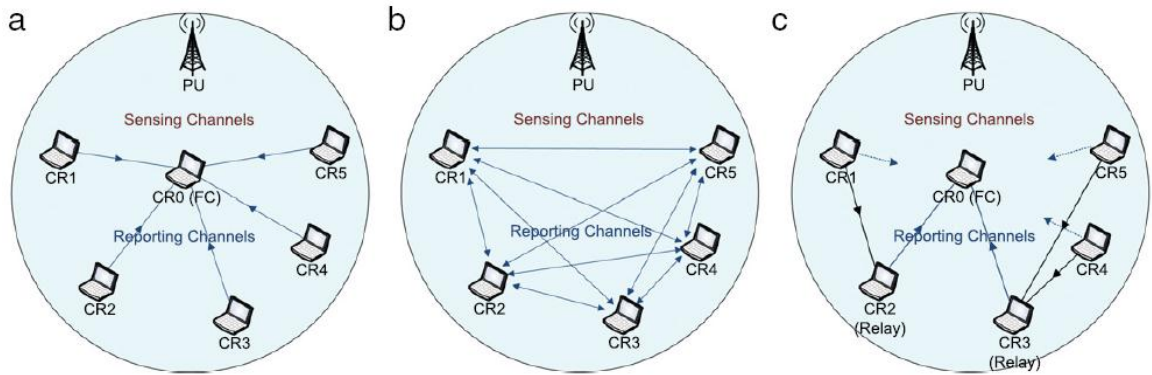


Figure 2.9: Classification of cooperative sensing: (a) Centralized, (b) Distributed, and (c) Relay-assisted [52]

In centralized cooperative sensing, the Central Unit, also known as the Fusion Centre (FC), manages the spectrum sensing process and makes a final decision about the

opportunistic spectrum access. The centralized cooperative sensing is carried out in three steps as mentioned below:

1. *Local Sensing*: A target frequency band is selected and each cooperating CR performs local spectrum sensing over that band.
2. *Reporting*: All the cooperating CRs individually forward their sensing information over their corresponding reporting channel to the fusion centre.
3. *Information Fusion*: Finally, the fusion centre combines all the received information to decide about the presence or the absence of PU.

After making the decision, the fusion centre either manages the opportunistic spectrum usage of the target band or it broadcasts the decision to all the cooperating CRs. In the literature, the central unit is addressed by different names such as fusion centre [54], [55], base station [56], [57], common receiver [47], [48], [58], [59], combining node [60], [61], master node [62], designated controller [46], etc.

In centralized CRN, a CR base station is the central unit. On the other hand, in CR ad hoc networks, as there is no central unit, any CR can work as a fusion centre and coordinate the cooperative sensing to receive the local sensing information from the cooperating CRs to make a final decision on the spectrum usage. Thus, centralized cooperative sensing can be performed in centralized as well as distributed networks. The centralized network is shown in Figure 2.9 (a), where, CR_0 is the fusion centre, and $CR_1 - CR_5$ are the cooperating CRs.

In distributed cooperative sensing (see Figure 2.9 (b)), there is no fusion centre to manage the cooperation and decide on the spectrum usage. Cooperating CRs exchange

information with each other to decide on the presence or the absence of a primary user iteratively [63], [64], [65]. The distributed sensing is performed in the three steps [14]:

1. Each CR performs local spectrum sensing and shares the sensing information with every other cooperating CR.
2. Each individual CR fuses its own local information with the received sensing information from other cooperating CRs to decide on the spectrum hole.
3. If CRs are unable to decide on the spectrum hole, each CR sends its fused sensing information to every other cooperating CR in the next iteration. This process continues until the cooperating CRs converge to a decision on the spectrum usage opportunity over the target frequency band.

Hence, with no fusion centre, each cooperating CR in the distributed network partly acts as the fusion centre.

The local sensing information shared by cooperating CRs, either with the fusion centre or with other cooperating CRs, can be either their observation values (*soft* results) or their local 1-bit binary (*hard* results) decisions about the spectrum usage opportunity. If the fusion centre combines all the received local 1-bit binary decisions, it is termed as *decision fusion* while if it combines all the received observation values, it is termed as *data fusion* [66]. These are also termed by some authors as *hard combination* and *soft combination* techniques respectively [21].

Each cooperating CR is linked with the primary receiver through a channel, called as *sensing channel*, to perform local sensing over the target frequency band. After performing local sensing, each cooperating CR reports its sensing information to the

fusion centre over the *reporting channel*, also known as the *control channel*. Implementation of the control channels can be using various techniques proposed like the use of ISM band or the ultra-wide band (UWB) which are non-licensed bands or even using a dedicated spectrum [67], [68]. The use of UWB is very interesting as it can function independently with the use of various spreading codes and it has less effect on other types of communication [67]. In [69], the authors proposed a TDMA based approach, wherein the network is divided into numerous clusters, represented by a cluster head. CRs in each cluster perform local sensing simultaneously and send the sensing data to the cluster head during the time slots assigned to these. Various cluster heads exchange information with each other to decide about the spectrum usage, and broadcast the decision to their respective cluster CRs. The reporting channels should be implemented such that the communication overhead remains low and the delay is minimized. Generally, medium access protocols (MAC) are used [70]. Many authors, for simplicity, have assumed the reporting channels to be perfect, wherein the cooperating CRs can report their sensing information with no error.

Practically, sensing as well as reporting channels are not perfect. Under such a scenario, certain cooperating CRs may observe a strong primary user signal but suffer from a weak reporting channel, due to fading/shadowing, while some others observe a weak primary user signal but have access to a strong reporting channel. This is when *relay-assisted* cooperative sensing can be used, as shown in Figure 2.9 (c). Here, CR_1 , CR_4 and CR_5 are observing weak reporting channels, whereas CR_2 and CR_3 have strong reporting channels. Hence, CR_2 and CR_3 can act as relays to report the sensing information from CR_1 , CR_4 and CR_5 to the fusion centre. Thus, the reporting channels of CR_2 and

CR_3 can be called as relay channels. Relay-assisted sensing can also work in distributed networks [52].

When the sensing information is reported to the fusion centre through multiple hops, each intermediate hop is a relay. Hence, relay-assisted sensing, shown in Figure 2.9 (c), is categorized as multi-hop cooperative sensing. The centralized and distributed sensing, shown in Figure 2.9 (a) and (b), are categorized as single hop cooperative sensing.

Cooperative spectrum sensing can also be broadly classified as *internal sensing* and *external sensing*. Centralized as well as distributed sensing, both single hop and multi-hop fall under the category of internal sensing. It is also called as *collocated sensing* [71], as sensing and operational (subsequent data transmission over the targeted band) functions are collocated in a single CR. Such CRs are more complex and consume higher energy. Moreover, each CR has to reserve certain time slot for sensing, hence, reducing the data transmission time. As a result, spectrum holes are sub-optimally used. Researchers, in [71] have proposed an external sensing technique, where a dedicated *external sensor network* is employed to continuously or periodically sense the target frequency band. The sensing results are reported to the central unit of the external network, which, then fuses the sensing results and shares the spectrum occupancy information with the *operational network*. Thus, rather than performing spectrum sensing, the CRs in the operational network only use the information from the external sensor network, to select the suitable frequency band as well as time duration for data transmission. Hence, apart from solving the multipath fading/shadowing and hidden primary transmitter problem, external sensing enhances spectrum usage efficiency, as CRs acquire the spectrum holes with minimum delay.

2.4.2 The Cooperative Spectrum Sensing Framework

The cooperative spectrum sensing framework [52] comprises of a primary user, cooperating CRs along with the fusion centre, the RF environment consisting of sensing as well as reporting channels and a database (optional) at a remote location. Figure 2.10 shows the physical layer framework of centralized cooperative sensing. In the framework, a group of cooperating (collaborating) CRs perform local spectrum sensing over the target frequency band.

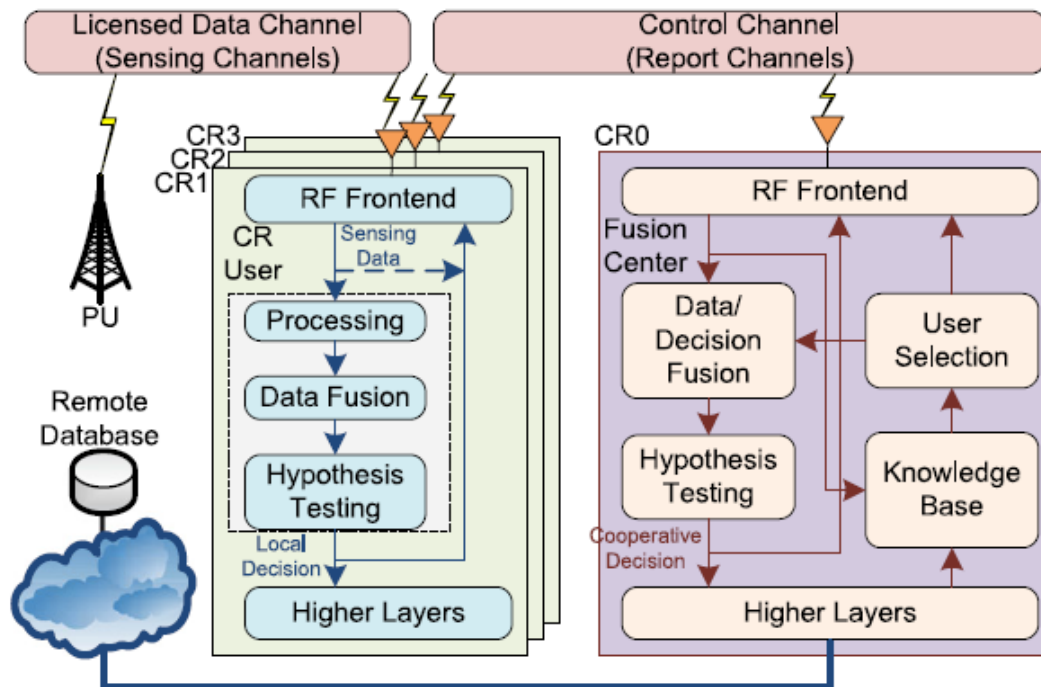


Figure 2.10: Framework of centralized cooperative spectrum sensing [52]

Each cooperating CR consists of an RF front end and a local processing unit which may include elements such as a signal processing unit, data fusion and hypothesis testing units. The RF front end has the capability of being configured for spectrum sensing or for data transmission. Moreover, it performs analog to digital conversion for received RF

signals. The local sensing information received by the RF front end can either be directly reported to the fusion centre or can be processed locally to reach a local decision. Generally, due to the bandwidth constraints over the reporting channel, it is required to perform some local processing of the sensing information, such as evaluating the test statistics and the thresholds. After the local decisions or the sensing observations are ready to be reported to the fusion centre, the reporting channels are accessed through the MAC layer and data is reported to the fusion centre.

In this framework, the fusion centre is a powerful CR, which, apart from having standard CR capabilities, also consists of user selection and knowledge base units to efficiently manage the cooperative sensing task. As per the requirement and based on the capability of the fusion centre, it can also be connected to the database at a remote location, which can provide information about primary user activity and spectrum holes. In the framework of distributed sensing, all the cooperating CRs have architecture identical to the fusion centre in centralized sensing. Each cooperating CR may also have an optional mini database for local use. As discussed in Section 2.4.1, cooperative spectrum sensing is generally a three step process. Apart from these steps, there exist other essential components of cooperative sensing, termed as *elements of cooperative spectrum sensing*. Thus, cooperative sensing technique consists of the following key elements [52]:

- *Cooperation Models*: These models decide how CRs in a network cooperate to perform sensing.
- *Sensing Techniques*: Various techniques are used to sense the environment to take observation samples and process them to detect a primary user.

- *Hypothesis Testing*: To detect the presence or the absence of a primary user, statistical test is performed, either by individual CRs or the fusion centre.
- *Control Channel and Reporting*: This takes care of how the sensing information can be efficiently reported over the control channel, which has certain bandwidth constraints and is susceptible to fading/shadowing.
- *Data Fusion*: It fuses the sensing information shared by cooperating CRs. Signal combining or decision fusion techniques are used as per the type of sensing information shared.
- *User Selection*: Here, cooperating CRs are optimally selected and the cooperation range is decided to optimize the cooperative gain with minimum overhead.
- *Knowledge Base*: It stores the apriori signal information or the knowledge due to past experience. Knowledge base assists the sensing process to enhance detection performance.

2.4.3 Cooperative Spectrum Sensing using Decision Fusion

As discussed in the previous section, generally, the reporting channel has certain bandwidth constraints. This requires the sensing information to be processed locally and only the 1-bit local decisions are reported to the fusion centre. These 1-bit decisions are combined using certain fusion rules and hence, the approach is termed as *decision fusion*. Each cooperating CR performs local sensing, wherein the locally observed energy value is compared with a calculated threshold value. If the energy value is greater than the threshold, the CR decides that a primary user is present and sends the result as binary 1 (H_1), otherwise it decides that primary user is absent and sends the result as binary 0

(H_0). The fusion centre receives 1-bit decision from N cooperating CRs and fuses them according to the logic rule given by [66]:

$$Z = \sum_{i=1}^N D_i \begin{cases} \geq K, & H_1 \\ < K, & H_0 \end{cases} \quad (2.23)$$

The fusion centre decides that a primary user is present (i.e. hypothesis H_1), if at least K out of N cooperating CRs have decided H_1 , or else, it infers that a primary user is absent (i.e. hypothesis H_0). This rule is referred as general K out of N rule [72]. The decision fusion rules generally used are OR, AND, and Majority rules, which are the special cases of general K out of N rule. Using the AND rule ($K = N$), fusion centre decides H_1 , if all the cooperating CRs report the decision as H_1 . If majority rule ($K \geq N/2$) is used, the fusion centre decides H_1 if more than half of the CRs report the decision as H_1 . Another rule used is the *half-voting* rule ($K = N/2$). The OR rule (1 out of N rule) gives the best detection performance compared to the other decision fusion rules for many practical cases [45]. The OR rule is the most conservative rule, as the fusion centre decides on the presence of the primary user signal if at least 1 out of N CRs has local decision H_1 . Thus, the likelihood of any interference caused to the primary user is minimized [66]. In [51], it was shown that the OR rule outperforms other rules for many practical cases. Hence, in this thesis, the focus will be on the OR rule for decision fusion.

The cooperative probabilities of detection, false alarm, and missed detection are given as [66]:

$$Q_d = 1 - \prod_{i=1}^N (1 - P_{d,i}) \quad (2.24)$$

$$Q_f = 1 - \prod_{i=1}^N (1 - P_{f,i}) \quad (2.25)$$

$$Q_m = \prod_{i=1}^N P_{m,i} \quad (OR) \quad Q_m = 1 - Q_d \quad (2.26)$$

Here, $P_{d,i}$, $P_{f,i}$ and $P_{m,i}$ are the probabilities of detection, false alarm and missed detection for the individual CRs.

When all the cooperating CRs are assumed to achieve identical probabilities of detection and false alarm, the cooperative probabilities above can be expressed as follows [50], [66]:

$$Q_d = 1 - (1 - P_d)^N \quad (2.27)$$

$$Q_f = 1 - (1 - P_f)^N \quad (2.28)$$

$$Q_m = (P_m)^N \quad (OR) \quad Q_m = 1 - Q_d \quad (2.29)$$

Here, P_d , P_f and P_m are the probabilities of detection, false alarm, and missed detection for the individual CRs.

As the number of cooperating CRs increase, we can easily show that the probability of missed detection decreases for a particular false alarm probability. Thus, N is termed as the “*sensing diversity order*” of cooperative spectrum sensing, since it characterizes the error component of Q_m ” in equations (2.26) and (2.29).

The advantage of sending the 1-bit local decisions to the fusion centre is that less bandwidth is consumed over the reporting channel.

2.4.4 Cooperative Spectrum Sensing using Data Fusion

In cooperative sensing, instead of sharing the 1-bit local decisions, cooperating CRs can just directly share the raw sensing information with the fusion centre. This approach is termed as *data fusion*. The combining of raw sensing information at the fusion centre provides the best detection performance, but enforces a large communication overhead [21]. Various data combining techniques have been proposed in the literature. In [6], Simon Haykin proposed a soft combining technique for cooperative sensing, called as *multitaper-method singular-value decomposition (MTM-SVD)*, which estimates the interference temperature of the environment. The Multitaper method [73] is used by cooperating CRs to analyze the wideband spectrum. Each of the M CRs evaluates the k^{th} eigenspectrum over the targeted band as follows:

$$Y_k^{(m)}(f) = \sum_{n=1}^N w_k(n) y_m(n) e^{-j2\pi f n}, \quad 1 \leq k \leq K \quad (2.30)$$

In the above equation, $y_m(n)$ is the signal received by m^{th} CR, $w_k(n)$ is the k^{th} Slepian sequence that is used for multitaper spectral analysis. The eigenspectrum vector sent by each cooperating CR to the fusion centre is as follows:

$$Y_m(f) = \left(Y_1^{(m)}(f), Y_2^{(m)}(f), \dots, Y_K^{(m)}(f) \right), \quad 1 \leq m \leq M \quad (2.31)$$

The fusion centre computes an $M \times K$ eigenvector matrix as follows:

$$\mathbf{A}(f) = \begin{bmatrix} w_1 Y_1^{(1)}(f) & \cdots & w_1 Y_K^{(1)}(f) \\ \vdots & \ddots & \vdots \\ w_M Y_1^{(M)}(f) & \cdots & w_M Y_K^{(M)}(f) \end{bmatrix} \quad (2.32)$$

In the above equation, w_m is the weight assigned for the m^{th} CR to take into consideration its geographical environment. Each CR's eigenspectrum vector comprises of the primary signal and noise. If we consider different CRs, their noise part is independent but the signal part is correlated. Thus, the MTM-SVD technique makes use of this correlation from the primary signal part by applying *Singular Value Decomposition (SVD)* to matrix $\mathbf{A}(f)$:

$$\mathbf{A}(f) = \sum_{k=1}^K \sigma_k(f) \mathbf{u}_k(f) \mathbf{v}_k^H(f) \quad (2.33)$$

In the above equation, $\sigma_k(f)$ is the k^{th} singular value of $\mathbf{A}(f)$, $\mathbf{u}_k(f)$ and $\mathbf{v}_k(f)$ are the corresponding left and right singular vectors respectively. Depending upon the largest singular value of $\mathbf{A}(f)$, the fusion centre makes a decision about spectrum occupancy. Thus, the MTM-SVD technique for cooperative sensing provides a near optimal performance [6], [21]. But it has a large communication overhead as each CR has to report K -dimensional eigenspectrum vector to the fusion centre, where SVD operation on $\mathbf{A}(f)$ is performed, which is computationally very complex.

In [74], the authors have proposed a cooperative spectrum sensing technique also using the eigenvalue approach, which was proposed in [42] (as discussed in Section 2.3.7). In [74], all the cooperating CRs evaluate the maximum eigenvalue (MEV) from the

estimated sample covariance matrix. The test statistic (i.e. MEV) is compared with the two thresholds, which are pre-fixed. This helps in determining the cooperating CRs that are reliable, and are allowed to report their decision to the fusion centre. The unreliable CRs directly report their maximum eigenvalues to the fusion centre. The fusion centre fuses all the received data to decide on the presence or the absence of primary user. As the sample covariance matrix can be estimated from the received signal samples, this approach neither requires apriori information about the primary user signal nor the noise power. This technique provides high detection performance but at the cost of higher computational complexity. Moreover, threshold values are set using the random matrix and hence, it is very difficult to determine the thresholds theoretically [42].

Various low complexity soft combining techniques were proposed by the authors in [75], wherein, the cooperating CRs report their observed energy values to the fusion centre. Here, a generalized soft combining technique is proposed, which can be reduced to *Maximal Ratio Combining (MRC)* for low SNR and to *Equal Gain Combining (EGC)* at high SNR. It was shown that MRC and EGC perform better than conventional hard combining scheme [75]. Moreover, to reduce the communication overhead of the soft combining scheme, the authors proposed a “new softened hard combination scheme with two-bit overhead for each cooperating CR” [75]. This algorithm achieves a performance similar to EGC, with a lower communication overhead. It was shown that MRC gives optimal performance for independent diversity branches [76]. But, MRC requires the complete information (both amplitude and phase) of the sensing channel. For MRC, using L diversity branches, the received signals $\{x_l(t)\}_{l=1}^L$ are weighted and combined to yield a new signal $x_{MRC}(t) = \sum_{l=1}^L h_l^* x_l(t)$, where h_l are the channel gains [77]. On the other

hand, EGC offers a less complex approach, as it doesn't require the sensing channel gain estimation. For EGC, using L diversity branches, the received signals $\{x_l(t)\}_{l=1}^L$ are weighted only by phase and combined to yield a new signal $x_{EGC}(t) = \sum_{l=1}^L e^{-j\phi_l} x_l(t)$, where ϕ_l is the phase of the l^{th} channel [77]. The MRC performs slightly better than EGC but it is more complex as it requires the estimation of the channel gains [51], [77]. The performance of EGC is comparable to MRC for Independent and Identically Distributed (IID) branches. Hence, in this thesis, since the performance analysis is done for IID signals, the EGC technique is used for data fusion, and it is compared with the data fusion technique using PSO, which will be discussed in the next chapter. The false alarm probability for EGC with L diversity branches, variance σ^2 and $u = TW$ (time-bandwidth product) is given by [25]:

$$P_{f,EGC} = \frac{\Gamma\left(Lu, \frac{\lambda}{2\sigma^2}\right)}{\Gamma(Lu)} \quad (2.34)$$

The probability of detection for EGC with L diversity branches, variance σ^2 and $u = TW$ under AWGN and Rayleigh fading respectively are given by [22], [25]:

$$P_{d,EGC,awgn} = Q_{Lu}\left(\sqrt{2\gamma_t}, \sqrt{\frac{\lambda}{\sigma^2}}\right) \quad (2.35)$$

Here, $\gamma_t = \sum_{l=1}^L \gamma_l$ is the sum of SNRs from L branches.

$$\begin{aligned}
P_{d,EGC,Ray} = \alpha & \left[G_1 \right. \\
& + \beta \sum_{n=1}^{Lu-1} \frac{(\lambda/2\sigma^2)^n}{2(n!)} {}_1F_1\left(L; n \right. \\
& \left. \left. + 1; \frac{\lambda}{2\sigma^2} \frac{L\bar{\gamma}}{L + L\bar{\gamma}} \right) \right]
\end{aligned} \tag{2.36}$$

Here, $\alpha = \frac{1}{\Gamma(L)2^{L-1}} \left(\frac{L}{L\bar{\gamma}}\right)^L$, $\beta = \Gamma(L) \left(\frac{2L\bar{\gamma}}{L+L\bar{\gamma}}\right)^L e^{-\lambda/2\sigma^2}$, and

$$\begin{aligned}
G_1 = \frac{2^{L-1}(L-1)!}{\left(\frac{L}{L\bar{\gamma}}\right)^L} \frac{L\bar{\gamma}}{L + L\bar{\gamma}} e^{-\frac{\lambda}{2\sigma^2} \frac{L}{L + L\bar{\gamma}}} & \left[\left(1 \right. \right. \\
& + \frac{L}{L\bar{\gamma}} \left) \left(\frac{L}{L + L\bar{\gamma}} \right)^{L-1} L_{L-1} \left(-\frac{\lambda}{2\sigma^2} \frac{L\bar{\gamma}}{L + L\bar{\gamma}} \right) \right. \\
& \left. + \sum_{n=0}^{L-2} \left(\frac{L}{L + L\bar{\gamma}} \right)^n L_n \left(-\frac{\lambda}{2\sigma^2} \frac{L\bar{\gamma}}{L + L\bar{\gamma}} \right) \right]
\end{aligned} \tag{2.37}$$

In the above equation, $L_n(\cdot)$ is the n degree Laguerre polynomial given by [78]:

$$L_n(x) = n! {}_1F_1(-n; 1; x) \tag{2.38}$$

Here, ${}_1F_1(\cdot; \cdot; \cdot)$ is the confluent hypergeometric function of the first kind, given by [79]:

$${}_1F_1(a; b; z) = \sum_{k=0}^{\infty} \frac{(a)_k}{(b)_k} \frac{z^k}{k!} \tag{2.39}$$

In [80], the authors used EGC for Nakagami-m fading channels, derived expressions for probability of detection using various number of diversity branches. The results were

used for finding the number of diversity branches and threshold value required to get a particular false alarm rate using EGC. Analysis of EGC using correlated non-identical Nakagami-m fading channels was discussed in [81], and the expression for the detection probability was derived for same. Estimation of diversity gain is obtained using the SNR's moment generating function. Results in [81] show that the performance degrades as correlation between the diversity increases. Analysis of correlated Rayleigh and Rician fading channels was carried using the de-correlation transformation [82], wherein it was shown that "the system can be transformed into an equivalent system with independent diversity branches" [83]. In [82], the results show that the performance of the de-correlator increases with the increase of correlation coefficient, unlike the traditional receiver. "Here, correlation increases the SNR of stronger de-correlated branch and decreases the SNR of weaker de-correlated branch, thus the effective SNR of the selected branch generally improves with increasing correlation".

In this thesis, the performance analysis is shown for Independent and Identically Distributed (IID) AWGN and Rayleigh fading cases, as the performance of the energy detector degrades for correlated channels. The transmission medium in the wireless communication networks encounters two major problems namely AWGN noise and Rayleigh Fading [84].

2.5 Simulation Results

This section discusses spectrum sensing performance using energy detection for the various cases discussed above. To summarize the results, the ROC and C-ROC curves are plotted under various scenarios.

2.5.1 Non-cooperative Spectrum Sensing

Here, a single CR is used to perform spectrum sensing. The performance of a conventional single threshold energy detector is shown for different SNRs under AWGN and Rayleigh fading channels. In [25], [51], [66], the authors use the time-bandwidth product $u = 5$ as a benchmark to analyze the performance of the energy detector. In this thesis, $u = 5$ is used for the experiments with the number of samples for the received signal $M = 2u = 10$. A received SNR of $\gamma = 5 \text{ dB}$ is considered.

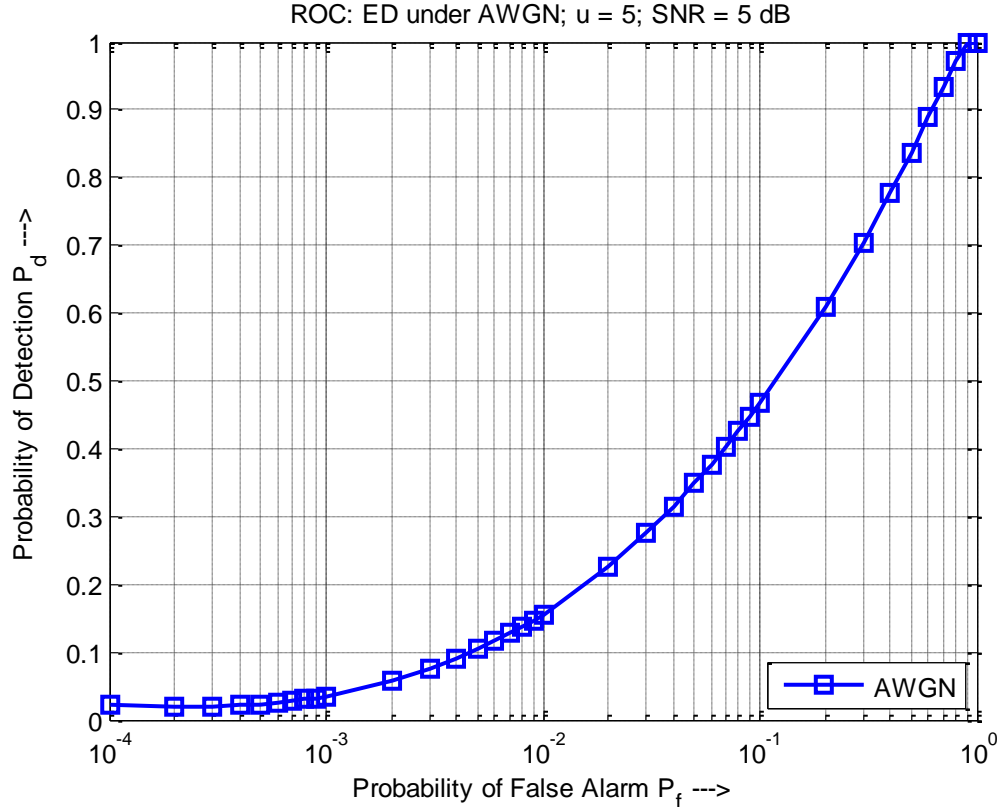


Figure 2.11: ROC for Conventional Energy Detector (SNR = 5 dB, AWGN Case)

In [4], the IEEE 802.22 specifies the acceptable values for the false alarm probability and the detection probability as 0.1 and 0.9 respectively. As can be seen in Figure 2.11, the performance of the energy detector is very low for non-cooperative spectrum sensing. For an SNR of 5 dB and a false alarm probability of 0.1, the detection performance is less than 50%. For SNRs lower than 5 dB, the detection performance degrades further.

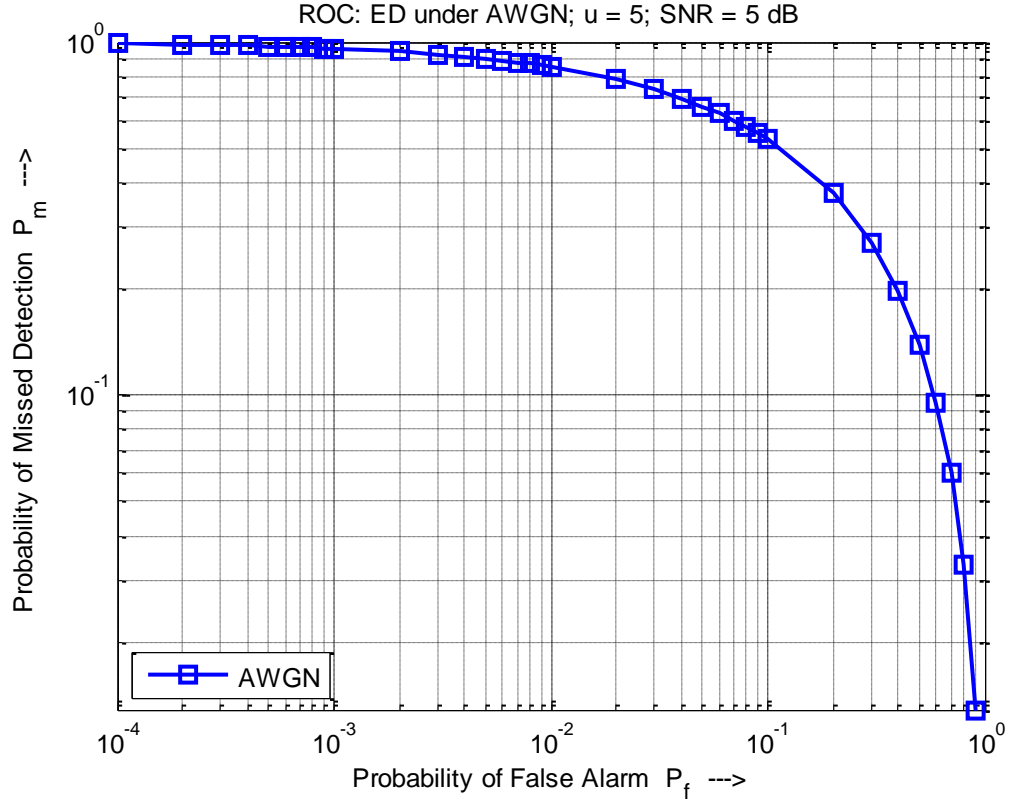


Figure 2.12: C-ROC for Conventional Energy Detector (SNR = 5 dB, AWGN Case)

The performance analysis can also be shown in terms of the Complementary Receiver Operating Characteristics (see Figure 2.12). For the false alarm probability of 0.1, the probability of missed detection is more than 0.5, which is much higher than acceptable values.

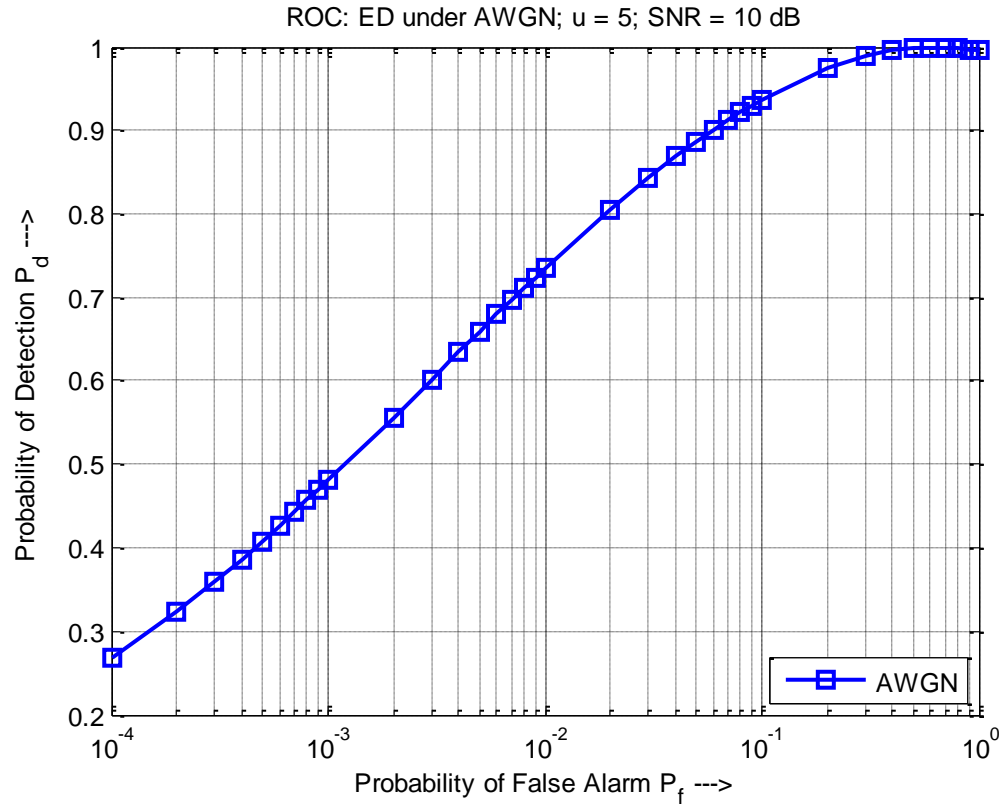


Figure 2.13: ROC for Conventional Energy Detector (SNR = 10 dB, AWGN Case)

The detection performance improves significantly for higher SNR values. For SNR value of 10 dB and a false alarm probability of 0.1, the detection performance is around 95% (see Figure 2.13).

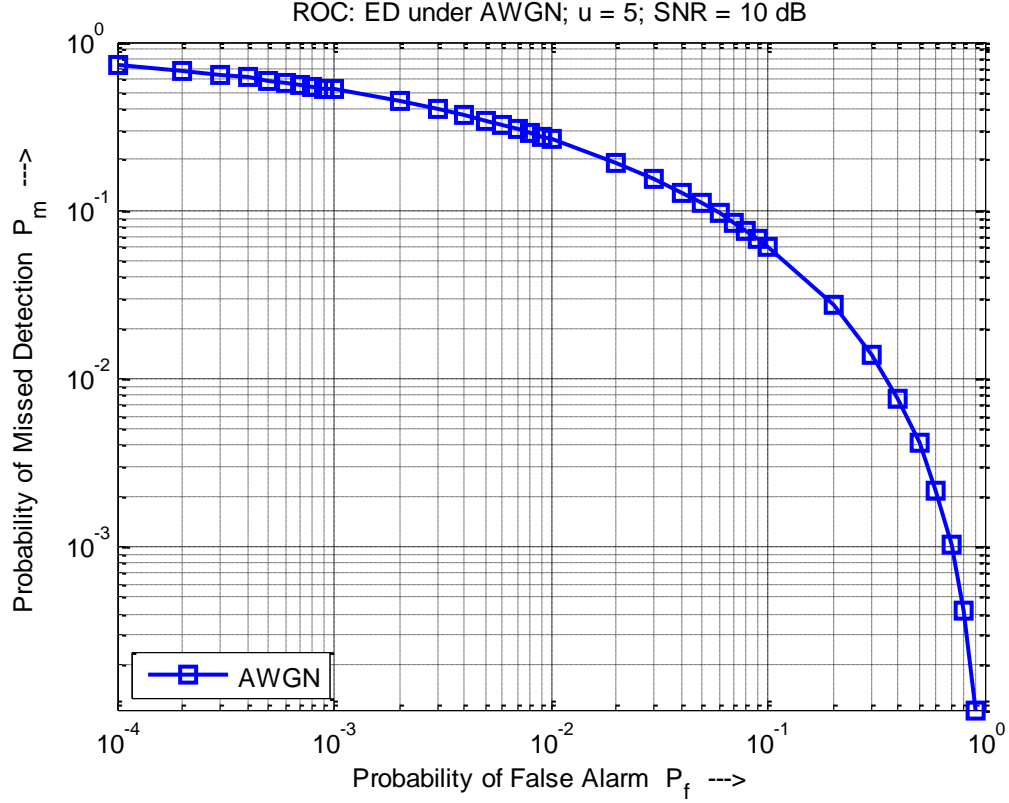


Figure 2.14: C-ROC for Conventional Energy Detector (SNR = 10 dB, AWGN Case)

By plotting the C-ROC curve, it is also observed that the missed detection probability is reduced considerably (see Figure 2.14).

Practically, various obstacles present in the environment, affect the radio signal before it reaches the receiver. Wireless systems are used mostly in urban environments, where a number of objects affect the radio signal. Rayleigh Fading is a practical model for the effect of such an environment. Hence, wireless channels are practically modeled as Rayleigh fading channels, wherein the channel gain follows the Rayleigh distribution, and hence, the received SNR follows the exponential distribution [22].

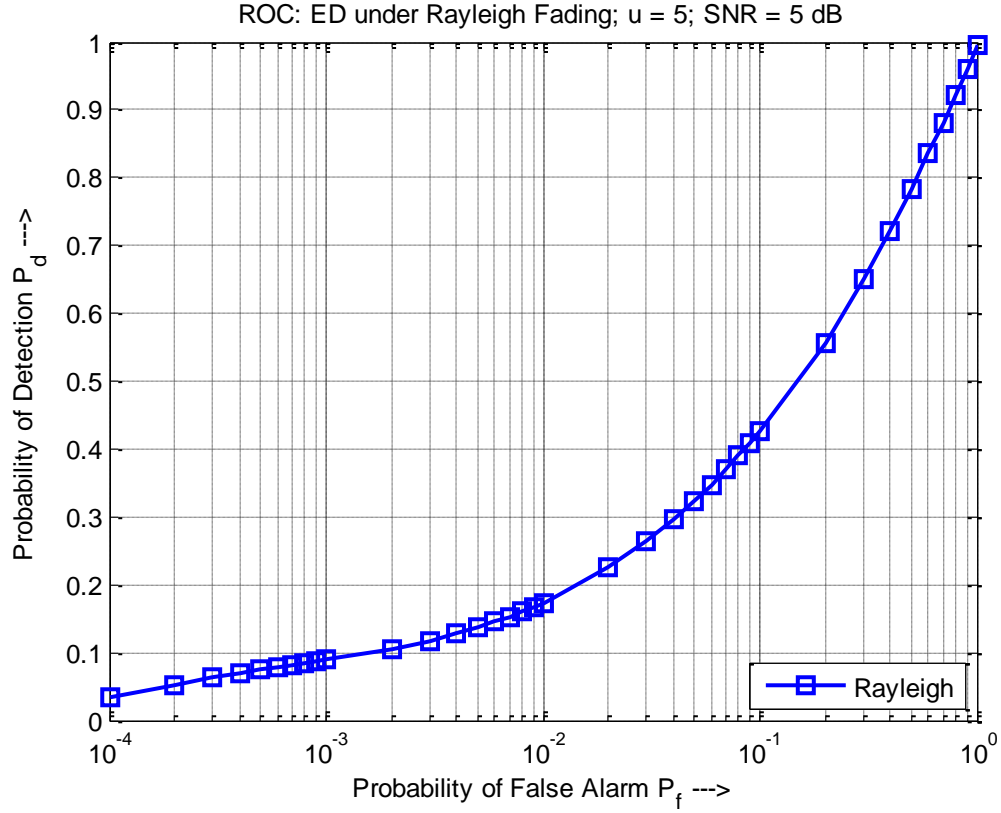


Figure 2.15: ROC for Conventional Energy Detector (Avg. SNR = 5 dB, Rayleigh Fading)

When a non-cooperative CR experiences Rayleigh fading, the performance degrades significantly, even more so at lower SNRs. For an average received SNR of 5 dB, the detection performance reduces to 42%, when the false alarm probability is fixed as 0.1 (see Figure 2.15). The C-ROC curve for this case is shown in Figure 2.16.

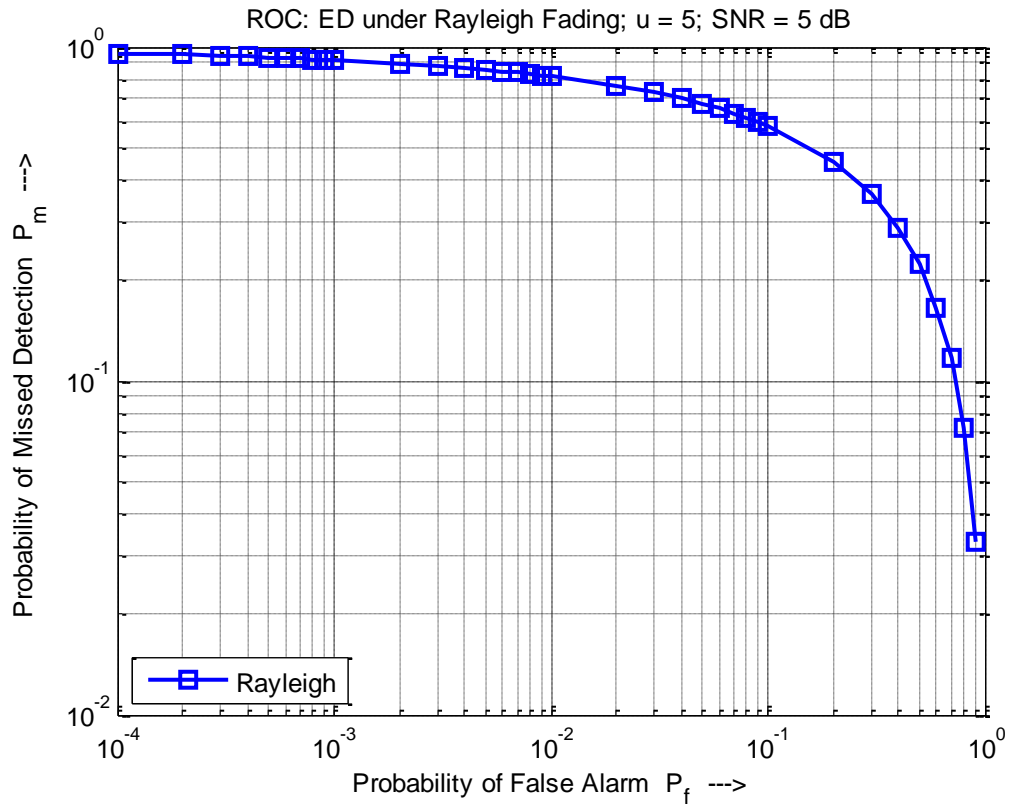


Figure 2.16: C-ROC for Conventional Energy Detector (Avg. SNR = 5 dB, Rayleigh Fading)

The probability of missed detection is around 58%, for a false alarm probability of 0.1, which is unacceptable for practical applications.

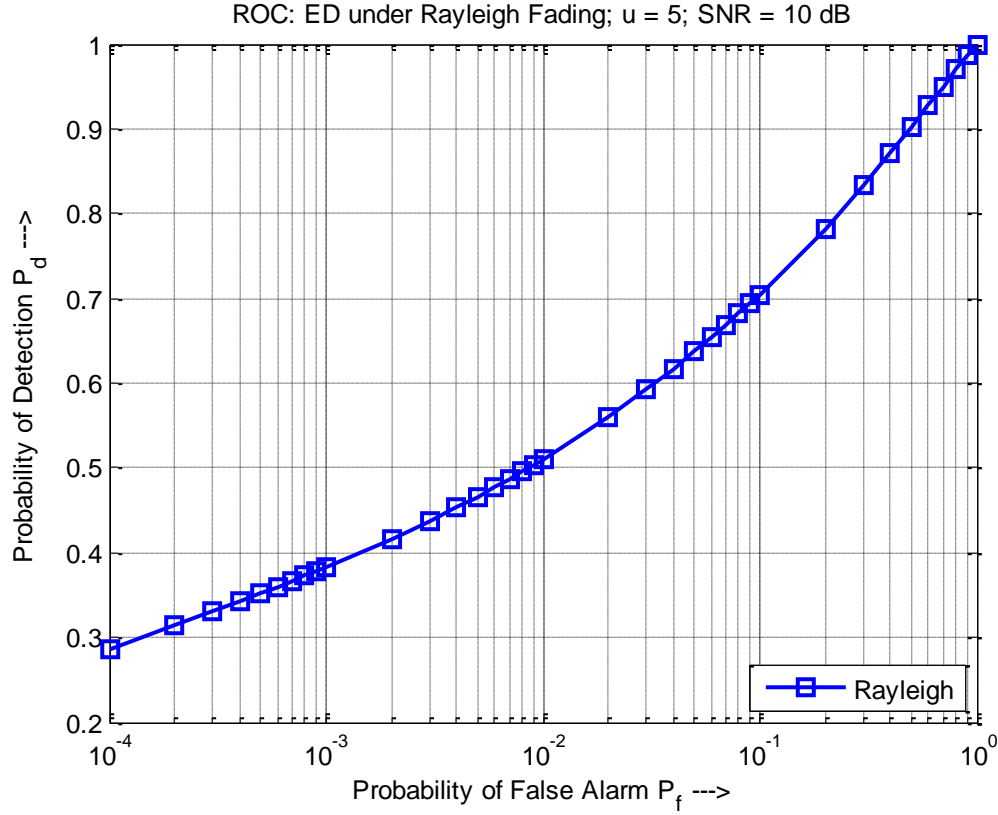


Figure 2.17: ROC for Conventional Energy Detector (Avg. SNR = 10 dB, Rayleigh Fading)

When the average received SNR is increased to 10 dB, for false alarm probability of 0.1, the detection performance is only 70% (see Figure 2.17). Hence, the performance improvement is lower compared to AWGN case, where detection performance goes above 90% for the same false alarm probability. The C-ROC plot for this case is shown in Figure 2.18.

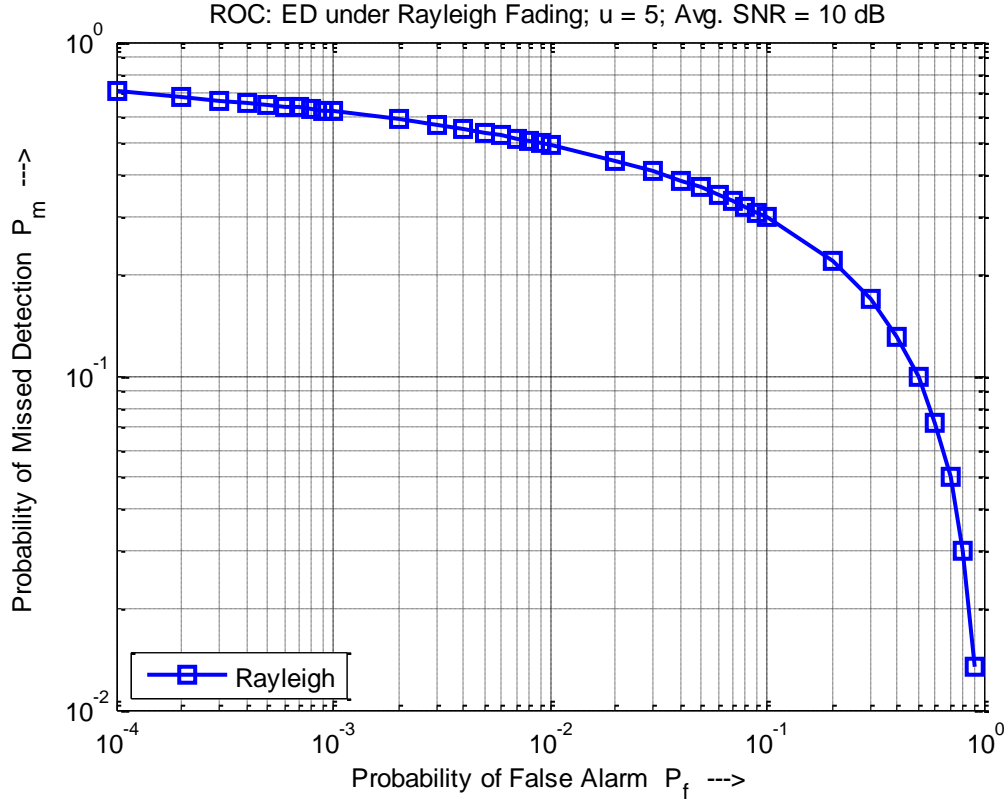


Figure 2.18: C-ROC for Conventional Energy Detector (Avg. SNR = 10 dB, Rayleigh Fading)

It is very clear from the results discussed above, that non-cooperative spectrum sensing yields very low performance under fading environment, even at high SNR. Hence, cooperative spectrum sensing is necessary to overcome the effects of multipath fading/shadowing and enhance detection performance.

2.5.2 Cooperative Spectrum Sensing

Cooperative spectrum sensing significantly reduces the effect of multipath fading/shadowing, thus increasing detection performance. For performance analysis, centralized cooperative sensing is used. At the fusion centre, OR-rule is used for decision fusion technique, and Equal Gain Combining (EGC) is used for data fusion technique.

Each cooperating CR performs energy detection and either reports its local decision or observation value, depending upon the type of fusion used. It was shown earlier, that for a given probability of false alarm, the probability of detection increases significantly when the number of cooperating CRs increase [50], [66]. In [51], the authors show that the use of 10 cooperating CRs sufficiently provides high detection performance as well as a very low false alarm rate, with reduced sensing time. Hence, we analyze the performance of cooperative spectrum sensing under AWGN and Rayleigh fading, for 10 cooperating CRs, and various SNR values. The results are shown in the following figures.

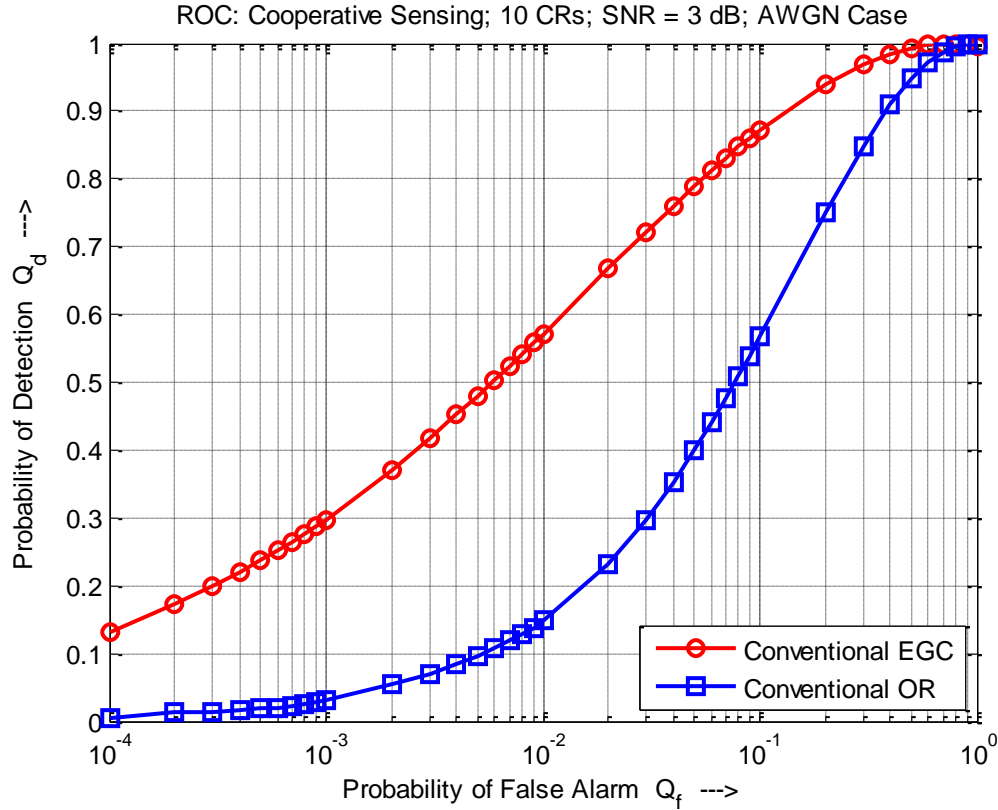


Figure 2.19: ROC – Comparison of Data and Decision Fusion (10 CRs, SNR = 3 dB, AWGN Case)

The OR-rule is compared with the EGC scheme, under AWGN, with the received SNR $\gamma = 3 \text{ dB}$ for each cooperating CR (see Figure 2.19). In this case, for the cooperative

false alarm probability of 0.01, the EGC scheme achieves 58% detection performance compared to the OR-rule which achieves only 14% detection performance.

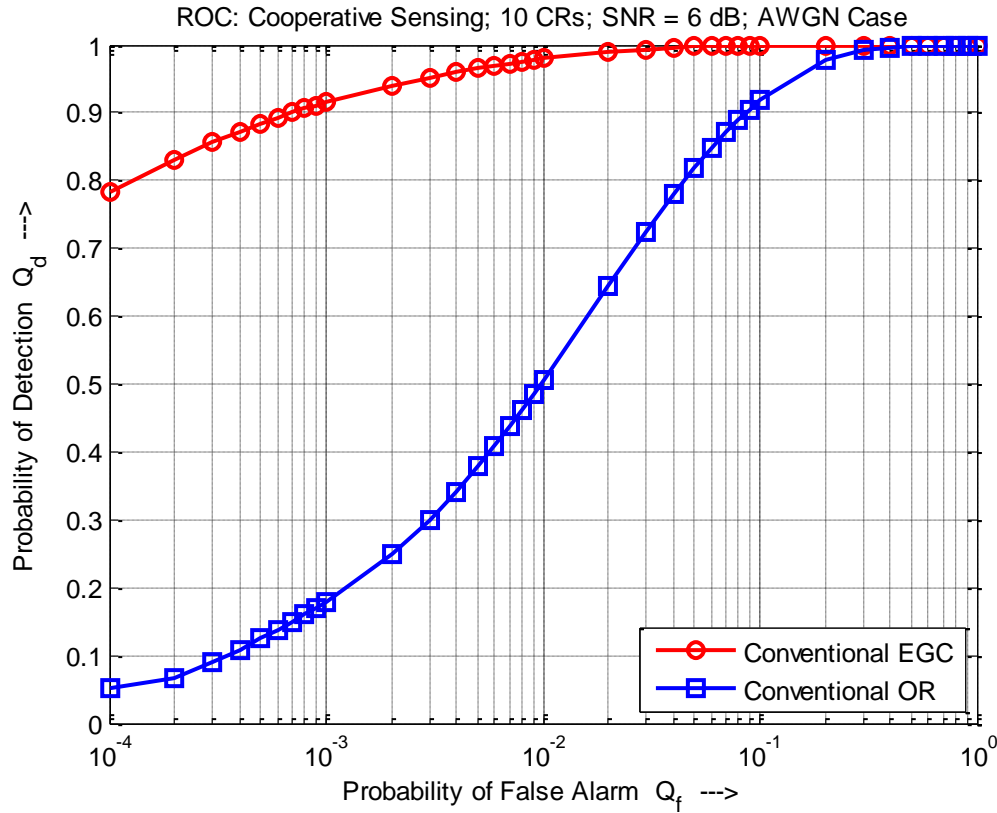


Figure 2.20: ROC – Comparison of Data and Decision Fusion (10 CRs, SNR = 6 dB, AWGN Case)

When the SNR for each CR is increased to 6 dB, and for $Q_f = 0.01$, the detection performance of the EGC scheme increases to 98%, whereas the detection performance of the OR-rule increases to only 51% (see Figure 2.20).

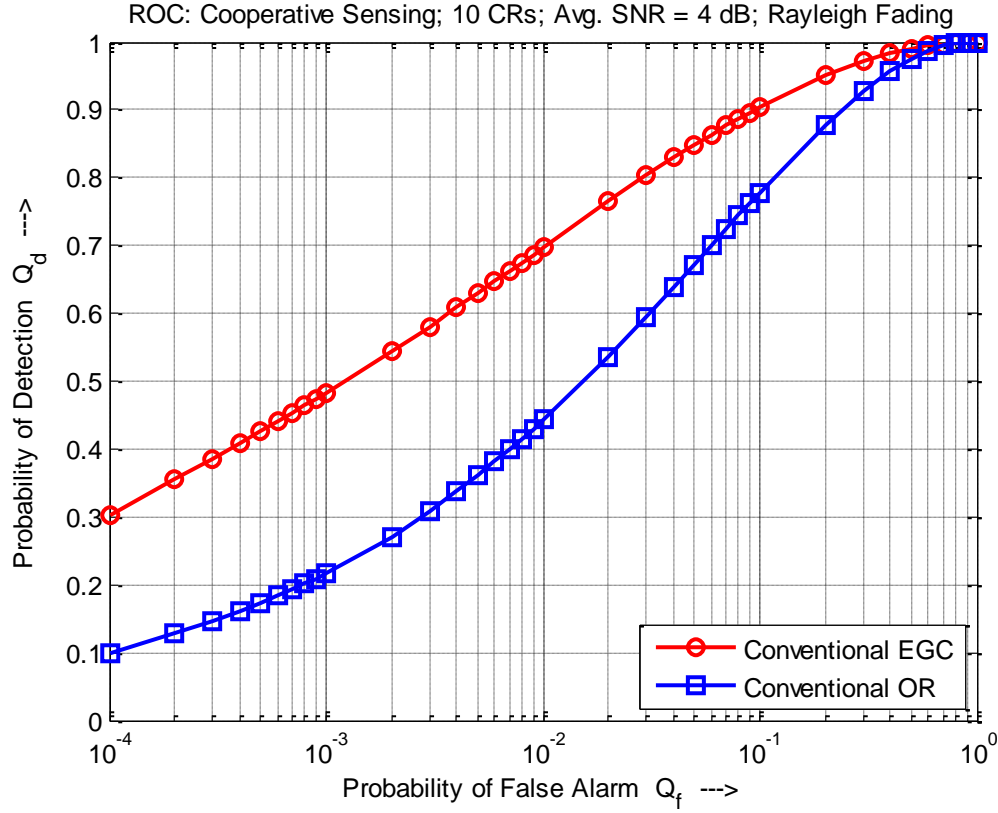


Figure 2.21: ROC – Comparison of Data and Decision Fusion (10 CRs, SNR = 4 dB, Rayleigh Fading)

In Figure 2.21, the OR-rule and the EGC scheme are compared under the case of Rayleigh fading. Here, the average received SNR $\gamma = 4 \text{ dB}$ for each cooperating CR. In this case, and for $Q_f = 0.01$, the EGC scheme achieves 70% detection performance compared to the OR-rule which achieves only 44% detection performance.

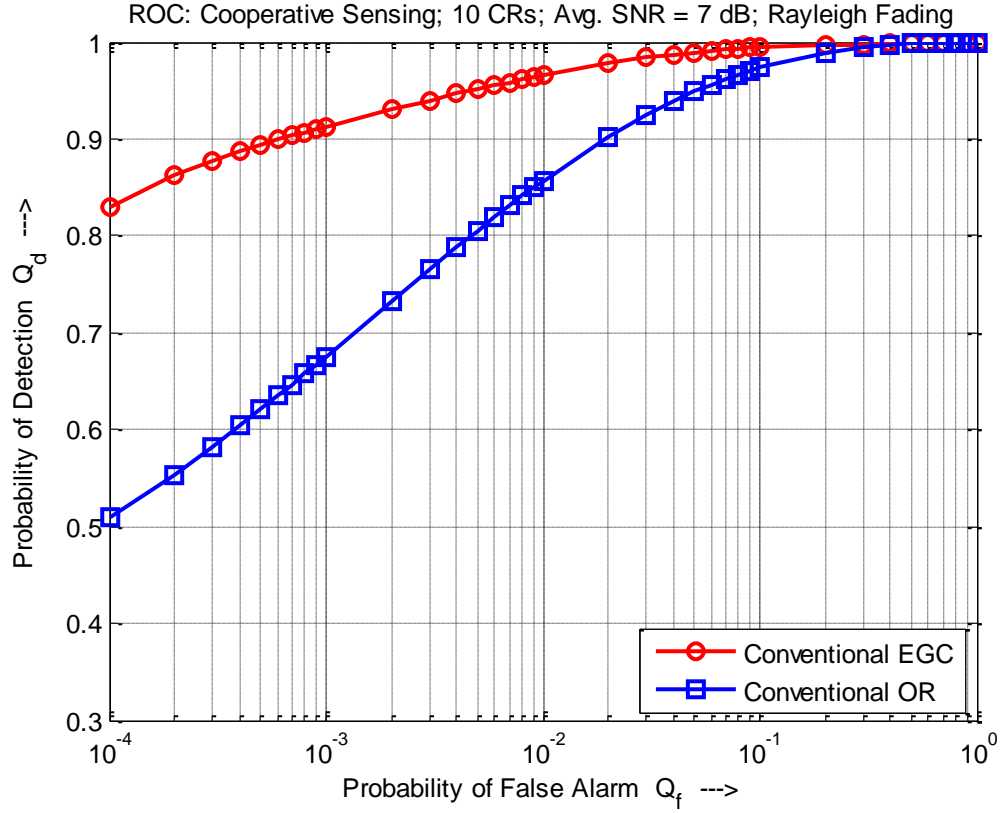


Figure 2.22: ROC – Comparison of Data and Decision Fusion (10 CRs, SNR = 7 dB, Rayleigh Fading)

In Figure 2.22, under Rayleigh fading, the average SNR is increased to $\gamma = 7 \text{ dB}$. For a given $Q_f = 0.01$, the detection performance of the EGC scheme increases to 96%, whereas the detection performance of the OR-rule increases to 85%.

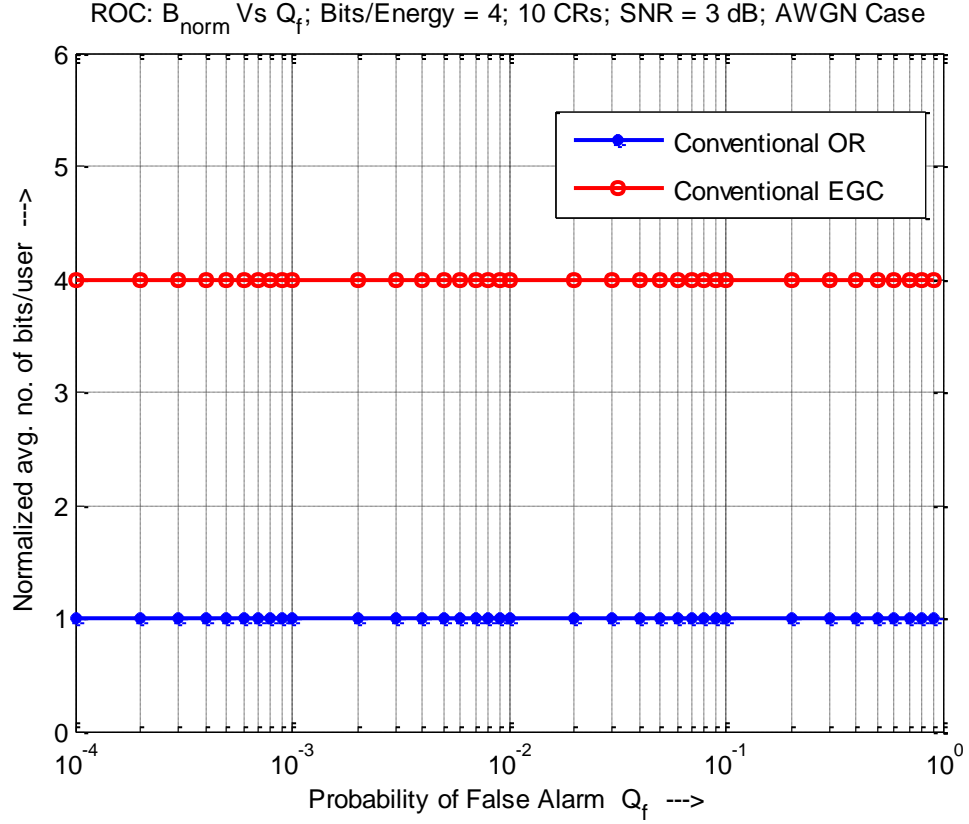


Figure 2.23: Normalized avg. number of bits/user \bar{B} vs. Q_f (10 CRs, SNR = 3 dB, AWGN Case)

The results show consistently that EGC outperforms the OR-rule, but it also requires more bits over the reporting channel to send the observed energy values. The normalized average number of bits/user for the OR-rule and the EGC scheme, under the case of AWGN are shown in Figure 2.23. For the OR-rule, each cooperating CR sends 1-bit binary decision to the fusion centre, whereas for the EGC scheme, each cooperating CR requires b bits to report the observed energy value. In Figure 2.23, we assume perfect reporting channels, and for the data fusion, each CR requires 4 bits to report the observed energy value.

2.6 Summary

This Chapter discussed the basics of spectrum sensing, various problems found in spectrum sensing, along with a detailed literature survey of different spectrum sensing techniques. The focus was mainly on energy detection using time domain approaches. Cooperative spectrum sensing using the decision fusion and the data fusion techniques was discussed at length. The simulation results show that cooperative spectrum sensing improves detection performance significantly compared to non-cooperative sensing. The decision fusion technique (OR-rule) was compared with the data fusion technique (EGC), and the results show that the EGC scheme outperforms the OR-rule, but significantly increases the communication burden over the reporting channel.

Among various data fusion techniques, the EGC scheme is computationally efficient, wherein the observed energy values from the cooperating CRs are simply combined without any sensing channel gain estimation. Hence, instead of blindly combining the energies, it will be attractive to develop a scheme that optimally combines the observed energy values from the cooperating CRs, hence, improving the detection performance. In the next chapter, data fusion technique using Particle Swarm Optimization is discussed.

CHAPTER 3

COOPERATIVE SPECTRUM SENSING USING PARTICLE SWARM OPTIMIZATION

3.1 Introduction

Cooperative Spectrum Sensing was discussed in detail in the previous chapter. The performance analysis of centralized spectrum sensing was carried out, and the results of OR-rule were compared to those of EGC. In a typical CRN, due to spatial diversity, it is highly unlikely for all the CRs to experience the same amount of fading/shadowing, and noise uncertainty. Hence, each cooperating CR will observe a different received SNR. While performing data combining for such a network, it is very important to smartly combine the observed energy values from the cooperating CRs. This can be achieved by weighing each CR differently, depending upon the amount of fading it undergoes and the corresponding noise variance. In other words, the observed energy value from the CR having a higher SNR should be assigned a higher weight value. Moreover, the weights for the CRs should be assigned such that the overall detection performance is optimized.

In this chapter, we discuss the use of Particle Swarm Optimization (PSO) technique, to optimally combine the observed energies from the cooperating CRs. We will then show that such an approach enhances detection performance. In the following section, the

Particle Swarm Optimization technique is discussed in detail, along with its advantages over the other optimization techniques.

3.2 Particle Swarm Optimization

Particle Swarm Optimization (PSO) is a robust, population based stochastic optimization technique, developed by James Kennedy and Russell Eberhart in [85]. PSO imitates the social behaviour of flocking in birds and animals [86]. PSO is initialized by a population of random candidate solutions, referred to as particles [87]. Each particle is treated as a point in N-dimensional space, which adjusts its flying according to its own flying experience as well as the flying experience of the other particles. PSO generally operates in real-valued spaces and almost exclusively in multi-dimensional metric, because the random candidate solutions are mutated to move towards the best solutions. Kennedy defined the concept of PSO as “A swarm is a population of interacting elements that is able to optimize some global objective through collaborative search of a space” [88]. As PSO is based on the movement and intelligence of swarms, the candidate solutions are referred to as swarm of particles. We can see the unique behaviour of PSO, wherein each particle, based on its past experience as well as its neighbours, moves towards the best solution. The performance of each particle is evaluated using the fitness (objective) function [89].

All the evolutionary algorithms, except PSO, incorporate survival of the fittest, wherein the particles with lower fitness are removed with higher probability [90]. PSO is different compared to other population based algorithms in a sense that “it does not resample the

population to produce the new ones, but it maintains a static population whose particles are adjusted in response to new discoveries about the space”, and hence, PSO has no selection, i.e. the particles never die [86]. The other major difference is that the evolutionary algorithms perform competitive search whereas the PSO algorithm performs cooperative search for the optimal solution. The PSO algorithm is more suitable because of its inherent advantages such as ease of hardware and software implementation, available guidelines to choose its parameters, ability to overcome the local minima problem, and faster convergence compared to other heuristic algorithms such as the Newton-based technique, Genetic Algorithms (GA), Differential Evolution, and Bacterial Foraging Algorithms.

The basic concept of PSO lies in accelerating each particle towards its personal best and the global best locations, with a random weighted acceleration at each time instant [85]. Hence, PSO doesn't depend on the set of initial population. In the PSO algorithm, each particle is governed by two parameters, its position in space and its velocity at a given time instant. In evolutionary algorithms, position of the particle is equivalent to the individual's genotype. The particles start at a random location with a random velocity vector [86]. The velocity and position of each particle are updated at every time step until a certain condition for termination is reached. The condition for termination can be fixed by specifying the maximum number of iterations, or a pre-defined number of iterations for which the global best solution doesn't change [89].

The position and velocity of each particle $i \{1 \leq i \leq S\}$, with dimension $d \{1 \leq d \leq D\}$, at any time instant t is represented by $\mathbf{x}_i^t = [x_{i1}^t, x_{i2}^t, \dots, x_{iD}^t]$ and $\mathbf{v}_i^t = [v_{i1}^t, v_{i2}^t, \dots, v_{iD}^t]$. At each time step, the velocity and position of a particle are updated as follows:

$$v_{id}^t = \omega v_{id}^{t-1} + c_1 \zeta (p_{id}^{t-1} - x_{id}^{t-1}) + c_2 \eta (p_{gd}^{t-1} - x_{id}^{t-1}) \quad (3.1)$$

$$x_{id}^t = x_{id}^{t-1} + v_{id}^t \quad (3.2)$$

Here, $\mathbf{p}_i^t = [p_{i1}^t, p_{i2}^t, \dots, p_{iD}^t]$ is the best solution of particle i at the time instant t and $\mathbf{p}_g^t = [p_{g1}^t, p_{g2}^t, \dots, p_{gD}^t]$ is the global best solution at time t , ω is the inertia weight, c_1 and c_2 are the acceleration coefficients (also called learning factors), and ζ and η are uniformly distributed random variables in the range $[0,1]$. These random variables formulate the stochastic behaviour in the algorithm. The local and global exploration of the swarm is balanced by the inertia weight, which keeps track of the previous velocity on the current velocity of each particle. The previous velocity v_{id}^{t-1} , keeps the particles on the right flight path, and stops them from suddenly changing direction. The cognition term $(p_{id}^{t-1} - x_{id}^{t-1})$, evaluates the particle's performance relative to the local best value and the social term $(p_{gd}^{t-1} - x_{id}^{t-1})$, evaluates the particle's performance relative to the global best value till that time instant. These terms significantly depend on the uniform random variables ζ and η . Such an adjustment towards the particle's local best and the global best is conceptually similar to the crossover operation (process of producing a child solution by combining the characteristics of more than one parent solutions [86]) in genetic algorithms [85]. The learning factors c_1 and c_2 control the local and global exploration of the particles respectively. The global best particle at the end of the iterations is the best possible solution for the entire swarm [89].

The generation of the random population set enhances the search space exploration and prevents the premature convergence to non-optimal points [87]. In relation to the effect of the number of particles S in the swarm, the results in [87] showed that increasing the

number of particles reduces the number of algorithm iterations. For practical applications, the fitness function evaluation, however, dominates the optimization cost. In Table 2 of [87], we note that, with very few particles used, the success rate is very low and there is a need for more iterations. On the other hand, using more particles increases the number fitness function evaluations. Intermediate number of particles provides the best results for most of the fitness functions. In [91], using the number of particles $S = 30$, the authors reported the best results. The proper selection of the algorithm parameters will guarantee global minimum in a lesser number of iterations, and hence, avoid premature convergence [92], [93].

The advantages of PSO over other traditional optimization techniques are summarized below [90], [92]:

- PSO is a derivative-free algorithm.
- Unlike Newton based optimization techniques, PSO uses payoff (objective function) information to guide the search in the problem space. Hence, PSO can easily deal with nonlinear, non-differential, and multi-modal objective functions. Moreover, this property relieves PSO of assumptions and approximations, which are often required by most optimization methods.
- Unlike GA and other heuristic algorithms, PSO has the flexibility to control the balance between the local and the global exploration of the search space. This unique feature of PSO overcomes the premature convergence problem and enhances the search capability.

- Unlike other optimization techniques, PSO is not dependent on a set of initial particles. Starting anywhere in the search space, the PSO algorithm ensures the convergence to the optimal solution.

The flowchart for the basic PSO algorithm is shown in Figure 3.1.

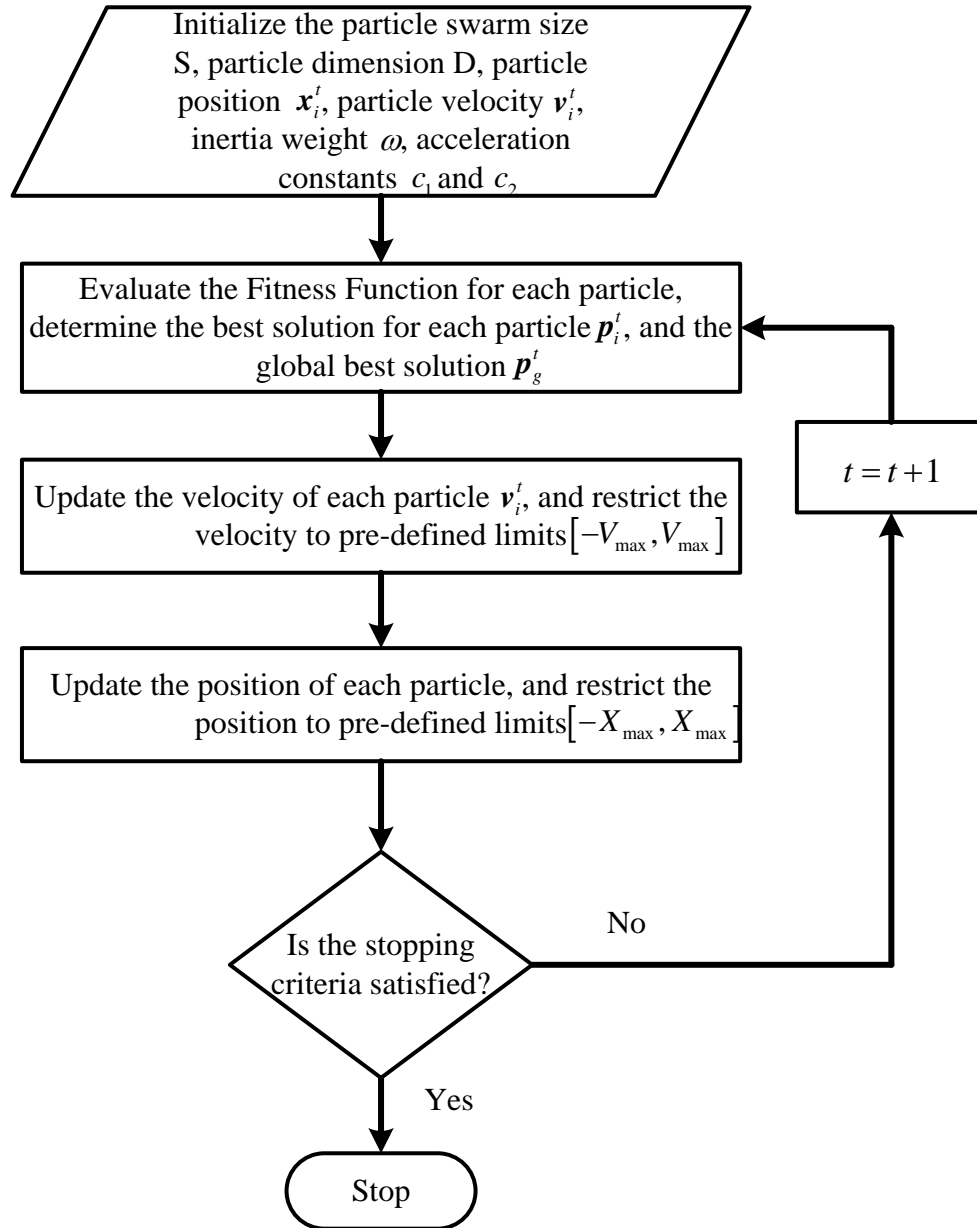


Figure 3.1: Flowchart for basic PSO algorithm

The particle's velocity and position is updated using the equations (3.1) and (3.2) respectively.

3.3 Applications of PSO in Communication Systems

PSO has been successfully used over a range of optimization problems given its very simple algorithm [85], high exploration ability, high convergence [89], and lower computational cost compared to other evolutionary algorithms. PSO is famous for its application in n-dimensional optimization problems [94]. Researchers have used PSO in a number of Wireless Sensor Network problems [95]:

- Optimal deployment of the sensor nodes, to achieve the desired coverage, connectivity, and energy efficiency, with minimum number of sensor nodes.
- Localization of sensor nodes with respect to the pre-determined location.
- Energy efficient clustering of sensor nodes for minimal communication with the fusion centre.
- Optimal data aggregation of large scale deployed sensor nodes.

Application of PSO for spectrum sensing has been very limited to date. In [94], the authors extended the use of PSO to the physical layer, and is applied for sub-carrier allocation in OFDMA. In PSO-aided sub-carrier allocation, with the knowledge that allocating only one sub-carrier with the best channel gain, increases data rate, the authors considered “the problem of optimizing the downlink sub-carrier allocation in OFDMA to minimize the transmit power with constraint on the user required bit rate” [94]. The results showed that PSO-aided sub-carrier allocation algorithm significantly reduces the

bit error rate compared to non-optimized sub-carrier allocation. PSO based sub-carrier allocation uses unsorted list of sub-carriers, and searches the solution space in a non-linear manner with a complexity of order $O(\log N)$, compared to conventional sort algorithms for OFDM/OFDMA [94].

The operational time frame of a CR is divided into two slots, sensing time and the data transmission time. Any CR has to perform spectrum sensing periodically to avoid interference with the primary user. Longer sensing time increases the detection performance, but reduces the time for data transmission, resulting in a less throughput of a CR. Researchers, in [89], study the trade-off between sensing time and achievable throughput of a CR. They proposed to use PSO for designing the sensing time slot duration, to maximize the achievable throughput for a given frame time. Initially, the sensing time was set as 10 ms, for a frame duration of 100 ms. Using PSO, the results show that 80% reduction in sensing time (reduced to 2 ms), and 8.89% higher throughput can be achieved. As the sensing time is reduced, the amount of energy consumed on sensing decreases significantly.

3.3.1 Conventional Data Fusion using PSO

In order to accurately detect a weak primary user signal, and overcome the effects of fading/shadowing, the authors in [96], proposed an “*optimal linear cooperation framework*”. Under the proposed framework, the local statistics from each CR are linearly combined for sensing the target frequency band. The sensing problem is formulated as a nonlinear optimization problem, wherein the aim is to maximize the

probability of detection. In order to reduce the computation complexity and obtain an optimal solution for a general CRN, the authors proposed “a heuristic method, where they optimized a *modified deflection coefficient (MDC)* that characterizes the PDF of global test statistic at the fusion centre”. MDC is the generalized method to find the weight vector for combining the observed energy values from the cooperating CRs, which reduces computation complexity, at the expense of a small amount of performance loss [96].

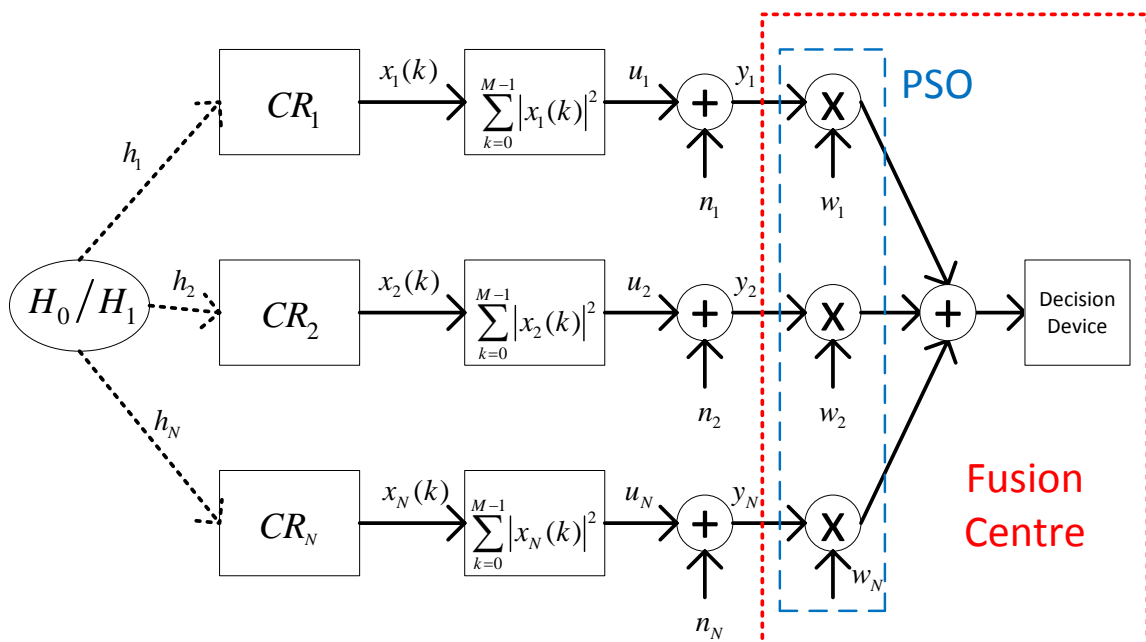


Figure 3.2: Cooperative Spectrum Sensing Framework using PSO

The authors, in [97], used the framework proposed in [96], to employ PSO technique for finding the optimal weight vector (see Figure 3.2), which would maximize the detection performance. The results showed that PSO based cooperative sensing yields a higher detection performance compared to MDC based methods. The linear cooperation framework shown in Figure 3.2 will now be discussed in more detail:

The received signal $x_l(k)$, at the l^{th} CR is given as by:

$$x_l(k) = \begin{cases} n_l(k), & H_0 \\ h_l s(k) + n_l(k), & H_1 \end{cases} \quad \text{for } l = 1, 2, \dots, N \quad (3.3)$$

In the above equation, $s(k)$ represents the transmitted primary user signal, h_l is the channel gain, $n_l(k)$ is the additive white Gaussian noise with zero mean and variance σ_l^2 .

Each cooperating CR evaluates the test statistic $u_l = \sum_{k=0}^{M-1} |x_l(k)|^2$ over a detection interval of M samples. Since this test statistic is the sum of squares of M Gaussian random variables, it follows the distribution given by:

$$\frac{u_l}{\sigma_l^2} \sim \begin{cases} \chi_M^2, & H_0 \\ \chi_M^2(2\gamma_l), & H_1 \end{cases} \quad (3.4)$$

Here, γ_l is the local SNR at the l^{th} CR and $E_s = \sum_{k=0}^{M-1} |s(k)|^2$ represents the transmitted signal energy.

The test statistic reported by each CR to the fusion centre is $y_l = u_l + n_l$, where the control channel noise n_l is a spatially uncorrelated Gaussian variable with zero mean and variance δ_l^2 . The fusion centre calculates the global decision statistic linearly as follows:

$$y_{FC} = \sum_{l=1}^N y_l w_l = \mathbf{w}^T \mathbf{y} \quad (3.5)$$

In the above equation, $\mathbf{w} = [w_1, w_2, \dots, w_N]^T$ is the weight vector assigned by PSO, and $\mathbf{y} = [y_1, y_2, \dots, y_N]$ is the received test statistic vector.

For the framework shown in Figure 3.2, the probabilities of detection and false alarm are derived as [96]:

$$P_{d,PSO} = Q \left(\frac{Q^{-1}(P_f) \sqrt{\mathbf{w}^T \mathbf{A} \mathbf{w}} - E_s \mathbf{h}^T \mathbf{w}}{\sqrt{\mathbf{w}^T \mathbf{B} \mathbf{w}}} \right) \quad (3.6)$$

$$P_f = Q \left(\frac{\lambda - M \boldsymbol{\sigma}^T \mathbf{w}}{\sqrt{\mathbf{w}^T \mathbf{A} \mathbf{w}}} \right) \quad (3.7)$$

For a given target probability of false alarm, the threshold value λ is given by:

$$\lambda = M \boldsymbol{\sigma}^T \mathbf{w} + Q^{-1}(P_f) \sqrt{\mathbf{w}^T \mathbf{A} \mathbf{w}} \quad (3.8)$$

Here, \mathbf{w} is the weight vector and E_s is the transmitted signal energy over M samples. The terms $\mathbf{w}^T \mathbf{A} \mathbf{w}$ and $\mathbf{w}^T \mathbf{B} \mathbf{w}$ are the received global test statistic variances under hypothesis H_0 and H_1 respectively. The expression for matrices \mathbf{A} and \mathbf{B} are given as [96]:

$$\mathbf{A} = 2N \begin{bmatrix} \sigma_1^4 & \cdots & 0 \\ \vdots & \ddots & \vdots \\ 0 & \cdots & \sigma_{N-K}^4 \end{bmatrix} + \begin{bmatrix} \delta_1^2 & \cdots & 0 \\ \vdots & \ddots & \vdots \\ 0 & \cdots & \delta_{N-K}^2 \end{bmatrix} \quad (3.9)$$

$$\begin{aligned} \mathbf{B} = 2N \begin{bmatrix} \sigma_1^4 & \cdots & 0 \\ \vdots & \ddots & \vdots \\ 0 & \cdots & \sigma_{N-K}^4 \end{bmatrix} + \begin{bmatrix} \delta_1^2 & \cdots & 0 \\ \vdots & \ddots & \vdots \\ 0 & \cdots & \delta_{N-K}^2 \end{bmatrix} \\ + 4E_s \begin{bmatrix} h_1^2 & \cdots & 0 \\ \vdots & \ddots & \vdots \\ 0 & \cdots & h_{N-K}^2 \end{bmatrix} \begin{bmatrix} \sigma_1^2 & \cdots & 0 \\ \vdots & \ddots & \vdots \\ 0 & \cdots & \sigma_{N-K}^2 \end{bmatrix} \end{aligned} \quad (3.10)$$

In this framework, $\mathbf{h} = [|h_1|^2, |h_2|^2, \dots, |h_N|^2]^T$ represents the squared amplitude channel gains for all the cooperating CRs, $\boldsymbol{\sigma} = [|\sigma_1|^2, |\sigma_2|^2, \dots, |\sigma_N|^2]^T$ are the sensing channel noise variances for all the CRs and $\boldsymbol{\delta} = [|\delta_1|^2, |\delta_2|^2, \dots, |\delta_N|^2]^T$ are the reporting channel noise variances. Matrices \mathbf{A} and \mathbf{B} are diagonal, as we consider that the received test statistics $\{y_l\}$, at the fusion centre, are independent. If the received test statistics $\{y_l\}$, are correlated, then the covariance matrices \mathbf{A} and \mathbf{B} will be non-diagonal.

Under this framework, the nonlinear optimization problem becomes an optimization of weight vector \mathbf{w} , to maximize the probability of detection. From equation (3.6), since the Q -function is a monotonically decreasing function, maximizing P_d is same as minimizing the following expression [96]:

$$f(\mathbf{w}) = \frac{Q^{-1}(P_f)\sqrt{\mathbf{w}^T \mathbf{A} \mathbf{w}} - E_s \mathbf{h}^T \mathbf{w}}{\sqrt{\mathbf{w}^T \mathbf{B} \mathbf{w}}} \quad (3.11)$$

If \mathbf{w} is the optimal weight vector which minimizes $f(\mathbf{w})$, then its scaled version $\alpha \mathbf{w}$, where α is a positive real number, is also an optimal vector which minimizes $f(\mathbf{w})$. Hence, to limit the number of optimal solutions, extra constraints are introduced to reduce the optimization problem as:

$$\begin{aligned} \min_{\mathbf{w}} f(\mathbf{w}) \text{ st. } & \sum_{l=1}^N w_l = 1, \quad 0 \leq w_l \leq 1, \\ & \text{for } l = 1, 2, \dots, N \end{aligned} \quad (3.12)$$

Applying the above mentioned constraint in PSO is helpful as it reduces the search space compared to the unconstrained problem. Under this framework, the dimension of the weight vector \mathbf{w} is equal to the number of cooperative CRs, N . Hence, for example, if we assume that each CR has the same received SNR, sensing channel gain and sensing noise, the weight value assigned to each CR will be $w_l = 1/N$ (as per equation (3.12)).

To calculate the system parameter matrices \mathbf{A} and \mathbf{B} at the fusion centre, the authors in [96] added some assumptions. Instead of using the channel gains at each CR, the authors directly used the local SNR at each CR. With this assumption, that channel coherence time is large enough, the local SNR at each CR γ_l can be estimated. Without this

assumption, the amplitude and phase of the channel would vary considerably. Moreover, assuming that each cooperating CR knows the power transmitted by the primary user, the exact channel gains $|h_l|^2$ can also be estimated. Hence, only apriori knowledge of local noise variances σ_l^2 at each CR is required at the fusion centre. Such information is obtainable in some circumstances. For instance, if the target spectrum is in TV bands, secondary users can possibly have a priori knowledge about the primary signal power, as most TV stations transmit at fixed power levels [96].

In this thesis, to calculate the optimal weight vector \mathbf{w} at the fusion centre, each CR is required to report its local noise variance σ_l^2 and the sensing channel gain $|h_l|^2$. It is assumed that local sensing noises at each CR are not time varying, hence, each CR sends its local noise level once to the fusion centre. For the AWGN case, the sensing channel gains remain constant, and without loss of generality, they are assumed to be unity. For Rayleigh fading, as the sensing channel gains follow the Rayleigh distribution, all the CRs report their estimated sensing channel gains along with the observed energy values during each sensing cycle. Hence, the total information reported by each CR under AWGN includes the local noise level initially, and then, only its observed energy value for every sensing cycle. Under Rayleigh fading, each CR reports the local noise level initially, and then, its observed energy value and the sensing channel gain for every sensing cycle.

The PSO algorithm for finding the optimal weight vector is implemented as follows [97]:

1. Set the number of particles S , dimensions of each particle N , inertia ω , learning factors c_1 and c_2 , maximum velocity V_{max} and maximum time iterations t . For

time $t = 1$, initialize each particle x_{id}^t randomly in the range $[0,1]$, and a random velocity v_{id}^t in the range $[-V_{max}, V_{max}]$.

2. Normalize each particle x_{id}^t as $x_{id}^t / \sum_{d=1}^D x_{id}^t$ (to satisfy the constraint given in equation (3.12)).
3. Assess the fitness value $f(\mathbf{x}_i^t)$ (see equation (3.11)) of each particle, set the best position of each particle $\mathbf{p}_i^t = [x_{i1}^t, x_{i2}^t, \dots, x_{iD}^t]$. The particle with the least fitness value is set as the global best particle $\mathbf{p}_g^t = [x_{g1}^t, x_{g2}^t, \dots, x_{gD}^t]$, where g is the particle index with the least fitness value.
4. At time $t = t + 1$, update the velocity v_{id}^t using equation (3.1). If the updated velocity is less than $-V_{max}$, set it to $-V_{max}$, and if it exceeds V_{max} , set it to V_{max} .
5. Update the position of each particle x_{id}^t using equation (3.2), and normalize it as shown in step 2.
6. Assess the fitness value $f(\mathbf{x}_i^t)$ (see equation (3.11)) of each particle. If each particle's fitness value is less than its previous fitness value \mathbf{p}_i^{t-1} , update the current particle position as its best position $\mathbf{p}_i^t = [x_{i1}^t, x_{i2}^t, \dots, x_{iD}^t]$, or else keep the particle's previous best position $\mathbf{p}_i^t = \mathbf{p}_i^{t-1}$.
7. Set the particle with the least fitness value as the current global best particle $\mathbf{p}_g^t = [x_{g1}^t, x_{g2}^t, \dots, x_{gD}^t]$. If the fitness value of current global best particle \mathbf{p}_g^t is less than the fitness value of previous global best particle \mathbf{p}_g^{t-1} , update the new global best particle $\mathbf{p}_g^t = [x_{g1}^t, x_{g2}^t, \dots, x_{gD}^t]$, or else keep the previous global best particle $\mathbf{p}_g^t = \mathbf{p}_g^{t-1}$.

8. If time t reaches the maximum iteration value, terminate the algorithm, or else go to step 4.

The global best particle \mathbf{p}_g^t at end of algorithm is the best solution of PSO, which is our optimal weight vector. The received energy from each CR is multiplied by its corresponding weight value calculated by PSO at the fusion centre.

3.4 Simulation Results

In this section, a detailed performance analysis is carried out for cooperative spectrum sensing technique under the framework discussed in the previous section. The time-bandwidth product is $u = TW = 5$, and the number of received signal samples is $M = 2u = 10$. For PSO, the intermediate number of particles ($S = 30$) was found to provide the best results for most objective functions [87]. The inertia weight $\omega = 1$ fully controls the impact of the previous velocities on the current velocity. In order to achieve uniformity of local and global explorations of the search space, the values of learning factors c_1 and c_2 are kept same (i.e. $c_1 = c_2 = 2$). For particle size of $S = 30$, the PSO algorithm for this framework converges before 50 iterations. Hence, the maximum number of iterations is set as $t = 50$.

The performance analysis is carried for different average SNR values under the case of AWGN and Rayleigh fading environments. For each case, the sensing noises are randomly generated, to get the desired average received SNR for each cooperating CR. Due to the spatial diversity in the CRN, the received SNR at each cooperating CR is different, depending on the amount of fading/shadowing it undergoes. For each case, different SNR values are randomly selected for each CR, to get the desired cooperative gain. These values eventually influence the detection performance. For simplicity, the reporting channels are assumed to be perfect, i.e. $\delta = 0$ in equations (3.9) and (3.10).

Here, 10 cooperating CRs are used as the benchmark to evaluate the performance of the algorithm, as it is shown in the literature that the use of 10 cooperating CRs sufficiently provides a high detection performance as well as keeps the falls alarm rate very low. The

performance of data fusion using PSO (called Conventional PSO) is compared with the conventional data fusion using EGC.

In Figure 3.3, performance evaluation is carried out under the case of AWGN, with 10 cooperating CRs, for average SNR of 4 dB (each CR with a different locally observed SNR value).

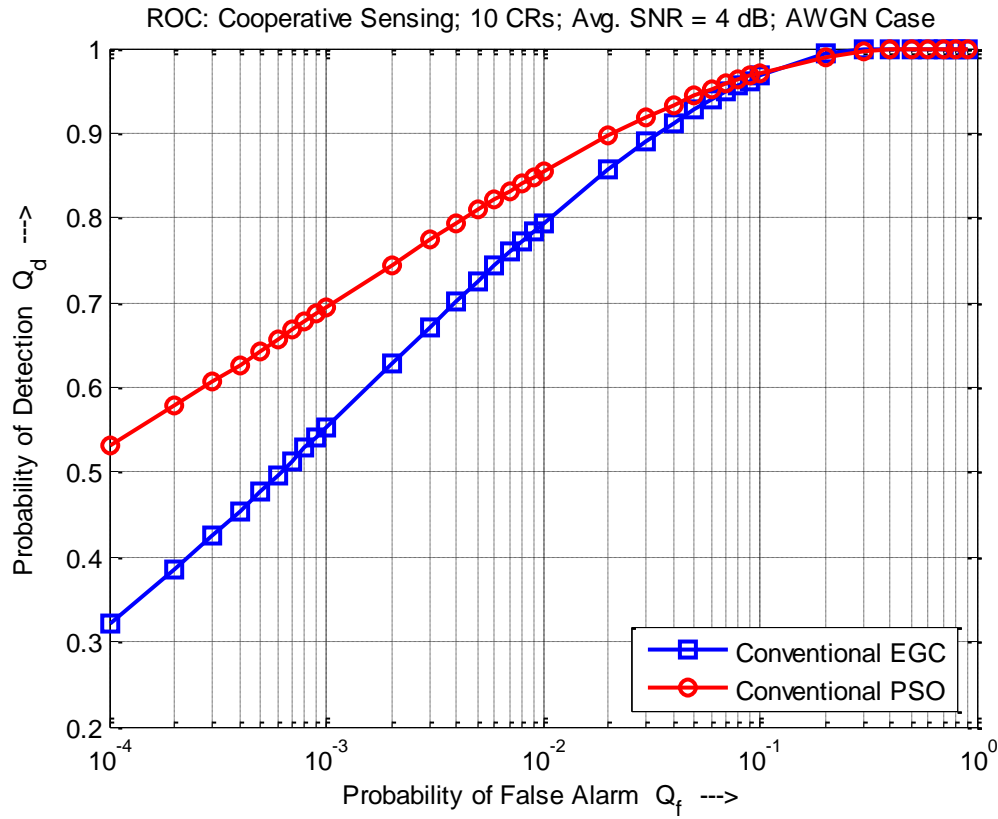


Figure 3.3: ROC – Data Fusion, EGC versus PSO (10 CRs, Avg. SNR = 4 dB, AWGN Case)

For $Q_f = 10^{-3}$, the conventional EGC achieves 55% detection performance, while the conventional PSO achieves 69% detection performance (see Figure 3.3).

Figure 3.4 shows the performance under the case of AWGN for average SNR of 6 dB, with 10 cooperating CRs.

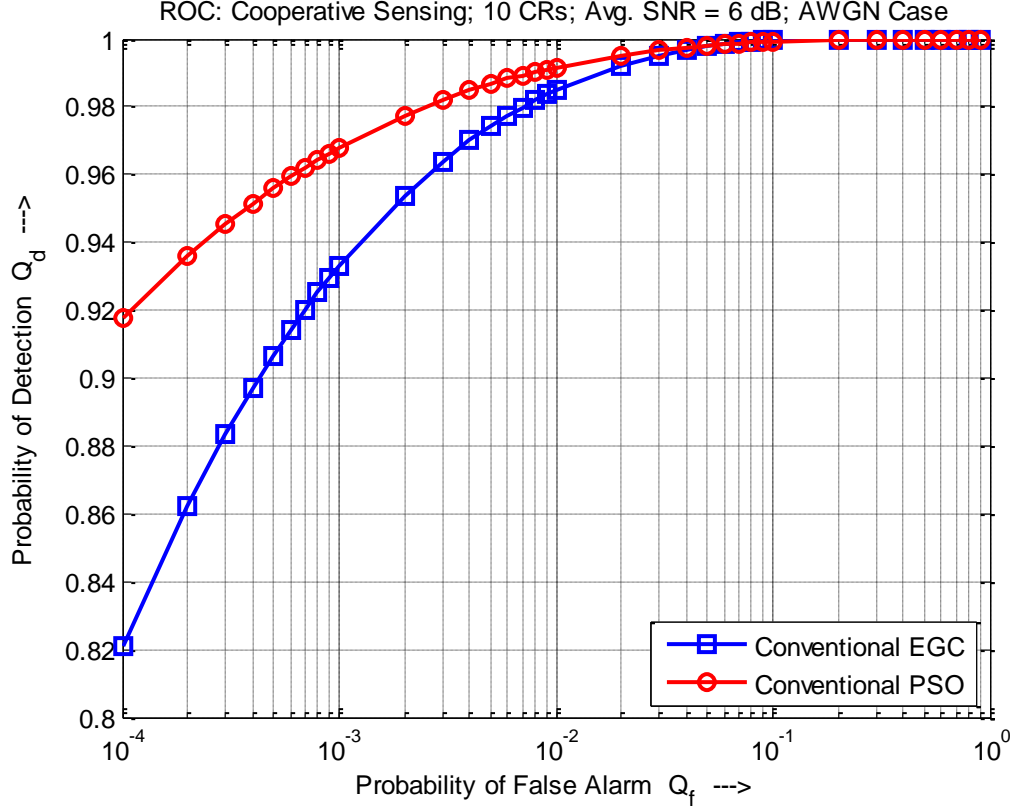


Figure 3.4: ROC – Data Fusion, EGC versus PSO (10 CRs, Avg. SNR = 6 dB, AWGN Case)

In the following, a representative scenario, with locally observed SNR values as $\mathbf{SNR}_{dB} = [7.5 \ 6.5 \ 6.0 \ 7.0 \ 5.5 \ 5.0 \ 8.0 \ 4.5 \ 6.0 \ 4.0]$ and corresponding sensing noise variances $\sigma = [1.77 \ 2.24 \ 2.52 \ 1.99 \ 2.82 \ 3.16 \ 1.58 \ 3.55 \ 2.52 \ 3.98]$ is analyzed. In Figure 3.4, for $Q_f = 10^{-3}$, the conventional EGC achieves 93% detection performance, while the conventional PSO achieves 97% detection performance. Hence, we observe that for lower average SNR values, the performance improvement of conventional PSO is higher. Here, PSO calculates the optimum weight vector for combining the received energies, and to optimize the detection performance. The CR with higher received SNR is

assigned a higher weight value by the PSO. In, Figure 3.4, for the given received SNR values, $\mathbf{w} = [0.15 \ 0.11 \ 0.09 \ 0.13 \ 0.08 \ 0.07 \ 0.17 \ 0.06 \ 0.10 \ 0.05]$ is the resulting weight vector found using PSO. In both cases above, the conventional PSO scheme outperforms the conventional EGC scheme, where the fusion centre blindly combines the received energies from the cooperating CRs.

We also carried an experiment considering Rayleigh fading (see Figure 3.5) for an average SNR of 5 dB, with 10 cooperating CRs.

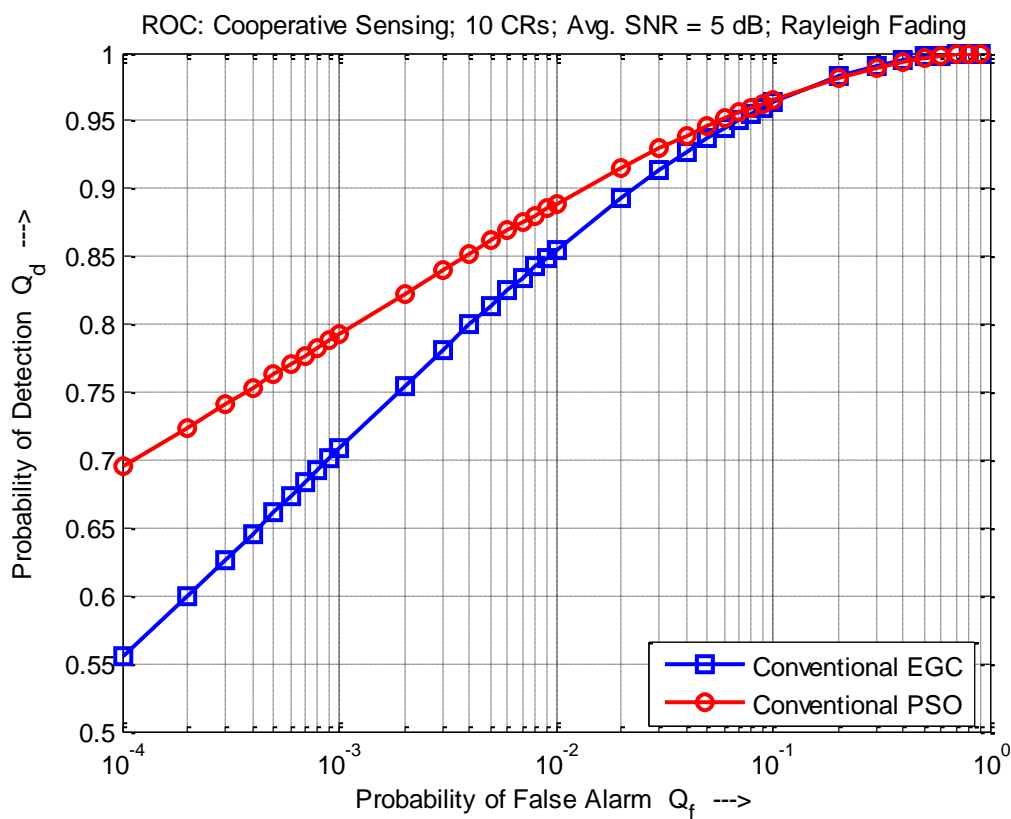


Figure 3.5: ROC – Data Fusion, EGC versus PSO (10 CRs, Avg. SNR = 5 dB, Rayleigh Fading)

In Figure 3.5, a representative scenario with locally observed average SNR values as $\mathbf{SNR}_{dB} = [7 \ 5 \ 6 \ 4 \ 2 \ 8 \ 6 \ 5 \ 4 \ 3]$ is analyzed. The sensing channel gains follow the

Rayleigh distribution to get the desired average received SNR for each cooperating CR. Here, for $Q_f = 10^{-3}$, the conventional PSO achieves 79% detection performance compared to the conventional EGC which achieves 71% detection performance.

Figure 3.6 shows the performance under Rayleigh fading for average SNR of 7 dB, with 10 cooperating CRs.

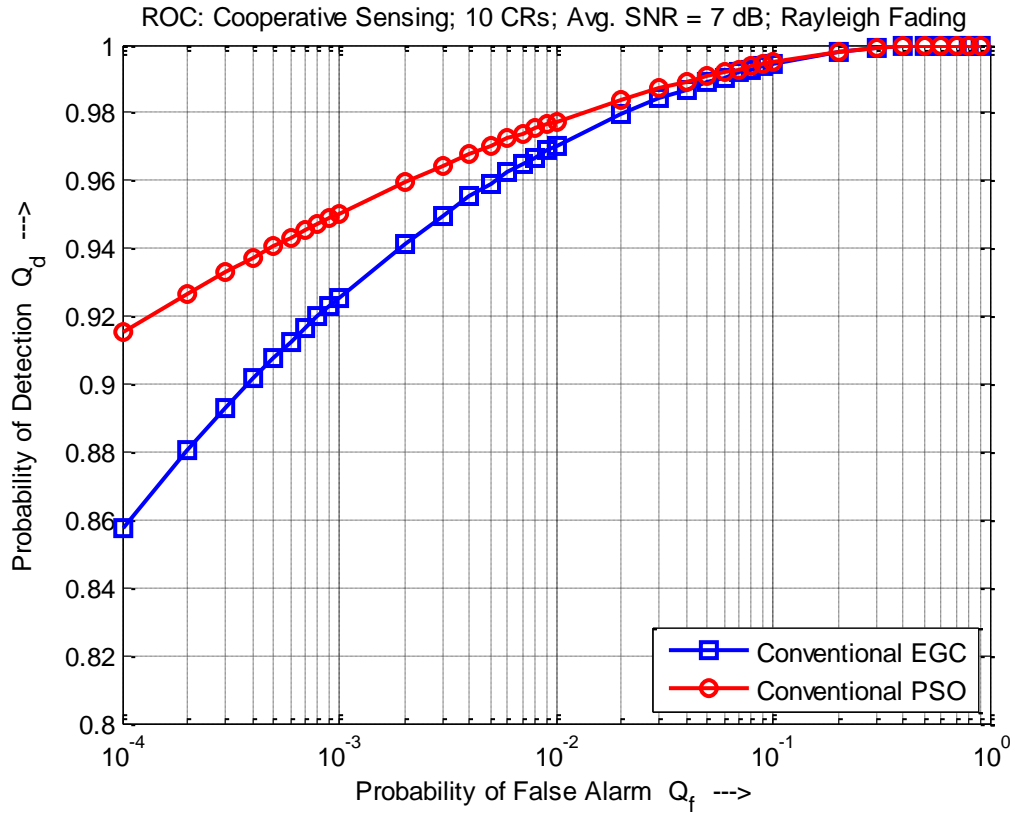


Figure 3.6: ROC – Data Fusion, EGC versus PSO (10 CRs, Avg. SNR = 7 dB, Rayleigh Fading)

In Figure 3.6, for $Q_f = 10^{-3}$, the conventional PSO achieves 94% detection performance compared to the conventional EGC which achieves 91% detection performance. Under Rayleigh fading, the sensing channel gains are reported to the fusion centre to calculate

the optimal weight vector. Again, the conventional PSO data fusion scheme outperforms the conventional EGC scheme.

3.5 Summary

In this chapter, the optimal linear cooperation framework proposed in [96] was discussed, wherein the spectrum sensing problem is formulated as a nonlinear optimization problem. In [97], using this framework, PSO is used at the fusion centre to calculate the optimum weight vector for combining the received energies from the cooperating CRs. The weight value assigned to the received energy from a particular CR determines its contribution to the final decision. The weighted energies are combined at the fusion centre to reach the final decision. CRs with high local SNRs are assigned larger weight values. Similarly, CRs with low local SNR values or experiencing deep fading/shadowing, are assigned smaller weight values, hence, their contribution to the final decision is weaker.

The conventional PSO technique optimizes the detection probability compared to the conventional EGC technique, which blindly combines the energies from cooperating CRs. Under the case of AWGN, conventional PSO and conventional EGC both have similar communication overhead. Under the case of Rayleigh fading, conventional PSO technique requires that each CR also reports its sensing channel gain, which is required by PSO to find the optimal weight vector at the fusion centre. On the other hand, in the conventional EGC scheme, sensing channel gains are not required at the fusion centre. Hence, under Rayleigh fading, conventional PSO technique achieves a higher detection performance, with increased communication burden compared to the conventional EGC

scheme. The computational complexity of the PSO depends on the swarm size and the number of iterations. A large number of iterations results in unnecessary added computations, hence increasing delay.

While PSO has been shown to optimally combine energies, it requires similar number of bits as EGC (same as EGC for AWGN, and more number of bits than EGC for the practical case of fading under Rayleigh). Next, the discussion will be to reduce the number of bits required to transmit the sensing information to the fusion centre. It will be shown that there is no need to transmit all energies, while some CRs effectively transmit their energies, some others can only transmit their decisions.

CHAPTER 4

A NEW HYBRID DOUBLE THRESHOLD COOPERATIVE

SPECTRUM SENSING ALGORITHM USING SWARM

INTELLIGENCE

4.1 Introduction

In this chapter, a new hybrid approach for cooperative spectrum sensing in CROWN is proposed, wherein the unreliable CRs are identified, and the reliable and the unreliable CRs are treated separately. Generally, using a single threshold approach, due to noise uncertainties and other environmental effects, the observed energy values from certain CRs are very close to the prefixed threshold value. Decisions from such CRs are unreliable, hence, such CRs can be considered as *Fuzzy* (unreliable). In the proposed approach, a double threshold energy detector is used at each cooperating CR to check its reliability. The reliable CRs report their local binary decision to the fusion centre, while the unreliable CRs report their observed energy values. The fusion centre uses Particle Swarm Optimization to optimally combine the reported energy values from the Fuzzy CRs. Since the hard and soft decisions are fused at the fusion centre, the proposed hybrid technique is termed as the Hybrid PSO-OR technique. It is shown that the proposed approach considerably reduces the number of reporting bits at the expense of a negligible

performance loss compared to the Conventional PSO technique, discussed in the previous chapter. The proposed algorithm is compared to other hybrid approaches, which combines energies from Fuzzy CRs using EGC (Hybrid EGC-OR), and also with the conventional OR rule. The expressions for the cooperative probabilities of detection and false alarm, and expression for the normalized average number of bits over the reporting channel are derived for the proposed algorithm.

4.2 The System Model

The system model uses a centralized cooperative spectrum sensing scheme with N CR users. Each cooperating CR uses a double threshold energy detector [59] as shown in Figure 4.1.

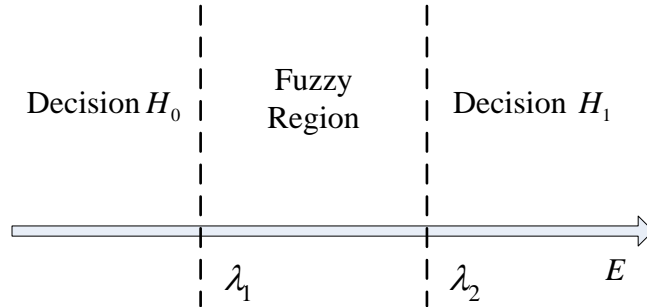


Figure 4.1: Double Threshold Energy Detector

The reliability of each cooperating CR is measured using two thresholds: λ_1 and λ_2 . The observed energy value of each CR falls in one of the three possible regions shown in Figure 4.1. If the observed energy value E_i , for i^{th} CR, is greater than the threshold value λ_2 , decision H_1 is sent to the fusion centre. If E_i is less than or equal to the threshold value λ_1 , decision H_0 is sent to the fusion centre. The region between the two

thresholds is termed as the Fuzzy region. If the observed energy value from any CR falls in the Fuzzy region, it is considered unreliable to send its local decision, and hence, it directly reports its observed energy value to the fusion centre. The proposed framework is shown in Figure 4.2, wherein PSO is used at the fusion centre to optimally combine the received energy values from all the Fuzzy CRs. The fusion centre finally combines the hard and the soft decisions, to give a final decision on whether the primary user is present or absent.

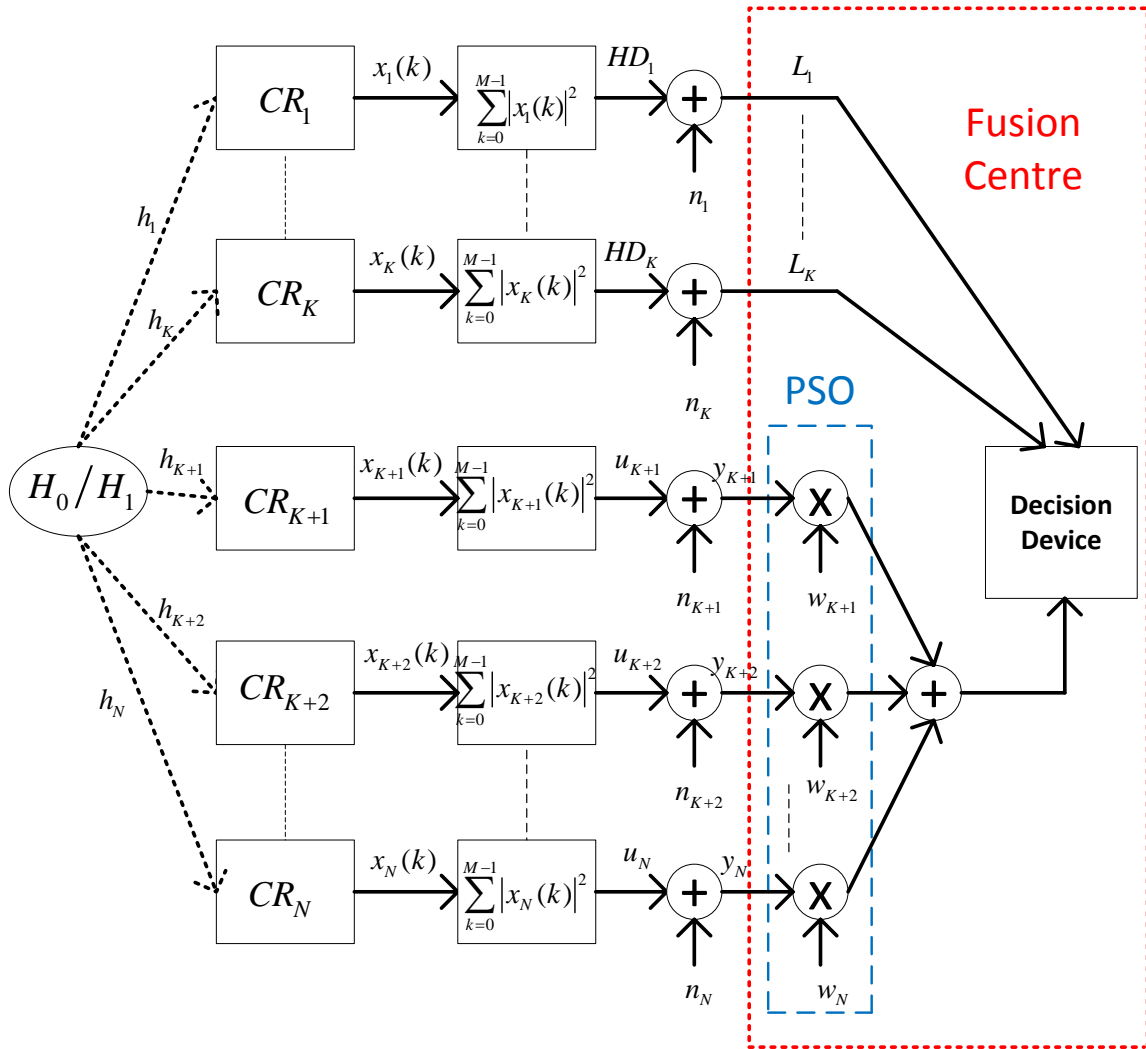


Figure 4.2: Framework for the proposed Hybrid PSO-OR algorithm

The cooperative sensing framework discussed in the previous chapter (see Figure 3.2) is modified to get the proposed Hybrid PSO-OR framework as evident from Figure 4.2.

The proposed hybrid cooperative sensing algorithm is implemented as follows:

1. Each of the cooperating CRs, for $i = 1, 2, \dots, N$, performs independent local spectrum sensing over the target frequency band to sense the primary transmitter energy value E_i . Based on the observed energy value E_i , each CR reports its local decision (H_0 or H_1) or the observed energy value to the fusion centre (FC). Thus, the information received at the fusion centre is:

$$FC_i = \begin{cases} E_i, & \lambda_1 < E_i \leq \lambda_2 \\ L_i, & \text{otherwise} \end{cases}, \quad \text{for } i = 1, 2, \dots, N \quad (4.1)$$

In the above equation, the hard decision L_i is either a binary 1 (if local decision is H_1) or a binary 0 (if local decision is H_0), given by:

$$L_i = \begin{cases} 0, & 0 \leq E_i \leq \lambda_1 \\ 1, & E_i > \lambda_2 \end{cases} \quad (4.2)$$

2. It is assumed that among the N cooperating CRs, the fusion centre receives K hard decisions and $(N - K)$ observed energy values. The fusion centre first makes a soft decision based on the received energy values. PSO is employed at the fusion centre [97], to assign an optimal weight vector \mathbf{w} with $(N - K)$ dimensions, for optimally combining the $(N - K)$ received energies. The soft decision is given as:

$$D = \begin{cases} 0, & 0 \leq \sum_{i=1}^{N-K} w_i E_i \leq \lambda \\ 1, & \sum_{i=1}^{N-K} w_i E_i > \lambda \end{cases} \quad (4.3)$$

Here, the threshold value λ is the threshold for data fusion using PSO, and is calculated using equation (3.8) discussed in Section 3.3.1.

3. The fusion centre makes a final decision in the following manner:

$$F = \begin{cases} 1, & D + \sum_{i=1}^K L_i \geq 1 \\ 0, & \text{otherwise} \end{cases} \quad (4.4)$$

Thus, only when the combination of all the hard decisions and the soft decision is zero, the fusion centre decides whether the target frequency band is vacant or not and ready for opportunistic access.

4.3 Performance Analysis of the Proposed Algorithm

In this section, the expressions for the cooperative probability of detection (Q_d), probability of missed detection (Q_m), and probability of false alarm (Q_f) are derived. The probability that a particular CR's observed energy value falls in the Fuzzy region, under hypothesis H_0 and H_1 respectively, is defined as follows:

$$\Delta_{0,i} = P(\lambda_1 < E_i \leq \lambda_2 | H_0) = F(\lambda_2) - F(\lambda_1) \quad (4.5)$$

$$\Delta_{1,i} = P(\lambda_1 < E_i \leq \lambda_2 | H_1) = G(\lambda_2) - G(\lambda_1) \quad (4.6)$$

The functions $F(\cdot)$ and $G(\cdot)$ are the CDFs of the observed energy value E , under hypothesis H_0 and H_1 respectively, and are defined as:

$$F(\lambda_2) = P(E < \lambda_2 | H_0) \quad (4.7)$$

$$G(\lambda_2) = P(E < \lambda_2 | H_1) \quad (4.8)$$

For a typical CR with local SNR γ , and local sensing noise variance σ_i^2 , the probability of detection ($P_{d,i}$), the probability of missed detection ($P_{m,i}$), and the probability of false alarm ($P_{f,i}$) are defined as follows:

- a. Under AWGN, the probability of detection is given as:

$$P_{d,i} = P(E_i > \lambda_2 | H_1) = Q_u\left(\sqrt{2\gamma}, \sqrt{\frac{\lambda_2}{2\sigma_i^2}}\right) \quad (4.9)$$

- b. Under Rayleigh fading, the probability of detection is given as:

$$\begin{aligned} P_{d,i} &= P(E_i > \lambda_2 | H_1) \\ &= e^{-\frac{\lambda_2}{2\sigma_i^2}} \sum_{k=0}^{u-2} \frac{1}{k!} \left(\frac{\lambda_2}{2\sigma_i^2}\right)^k \\ &\quad + \left(\frac{1+\bar{\gamma}}{\bar{\gamma}}\right)^{u-1} \left(e^{-\frac{\lambda_2}{2(1+\bar{\gamma})}}\right. \\ &\quad \left.- e^{-\frac{\lambda_2}{2\sigma_i^2}} \sum_{k=0}^{u-2} \frac{1}{k!} \left(\frac{\lambda_2 \bar{\gamma}}{2\sigma_i^2(1+\bar{\gamma})}\right)^k\right) \end{aligned} \quad (4.10)$$

$$P_{m,i} = P(E_i \leq \lambda_1 | H_1) = 1 - \Delta_{1,i} - P_{d,i} \quad (4.11)$$

$$P_{f,i} = P(E_i > \lambda_2 | H_0) = \frac{\Gamma\left(u, \frac{\lambda_2}{2\sigma_i^2}\right)}{\Gamma(u)} \quad (4.12)$$

The cooperative probability of missed detection (Q_m) is defined as follows:

$$Q_m = P(F = 0 | H_1) \quad (4.13)$$

Using the total probability theorem, Q_m can be expressed as follows:

$$Q_m = P(F = 0, K \neq N | H_1) + P(F = 0, K = N | H_1)$$

$$Q_m = P\left(\sum_{i=1}^K L_i = 0 \cap D = 0, K \neq N \middle| H_1\right) + P\left(\sum_{i=1}^K L_i = 0, K = N \middle| H_1\right)$$

$$Q_m = P\left(\sum_{i=1}^K L_i = 0, K \neq N \middle| H_1\right) P(D = 0, K \neq N | H_1) + P\left(\sum_{i=1}^K L_i = 0, K = N \middle| H_1\right)$$

$$Q_m = \sum_{K=0}^{N-1} \binom{N}{K} \prod_{i=1}^K \{P(E_i \leq \lambda_1 | H_1)\} \prod_{i=1}^{N-K} \{P(\lambda_1 < E_i \leq \lambda_2 | H_1)\} P\left(\sum_{i=1}^{N-K} w_i E_i \leq \lambda | H_1\right) \\ + \prod_{i=1}^N \{P(E_i \leq \lambda_1 | H_1)\}$$

$$Q_m = \sum_{K=0}^{N-1} \binom{N}{K} \prod_{i=1}^K \{P_{m,i}\} \prod_{i=1}^{N-K} \{\Delta_{1,i}\} \left[1 - P\left(\sum_{i=1}^{N-K} w_i E_i > \lambda | H_1\right)\right] + \prod_{i=1}^N \{P_{m,i}\}$$

$$Q_m = \sum_{K=0}^{N-1} \binom{N}{K} \prod_{i=1}^K \{P_{m,i}\} \prod_{i=1}^{N-K} \{\Delta_{1,i}\} [1 - P_{d,PSO(N-K)}] + \prod_{i=1}^N \{P_{m,i}\}$$

$$Q_m = \sum_{K=0}^N \binom{N}{K} \prod_{i=1}^K \{P_{m,i}\} \prod_{i=1}^{N-K} \{\Delta_{1,i}\} [1 - P_{d,PSO(N-K)}] \quad (4.14)$$

Here, $P_{d,PSO(N-K)}$ is probability of detection for the Conventional PSO (see equation (3.6)) with $N - K$ CR users, and can be expressed as:

$$P_{d,PSO(N-K)} = P\left(\sum_{i=1}^{N-K} w_i E_i > \lambda | H_1\right) \quad (4.15)$$

The cooperative probability of detection (Q_d) is obtained using:

$$Q_d = 1 - Q_m \quad (4.16)$$

The cooperative probability of false alarm (Q_f) is simply defined as:

$$Q_f = P(F = 1 | H_0) = 1 - P(F = 0 | H_0) \quad (4.17)$$

Using the total probability theorem again, Q_f can be expressed as:

$$Q_f = 1 - [P(F = 0, K \neq N | H_0) + P(F = 0, K = N | H_0)]$$

$$Q_f = 1 - \left[P\left(\sum_{i=1}^K L_i = 0 \cap D = 0, K \neq N \middle| H_0\right) + P\left(\sum_{i=1}^K L_i = 0, K = N \middle| H_0\right) \right]$$

$$Q_f = 1 - \left[P\left(\sum_{i=1}^K L_i = 0, K \neq N \middle| H_0\right) P(D = 0, K \neq N | H_0) \right. \\ \left. + P\left(\sum_{i=1}^K L_i = 0, K = N \middle| H_0\right) \right]$$

$$\begin{aligned}
Q_f &= 1 - \left[\sum_{K=0}^{N-1} \binom{N}{K} \prod_{i=1}^K \{P(E_i \leq \lambda_1 | H_0)\} \prod_{i=1}^{N-K} \{P(\lambda_1 < E_i \leq \lambda_2 | H_0)\} P\left(\sum_{i=1}^{N-K} w_i E_i \right. \right. \\
&\quad \left. \left. \leq \lambda | H_0\right) + \prod_{i=1}^N \{P(E_i \leq \lambda_1 | H_0)\} \right] \\
Q_f &= 1 - \left[\sum_{K=0}^{N-1} \binom{N}{K} \prod_{i=1}^K \{1 - \Delta_{0,i} - P_{f,i}\} \prod_{i=1}^{N-K} \{\Delta_{0,i}\} \left[1 - P\left(\sum_{i=1}^{N-K} w_i E_i > \lambda | H_0\right) \right] \right. \\
&\quad \left. + \prod_{i=1}^N \{1 - \Delta_{0,i} - P_{f,i}\} \right] \\
Q_f &= 1 - \left[\sum_{K=0}^{N-1} \binom{N}{K} \prod_{i=1}^K \{1 - \Delta_{0,i} - P_{f,i}\} \prod_{i=1}^{N-K} \{\Delta_{0,i}\} [1 - P_{f,PSO(N-K)}] \right. \\
&\quad \left. + \prod_{i=1}^N \{1 - \Delta_{0,i} - P_{f,i}\} \right] \\
Q_f &= 1 - \left[\sum_{K=0}^N \binom{N}{K} \prod_{i=1}^K \{1 - \Delta_{0,i} - P_{f,i}\} \prod_{i=1}^{N-K} \{\Delta_{0,i}\} [1 \right. \\
&\quad \left. - P_{f,PSO(N-K)}] \right] \tag{4.18} \\
Q_f &= 1 - \left[\sum_{K=0}^N \binom{N}{K} \prod_{i=1}^K \{F(\lambda_{1,i})\} \prod_{i=1}^{N-K} \{\Delta_{0,i}\} [1 \right. \\
&\quad \left. - P_{f,PSO(N-K)}] \right] \tag{4.19}
\end{aligned}$$

Here, $F(\lambda_{1,i})$ is the CDF for i^{th} CR, as defined in equation (4.7), and $P_{f,PSO(N-K)}$ is the probability of false alarm for the Conventional PSO (see equation (3.7)) for $N - K$ CR users, and is given by:

$$P_{f,PSO(N-K)} = P\left(\sum_{i=1}^{N-K} w_i E_i > \lambda | H_0\right) \quad (4.20)$$

The expression for $P_{d,PSO(N-K)}$ in equation (4.14), for both AWGN case and Rayleigh fading, is the same as equation (3.6), with $(N - K)$ CR users. The difference for Rayleigh fading is that the channel gains h_i follow the Rayleigh distribution. Similarly, the expression for $P_{f,PSO(N-K)}$ in equation (4.19), for both the AWGN case and the Rayleigh fading, is the same as equation (3.7).

In the proposed algorithm, if the energies from the Fuzzy CRs are combined using the EGC technique, the cooperative probabilities of missed detection and false alarm become:

$$Q_m = \sum_{K=0}^N \binom{N}{K} \prod_{i=1}^K \{P_{m,i}\} \prod_{i=1}^{N-K} \{\Delta_{1,i}\} [1 - P_{d,EGC(N-K)}] \quad (4.21)$$

$$Q_f = 1 - \left[\sum_{K=0}^N \binom{N}{K} \prod_{i=1}^K \{F(\lambda_{1,i})\} \prod_{i=1}^{N-K} \{\Delta_{0,i}\} [1 - P_{f,EGC(N-K)}] \right] \quad (4.22)$$

The expression for $P_{d,EGC(N-K)}$ in equation (4.21) varies as per the wireless channel behaviour. For the case of AWGN, equation (2.35) is used, while for Rayleigh fading,

equation (2.36) is used as the expression for $P_{d,EGC(N-K)}$, $N - K$ CR users. The expression for $P_{f,EGC(N-K)}$ in equation (4.22) is independent of the channel behaviour. Hence, for both the AWGN case and the Rayleigh fading case, equation (2.34) is used as the main expression for $P_{f,EGC(N-K)}$.

On the other hand, if the CRs whose observed energy values fall in the fuzzy region are neglected, the final decision will then be based only on the local hard decisions reported by the reliable CRs [59]. Under such a scenario, the cooperative probabilities of detection, missed detection and false alarm become:

$$Q_d = P(F = 1, K \geq 1 | H_1) = 1 - \prod_{i=1}^N \{G(\lambda_{2,i})\} \quad (4.23)$$

$$\begin{aligned} Q_m &= P(F = 0, K \geq 1 | H_1) = 1 - \prod_{i=1}^N \Delta_{1,i} - Q_d \\ &= \prod_{i=1}^N \{G(\lambda_{2,i})\} - \prod_{i=1}^N \Delta_{1,i} = \prod_{i=1}^N \{G(\lambda_{1,i})\} \end{aligned} \quad (4.24)$$

$$Q_f = P(F = 1, K \geq 1 | H_0) = 1 - \prod_{i=1}^N \{F(\lambda_{2,i})\} \quad (4.25)$$

Here, $F(\lambda_i)$ and $G(\lambda_i)$ are the CDFs for i^{th} CR, under H_0 and H_1 respectively, as defined in equations (4.7) and (4.8) respectively.

Equations (4.23), (4.24) and (4.25) are the corrected version of the expressions derived in [59].

4.4 Bit Savings over the Reporting Channel for the proposed algorithm

As discussed in the previous chapter, the conventional EGC and the conventional PSO data fusion schemes achieve higher detection performance compared to the decision fusion techniques, but at the expense of high communication burden over the reporting channel. Hence, due to the bandwidth constraints over the reporting channel, there is a need to reduce the number of reporting bits, with preferably a negligible loss in performance.

In this section, the average communication overhead over the reporting channel is evaluated. In the proposed algorithm, during each spectrum sensing cycle, the fusion centre receives K hard decisions and $(N - K)$ observation values (energies, local noise variances and channel gains). Each CR uses 1 bit to report its hard decision, and b bits to report its observation values. The total number of bits received by the fusion centre is given as:

$$B = K + b(N - K) \quad (4.26)$$

In the proposed algorithm, as PSO is used at the fusion centre to calculate the optimal weight vector for combining the energies from Fuzzy CRs, it requires the information about the local sensing noise variances as well as the sensing channel gains for each CR. Here, it is assumed that the sensing noise variances of the cooperating CRs remain unchanged. Hence, each CR has to send its local noise variance only once to the fusion centre. While calculating the average number of reporting bits, the one-time reporting of local noise variances is neglected. The reporting of sensing channel gains varies as per the wireless channel behaviour. For the case of AWGN, the sensing channel gains remain

constant, and without loss of generality, these are assumed to be unity. For the case of Rayleigh fading, as the channel gains follow the Rayleigh distribution, each cooperating CR has to report its sensing channel gain during each sensing cycle. Hence, under AWGN, each CR uses b bits to report only its observed energy value during each sensing cycle. For Rayleigh fading, each CR uses b bits in total to report its observed energy value as well as the sensing channel gain.

Firstly, let us define event V_K , as the case in which K CRs report their hard decisions to the fusion centre. Thus, the probability of event V_K is given by:

$$P(V_K) = [1 - P(\lambda_1 < E \leq \lambda_2)]^K \quad (4.27)$$

The other event W_{N-K} is defined, when $(N - K)$ CRs report their observed information to the fusion centre. The probability of event W_{N-K} is given by:

$$P(W_{N-K}) = [P(\lambda_1 < E \leq \lambda_2)]^{N-K} \quad (4.28)$$

Also, P_1 and P_0 are denoted as the probabilities of a primary user being present and absent respectively. Using these equations, the expression for the average number of CRs reporting their observed information is given as:

$$K_{soft} = \sum_{K=0}^N (N - K) \left[\binom{N}{K} P(W_{N-K}|H_0) P(V_K|H_0) P_0 \right. \\ \left. + \binom{N}{K} P(W_{N-K}|H_1) P(V_K|H_1) P(H_1) P_1 \right]$$

$$\begin{aligned}
K_{soft} &= \sum_{K=0}^N N \left[\binom{N}{K} P(W_{N-K}|H_0)P(V_K|H_0)P_0 + \binom{N}{K} P(W_{N-K}|H_1)P(V_K|H_1)P(H_1)P_1 \right] \\
&\quad - K \left[\binom{N}{K} P(W_{N-K}|H_0)P(V_K|H_0)P_0 \right. \\
&\quad \left. + \binom{N}{K} P(W_{N-K}|H_1)P(V_K|H_1)P(H_1)P_1 \right] \\
K_{soft} &= N - P_0 \sum_{K=1}^N K \binom{N}{K} P(W_{N-K}|H_0)P(V_K|H_0) \\
&\quad - P_1 \sum_{K=1}^N K \binom{N}{K} P(W_{N-K}|H_1)P(V_K|H_1) \\
K_{soft} &= N - K_{hard} \tag{4.29}
\end{aligned}$$

Here, K_{hard} is the average number of CRs reporting the hard decisions, which is also expressed as:

$$K_{hard} = N[P_0(1 - \Delta_0) + P_1(1 - \Delta_1)] \tag{4.30}$$

The average total number of bits can hence be expressed as:

$$B_{avg} = K_{hard} + bK_{soft}$$

$$B_{avg} = K_{hard} + b(N - K_{hard})$$

$$B_{avg} = K_{hard} + bN - bK_{hard}$$

$$B_{avg} = bN - (b - 1)K_{hard} \tag{4.31}$$

The normalized average number of bits over the reporting channel is given as:

$$\bar{B} = \frac{B_{avg}}{N} = b - (b - 1)\bar{K} \quad (4.32)$$

Here, $\bar{K} = \frac{K_{hard}}{N}$ is the normalized average number of hard decisions [59].

From equation (4.32), it is observed that the normalized average number of bits over the reporting channel is obviously less than b bits. Hence, the normalized average number of reporting bits for the proposed algorithm is low in comparison to the conventional single threshold PSO algorithm, wherein each CR uses b bits to report its observed information. For the case of $\Delta_0 = 0$, the two thresholds λ_1 and λ_2 coincide, and the normalized average number of reporting bits $\bar{B} = 1$ (corresponding to the conventional OR rule). On the other hand, for $\Delta_0 = 1$, the two thresholds λ_1 and λ_2 are infinitely apart, and the normalized average number of reporting bits $\bar{B} = b$ (corresponding to the conventional PSO algorithm).

4.5 Simulation Results

In this section, the performance analysis is carried for the proposed hybrid cooperative spectrum sensing algorithm (Hybrid PSO-OR). The proposed Hybrid PSO-OR algorithm is compared to the Hybrid EGC-OR algorithm, the conventional single threshold PSO algorithm, and the conventional OR rule algorithm.

The time-bandwidth product is taken as $u = TW = 5$, and the number of received signal samples is $M = 2u = 10$. The parameters used for PSO are: number of particles $S = 30$, maximum number of iterations $t = 50$, inertia weight $\omega = 1$, and the learning factors $c_1 = c_2 = 2$.

The performance analysis is carried for 10 cooperating CRs, for different average SNR values under both AWGN and Rayleigh fading. For simplicity, the reporting channels are assumed to be perfect, i.e. $\delta = 0$ in equations (3.9) and (3.10).

4.5.1 Simulation Results under AWGN

In Figure 4.3, the performance of the proposed Hybrid PSO-OR algorithm is analyzed for an average SNR of 4 dB, and different values of Δ_0 .

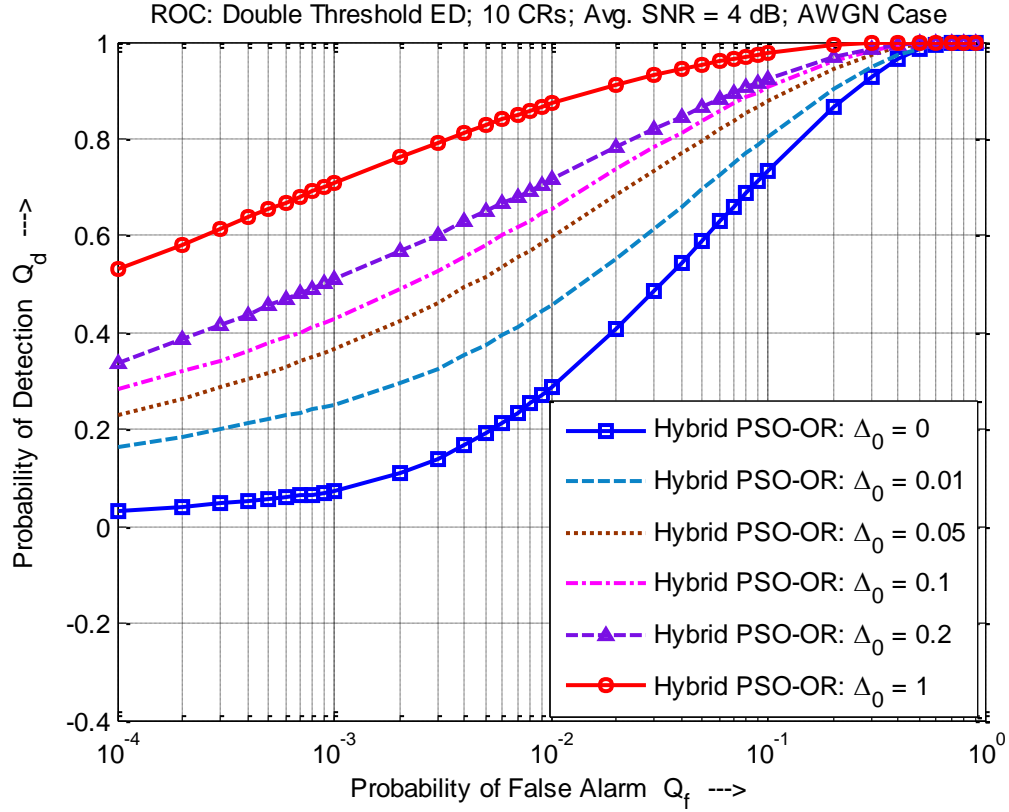


Figure 4.3: ROC – Proposed Hybrid PSO-OR algorithm (10 CRs, Avg. SNR = 4 dB, AWGN Case)

Here, $SNR_{dB} = [6 \ 4 \ 5 \ 3 \ 2 \ 6 \ 5 \ 4 \ 3 \ 2]$ represents the local SNR values of the cooperating CRs. As the value of Δ_0 increases, the detection performance of the proposed algorithm increases (see Figure 4.3). For the proposed algorithm, $\Delta_0=0$ corresponds to the conventional OR rule, where the two thresholds λ_1 and λ_2 coincide. On the other hand, $\Delta_0=1$ corresponds to the conventional PSO algorithm, where all the CRs fall in fuzzy

region, and the received energies are combined using the optimal weight vector calculated using PSO.

For the same setup, the performance of the Hybrid EGC-OR algorithm for different values of Δ_0 is shown in Figure 4.4.

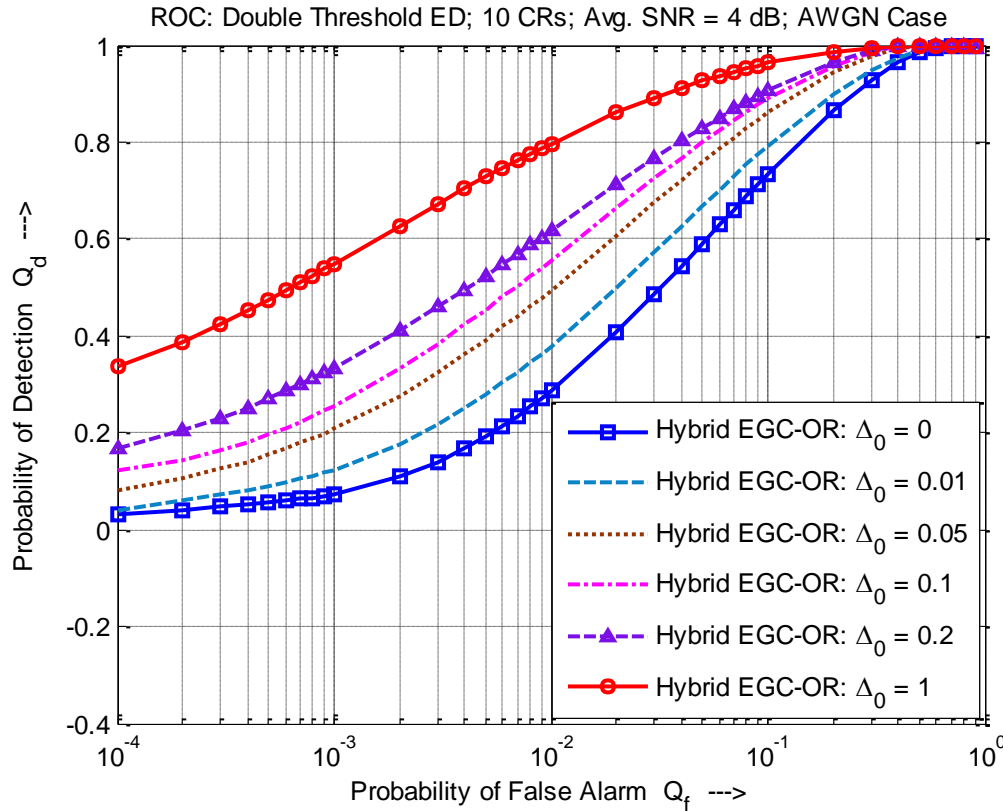


Figure 4.4: ROC – Hybrid EGC-OR algorithm (10 CRs, Avg. SNR = 4 dB, AWGN Case)

For the Hybrid EGC-OR technique, $\Delta_0 = 0$ corresponds to the Conventional OR rule, where the two thresholds λ_1 and λ_2 coincide. On the other hand, $\Delta_0 = 1$ corresponds to the conventional EGC data fusion technique, where the received energies are blindly combined to make a soft decision. As the value of Δ_0 increases, the detection performance of Hybrid EGC-OR algorithm increases. Comparing Figure 4.3 and

Figure 4.4, it is seen that the proposed Hybrid PSO-OR algorithm outperforms the Hybrid EGC-OR algorithm for all the values of Δ_0 .

The quantitative analysis is performed for $\Delta_0 = 0.2$ (see Figure 4.5), where the proposed algorithm is compared with the Hybrid EGC-OR algorithm, the conventional PSO data fusion technique and the conventional OR rule (decision fusion).

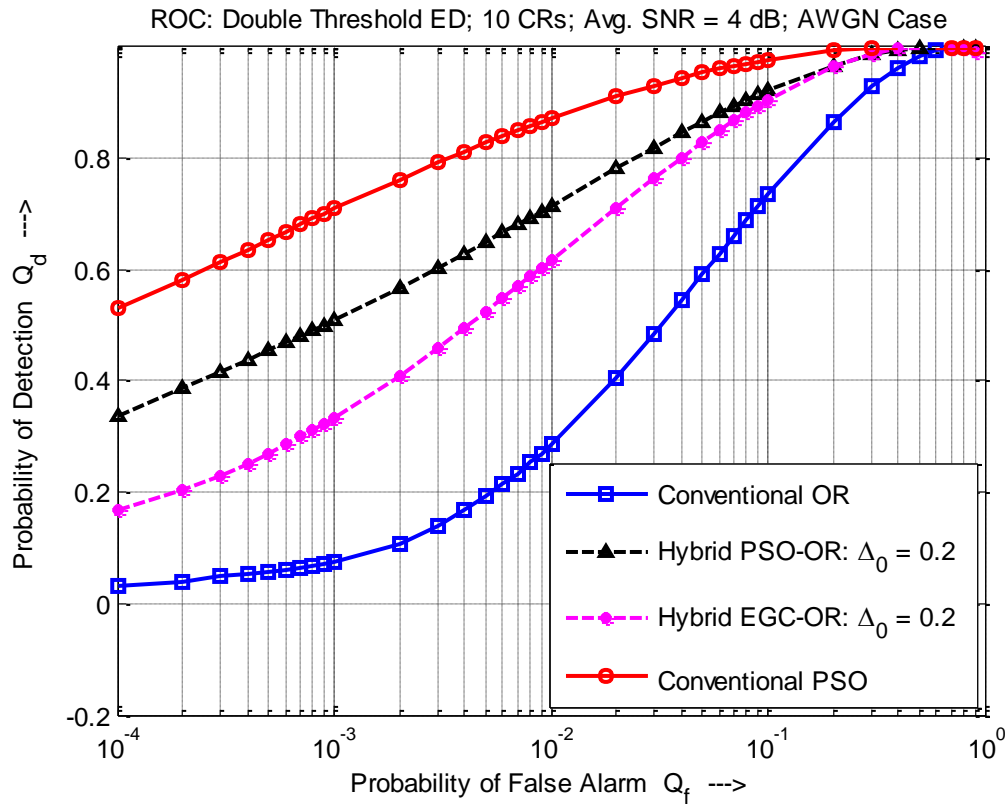


Figure 4.5: ROC – Comparison of proposed Hybrid PSO-OR algorithm with existing techniques (10 CRs, Avg. SNR = 4 dB, AWGN Case)

The performance of the proposed Hybrid PSO-OR algorithm, for any value of Δ_0 , lies in between the conventional OR rule and the conventional PSO data fusion technique. For $Q_f = 10^{-3}$ and $\Delta_0 = 0.2$, the proposed Hybrid PSO-OR algorithm achieves 51%

detection performance compared to the Hybrid EGC-OR algorithm, which achieves only 33% detection performance.

To compare the proposed algorithm with other techniques in terms of missed detection probability, the C-ROC curves are plotted and shown in Figure 4.6.

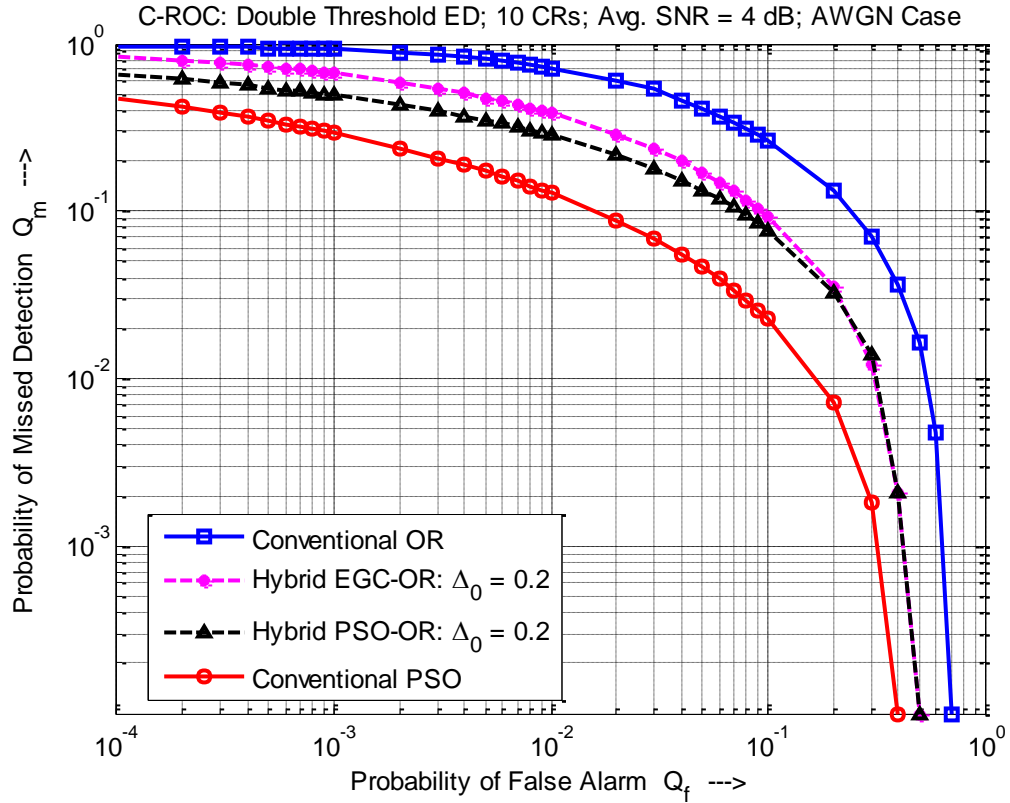


Figure 4.6: C-ROC – Comparison of proposed Hybrid PSO-OR algorithm with existing techniques (10 CRs, Avg. SNR = 4 dB, AWGN Case)

For $Q_f = 10^{-3}$ and $\Delta_0 = 0.2$, the proposed Hybrid PSO-OR algorithm gives 49% missed detection as opposed to the Hybrid EGC-OR algorithm which gives 66% missed detection.

In Figure 4.7, the performance of the proposed Hybrid PSO-OR algorithm is analyzed for an average SNR of 6 dB, and different values of Δ_0 .

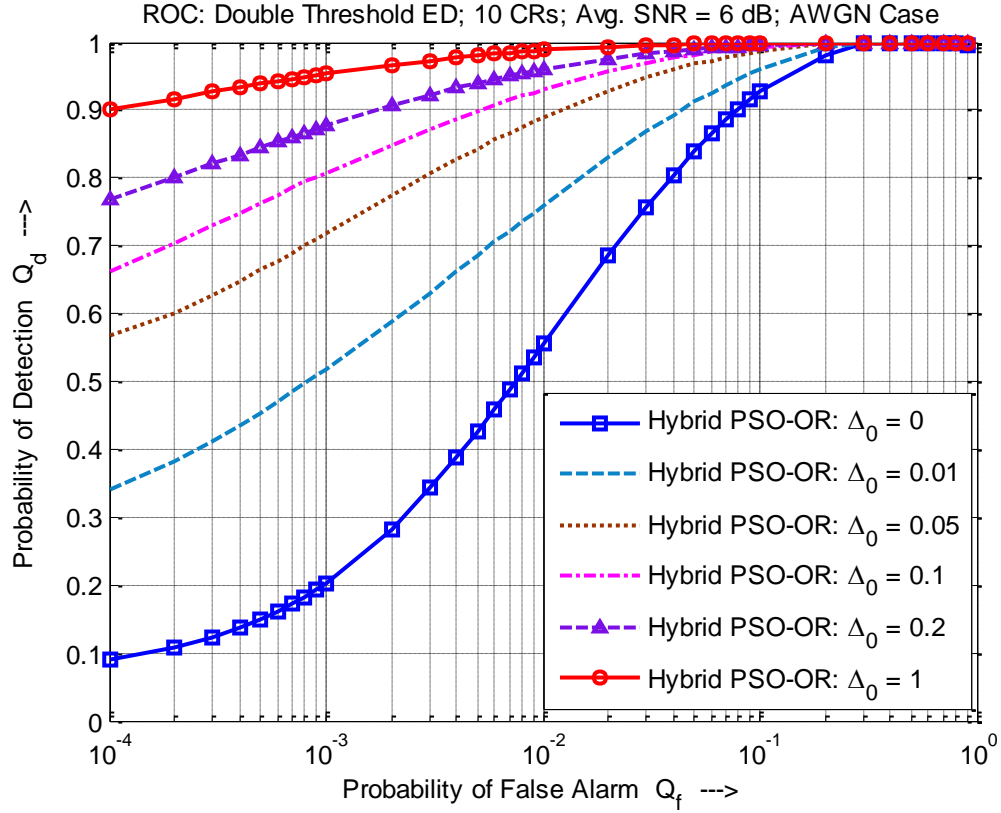


Figure 4.7: ROC – Proposed Hybrid PSO-OR algorithm (10 CRs, Avg. SNR = 6 dB, AWGN Case)

For a higher average SNR value, the detection performance improves significantly for different values of Δ_0 , and outperforms the conventional OR rule. For $\Delta_0 = 0.2$, the detection performance is very close to that of the conventional PSO algorithm.

Using the same scenario, the performance of Hybrid EGC-OR technique is shown in Figure 4.8.

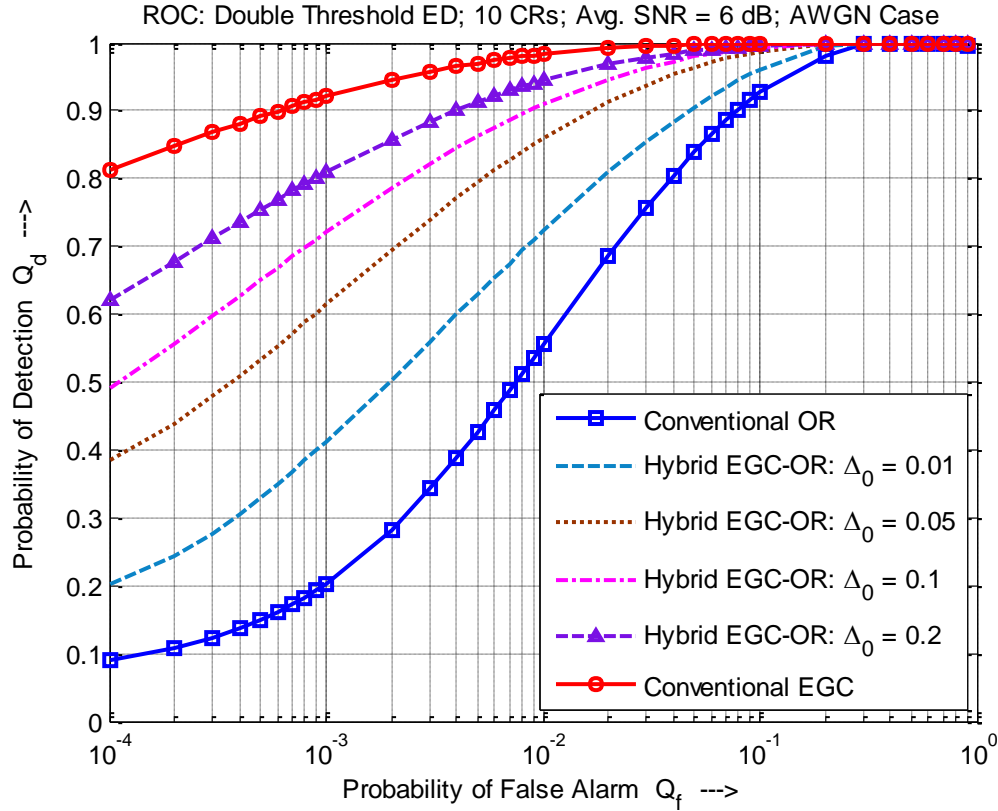


Figure 4.8: ROC – Hybrid EGC-OR algorithm (10 CRs, Avg. SNR = 6 dB, AWGN Case)

The proposed Hybrid PSO-OR algorithm outperforms the Hybrid EGC-OR algorithm for all the values of Δ_0 (see Figure 4.7 and Figure 4.8). For the case of $\Delta_0 = 0.2$, the Hybrid PSO-OR algorithm is compared with other techniques, as shown in Figure 4.9.

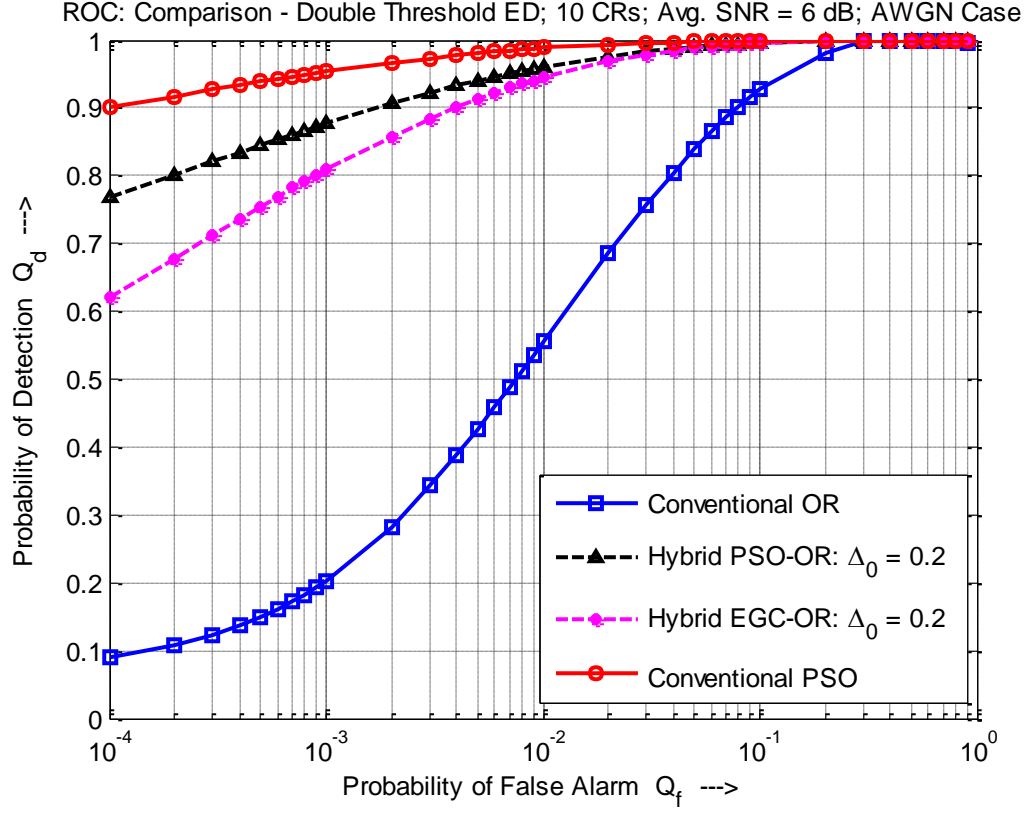


Figure 4.9: ROC – Comparison of proposed Hybrid PSO-OR algorithm with existing techniques (10 CRs, Avg. SNR = 6 dB, AWGN Case)

For $Q_f = 10^{-3}$ and $\Delta_0 = 0.2$, the proposed Hybrid PSO-OR algorithm achieves 87% detection performance compared to the Hybrid EGC-OR algorithm, which achieves only 81% detection performance.

4.5.2 Simulation Results under Rayleigh Fading

In Figure 4.10, the performance of the proposed Hybrid PSO-OR algorithm is analyzed for an average SNR of 5 dB, and different values of Δ_0 .

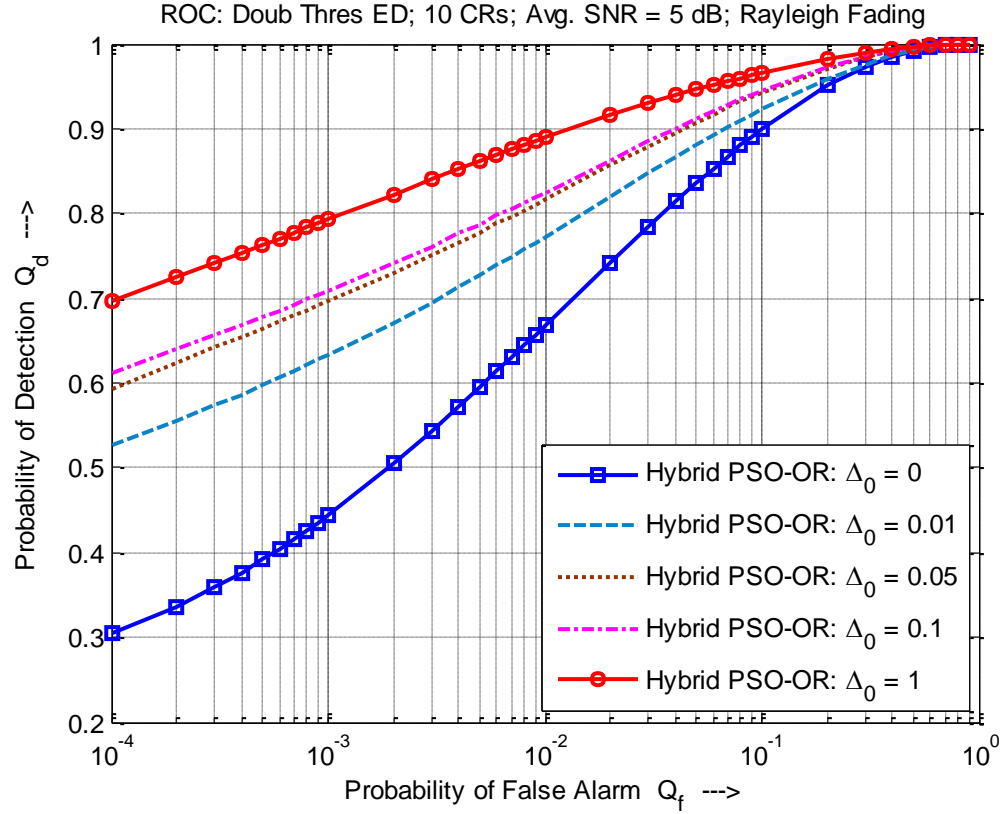


Figure 4.10: ROC – Proposed Hybrid PSO-OR algorithm (10 CRs, Avg. SNR = 5 dB, Rayleigh Fading)

Here, the representative scenario with the locally observed average SNR values for the CRs as $\mathbf{SNR}_{dB} = [7 \ 5 \ 6 \ 4 \ 2 \ 8 \ 6 \ 5 \ 4 \ 3]$ is analyzed. The sensing channel gains follow a Rayleigh distribution. Similar to the AWGN case, the performance of the proposed Hybrid PSO-OR algorithm, for different values of Δ_0 , lies in between the conventional OR rule and the conventional PSO technique.

The performance of the Hybrid EGC-OR algorithm, for the same scenario, is shown in Figure 4.11.

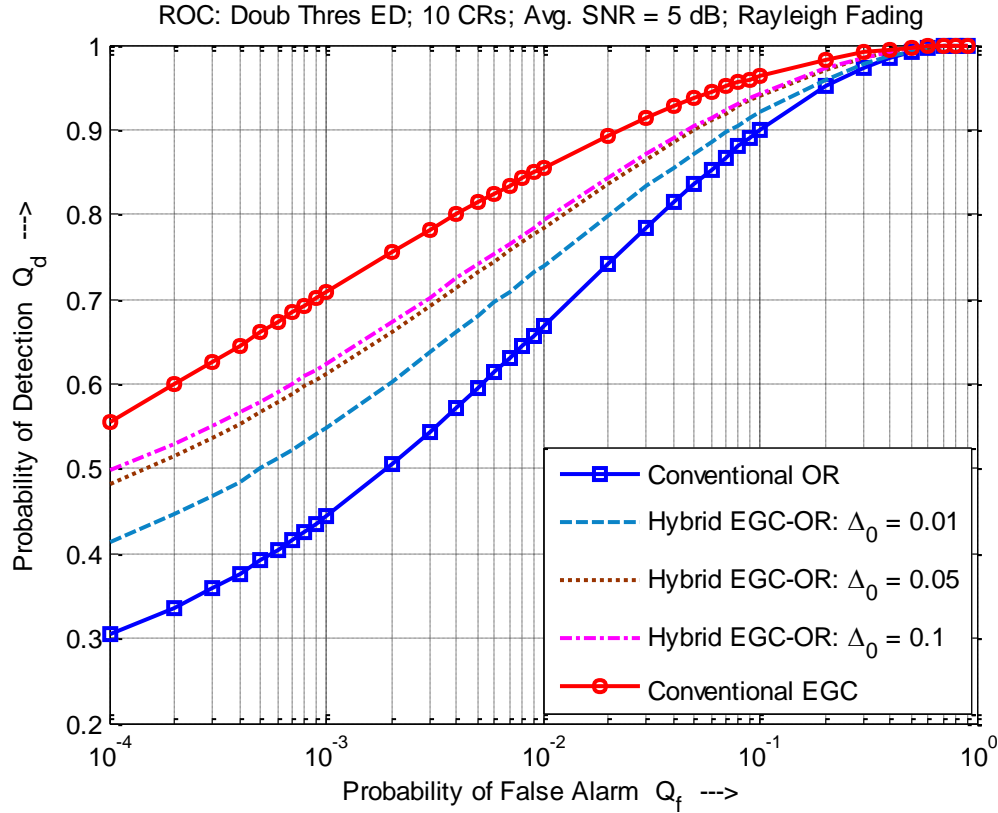


Figure 4.11: ROC – Hybrid EGC-OR algorithm (10 CRs, Avg. SNR = 5 dB, Rayleigh Fading)

The proposed Hybrid PSO-OR algorithm outperforms the Hybrid EGC-OR technique under Rayleigh fading. In Figure 4.12, the case of $\Delta_0 = 0.05$ is used to show the performance of the Hybrid PSO-OR algorithm in comparison with other existing techniques.

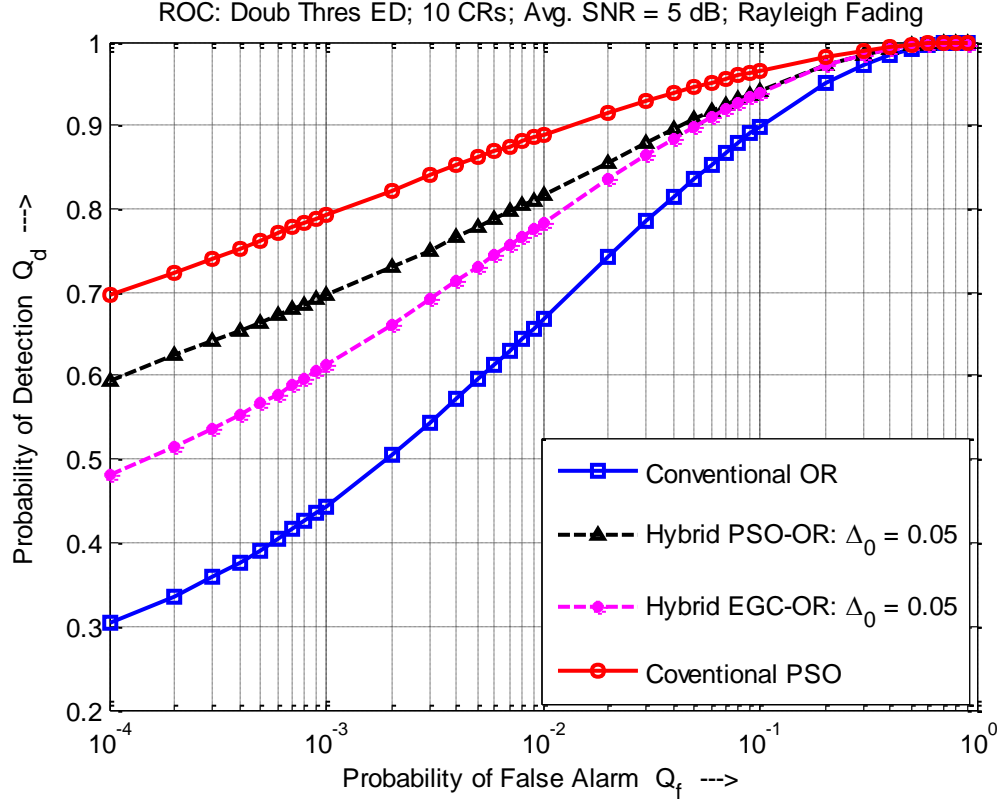


Figure 4.12: ROC – Comparison of proposed Hybrid PSO-OR algorithm with existing techniques (10 CRs, Avg. SNR = 5 dB, Rayleigh Fading)

For $Q_f = 10^{-3}$, the proposed Hybrid PSO-OR algorithm achieves 70% detection performance compared to the Hybrid EGC-OR algorithm, which only achieves 61% detection performance.

To compare the proposed algorithm with other techniques in terms of missed detection probability, the C-ROC curves are displayed in Figure 4.13.

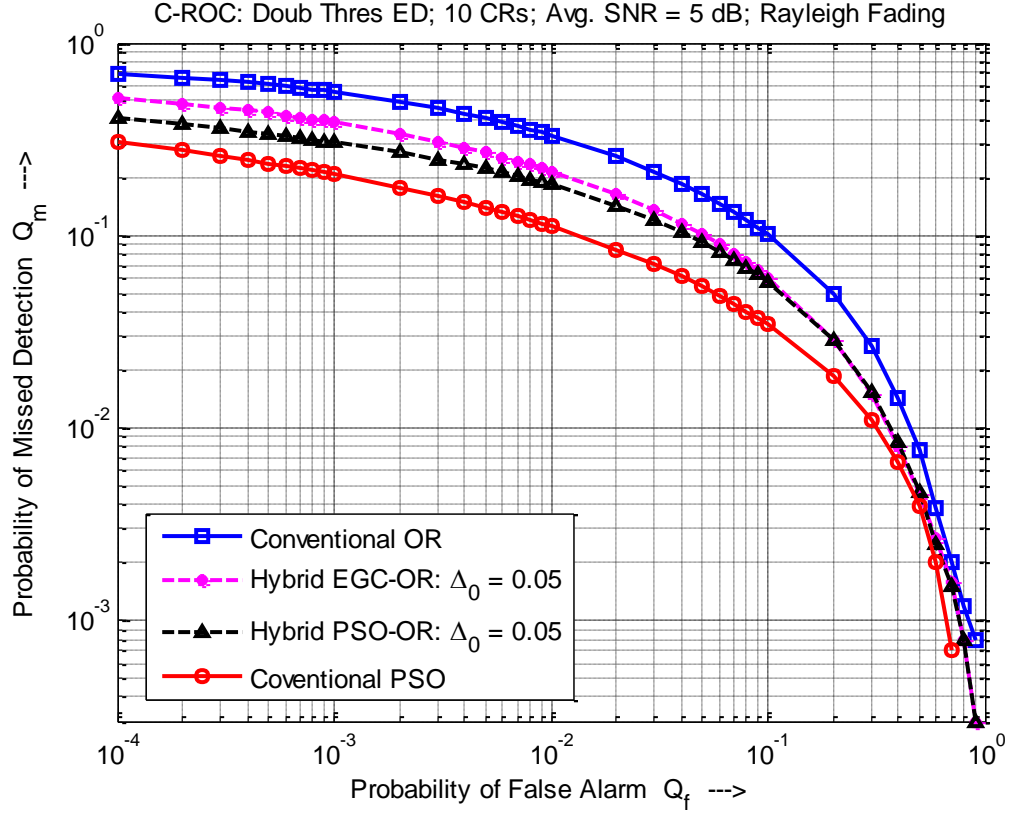


Figure 4.13: C-ROC – Comparison of proposed Hybrid PSO-OR algorithm with existing techniques (10 CRs, Avg. SNR = 5 dB, Rayleigh Fading)

For $Q_f = 10^{-3}$ and $\Delta_0 = 0.05$, the proposed Hybrid PSO-OR algorithm gives 30% missed detection as opposed to Hybrid EGC-OR algorithm which gives 39% missed detection.

Figure 4.14 shows the performance of the proposed algorithm for an average SNR of 7 dB, under Rayleigh fading.

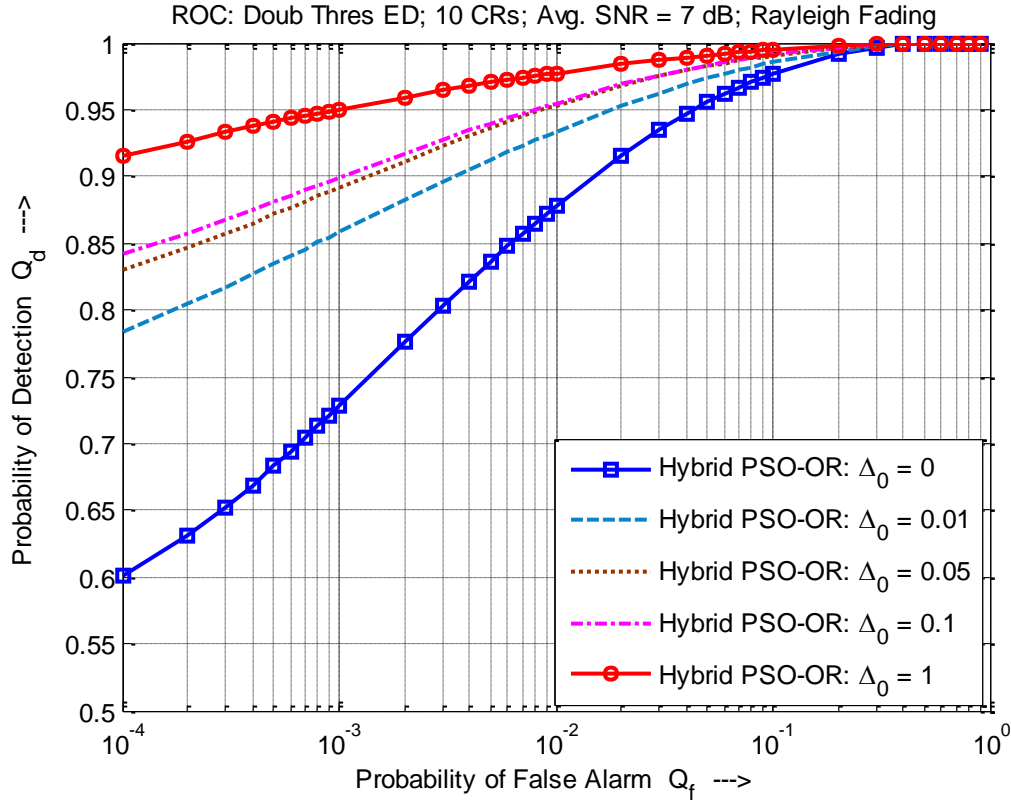


Figure 4.14: ROC – Proposed Hybrid PSO-OR algorithm (10 CRs, Avg. SNR = 7 dB, Rayleigh Fading)

Similar to the AWGN case, for a higher average SNR value, the detection performance improves significantly for different values of Δ_0 , and outperforms the conventional OR rule. For $\Delta_0 = 0.1$, the detection performance is close to that of the conventional PSO algorithm.

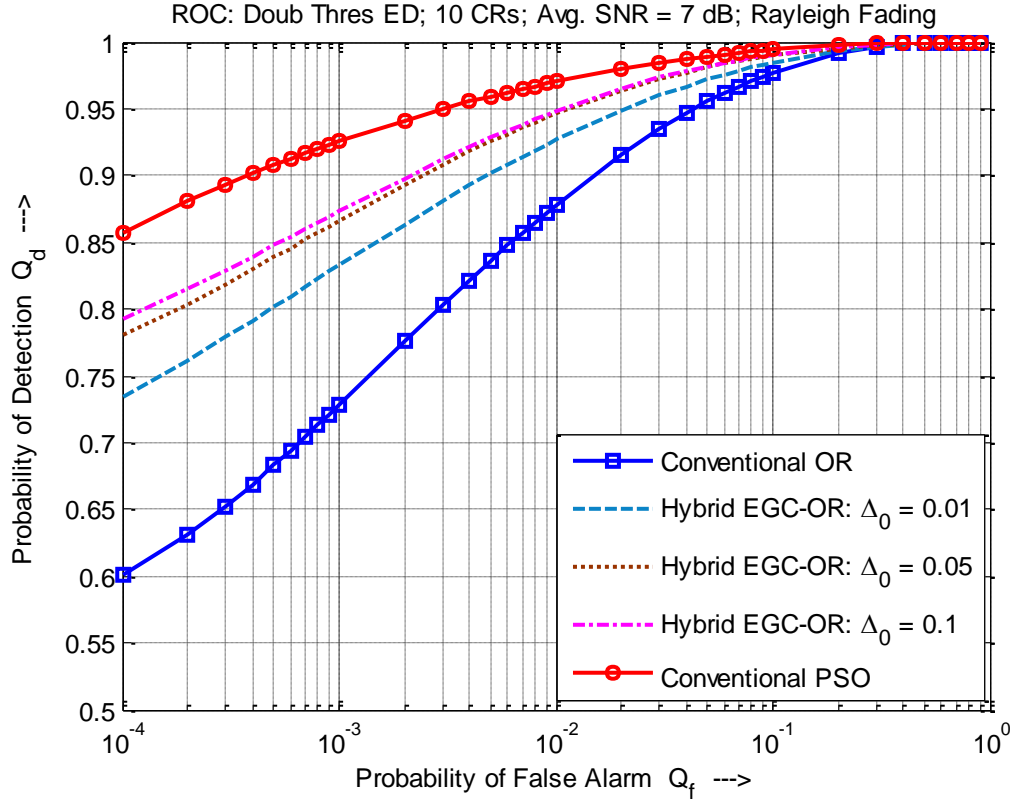


Figure 4.15: ROC – Hybrid EGC-OR algorithm (10 CRs, Avg. SNR = 7 dB, Rayleigh Fading)

The performance of the Hybrid EGC-OR technique, for the same scenario, is displayed in Figure 4.15. In Figure 4.16, the Hybrid PSO-OR algorithm is compared to the existing techniques for $\Delta_0 = 0.05$.

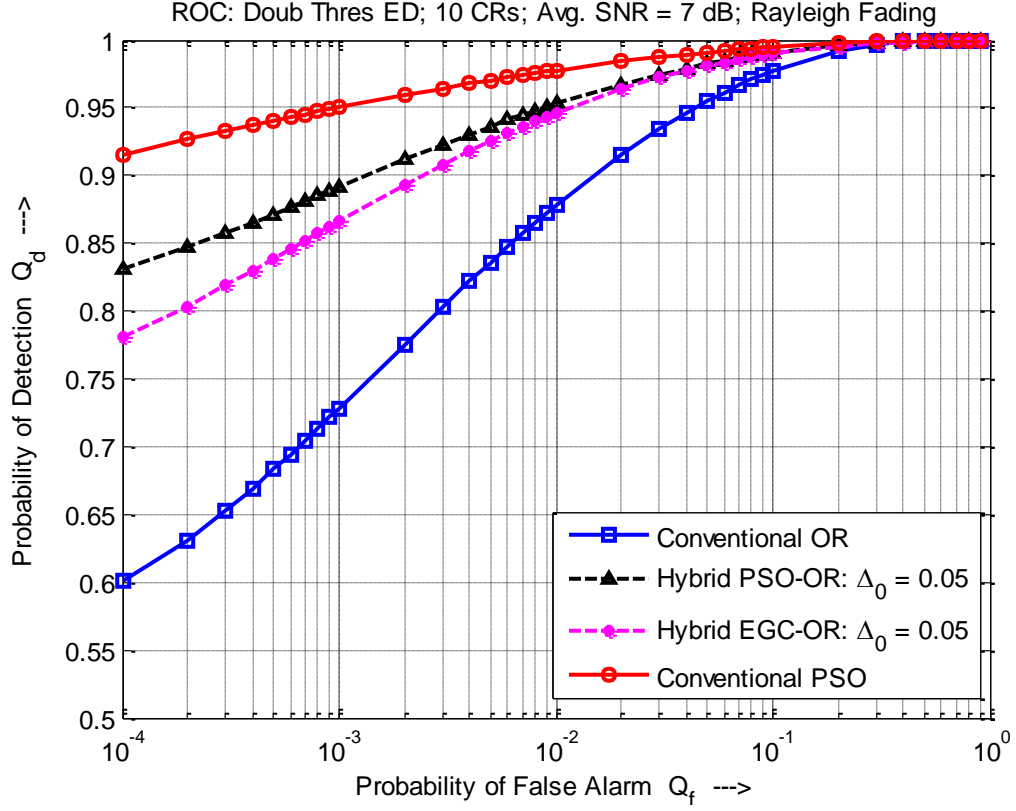


Figure 4.16: ROC – Comparison of proposed Hybrid PSO-OR algorithm with existing techniques (10 CRs, Avg. SNR = 7 dB, Rayleigh Fading)

For $Q_f = 10^{-3}$, the proposed Hybrid PSO-OR algorithm achieves 89% detection performance in comparison to the Hybrid EGC-OR algorithm, which achieves 86.5% detection performance.

4.5.3 Simulation Results for Bit Savings over the Reporting Channel

Figure 4.17 shows the normalized average number of reporting bits (\bar{B}) required by the proposed Hybrid PSO-OR algorithm, for the scenario used in Figure 4.3.

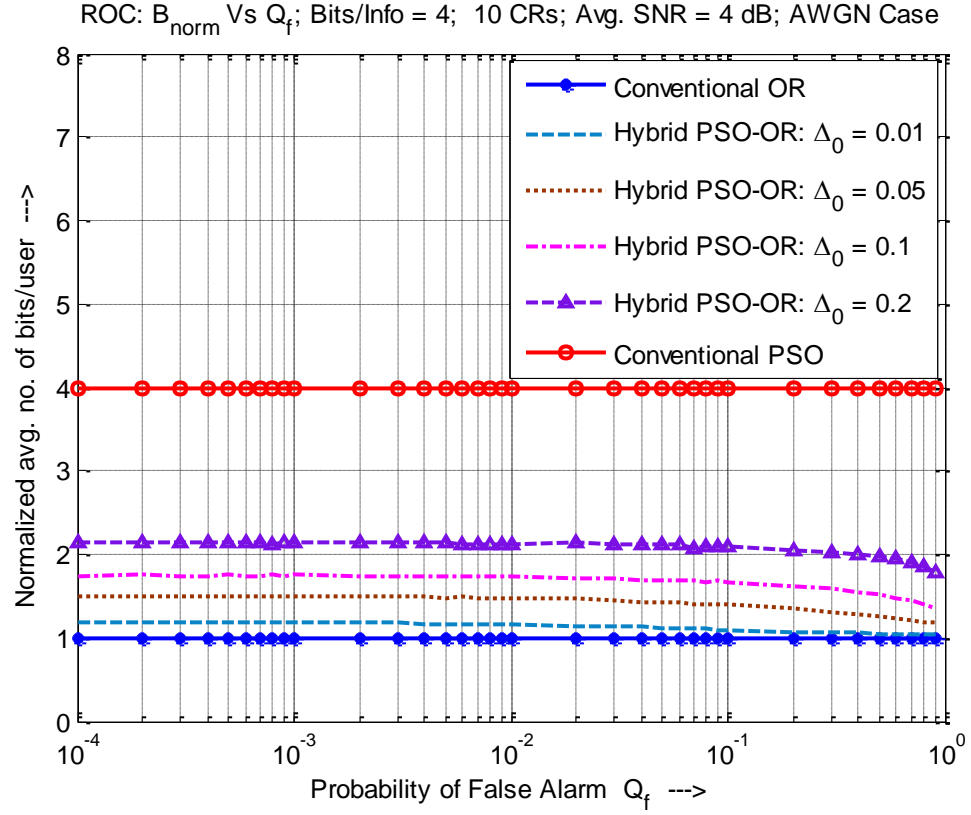


Figure 4.17: Normalized avg. number of bits/user \bar{B} vs. Q_f (10 CRs, Avg. SNR = 4 dB, AWGN Case)

The results are compared to those of the conventional OR rule, and the conventional single threshold PSO technique. As discussed in Section 4.4, the one time reporting of the local noise variances to the fusion centre is neglected, and the sensing channel gains are assumed to be unity. For the proposed algorithm under AWGN, each Fuzzy CR requires 4 bits to report its observed energy value. In Figure 4.17, for the case of $\Delta_0 = 0.2$, across most of the Q_f values, \bar{B} reduces from 4 bits/CR to 2.13 bits/CR (almost 50% reduction)

for each sensing cycle, but the detection performance is still close to the conventional PSO technique (see Figure 4.3). Hence, there is a significant reduction in the communication overhead over the reporting channel. Under AWGN, the average number of reporting bits required for the proposed Hybrid PSO-OR and Hybrid EGC-OR is the same. Hence, under AWGN, for a given value of Δ_0 , the Hybrid PSO-OR gives a better detection performance than Hybrid EGC-OR, with the same number of reporting bits.

For the conventional OR rule (corresponding to $\Delta_0 = 0$), each CR reports its local hard decision, hence, only 1 bit is required over the reporting channel. On the other hand, for the conventional PSO technique (corresponding to $\Delta_0 = 1$), each CR reports the observed energy value, hence, requires 4 bits over the reporting channel. The average number of bits required by the proposed Hybrid PSO-OR algorithm falls in between these two techniques. As the value of Δ_0 increases, the number of CRs falling in the Fuzzy region increases, and hence, \bar{B} increases.

Figure 4.18 shows the normalized average number of reporting bits for the scenario discussed in Figure 4.7.

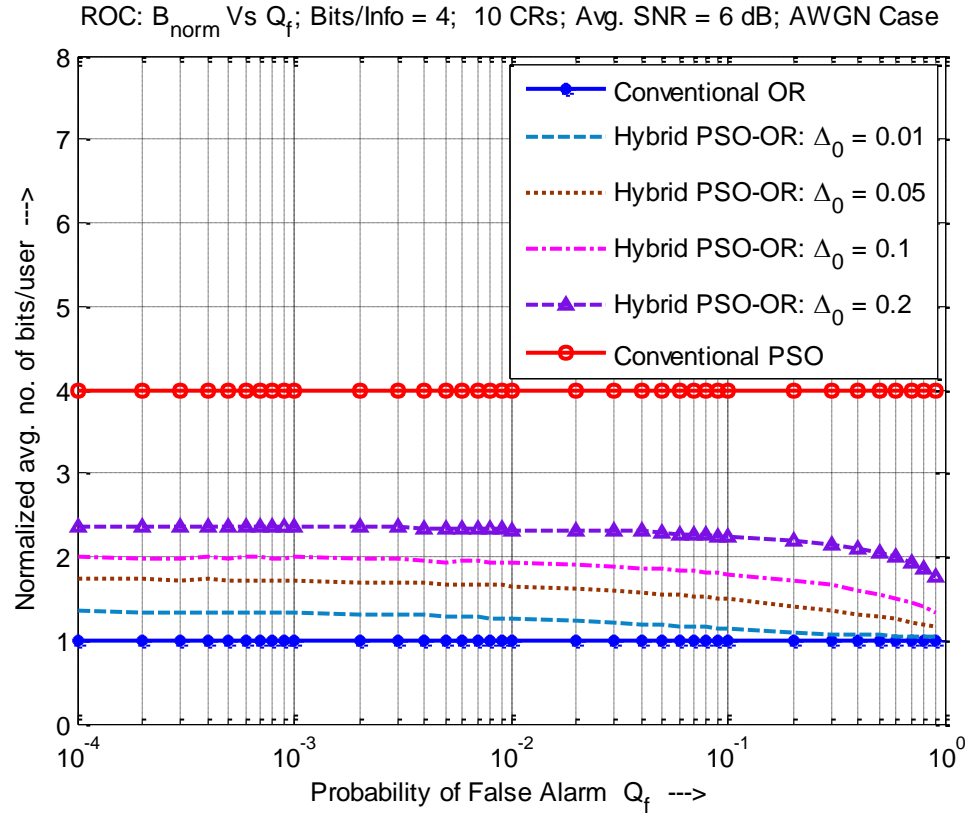


Figure 4.18: Normalized avg. number of bits/user \bar{B} vs. Q_f (10 CRs, Avg. SNR = 6 dB, AWGN Case)

In this case, for $\Delta_0 = 0.2$, \bar{B} reduces from 4 bits/CR to 2.35 bits/CR, but the detection performance is still close to the conventional PSO technique. For smaller values of Δ_0 , the performance of Hybrid PSO-OR remains close to that of the conventional OR rule. As Δ_0 increases further, the performance of Hybrid PSO-OR starts getting close to the conventional PSO technique, but with a lesser number of reporting bits.

Figure 4.19 shows the normalized average number of reporting bits for Hybrid PSO-OR algorithm, for the scenario used in Figure 4.10.

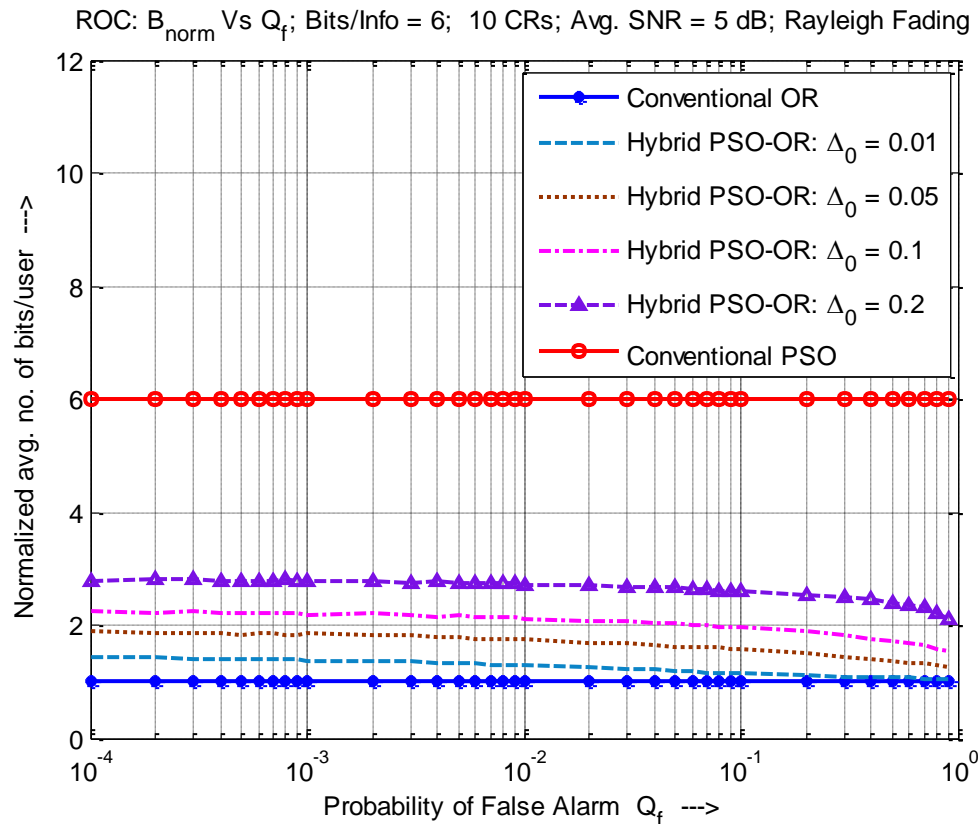


Figure 4.19: Normalized avg. number of bits/user \bar{B} vs. Q_f (10 CRs, Avg. SNR = 5 dB, Rayleigh Fading)

As discussed in Section 4.4, under Rayleigh fading, sensing channel gains follow the Rayleigh distribution. Hence, each Fuzzy CR has to report its sensing channel gain, along with the observed energy value, during each sensing cycle. Here, it is assumed that each CR uses 6 bits to report the required information, during each sensing cycle. Hence, for the conventional PSO technique (corresponds to $\Delta_0 = 1$), each CR uses 6 bits to report its observed energy value as well as the sensing channel gain. For $\Delta_0 = 0.1$, the required number of reporting bits reduces from 6 bits/CR to 2.2 bits/CR, with a detection performance very close to that of the conventional PSO technique (see Figure 4.10).

Figure 4.20 shows the normalized average number of reporting bits, for the scenario used in Figure 4.14.

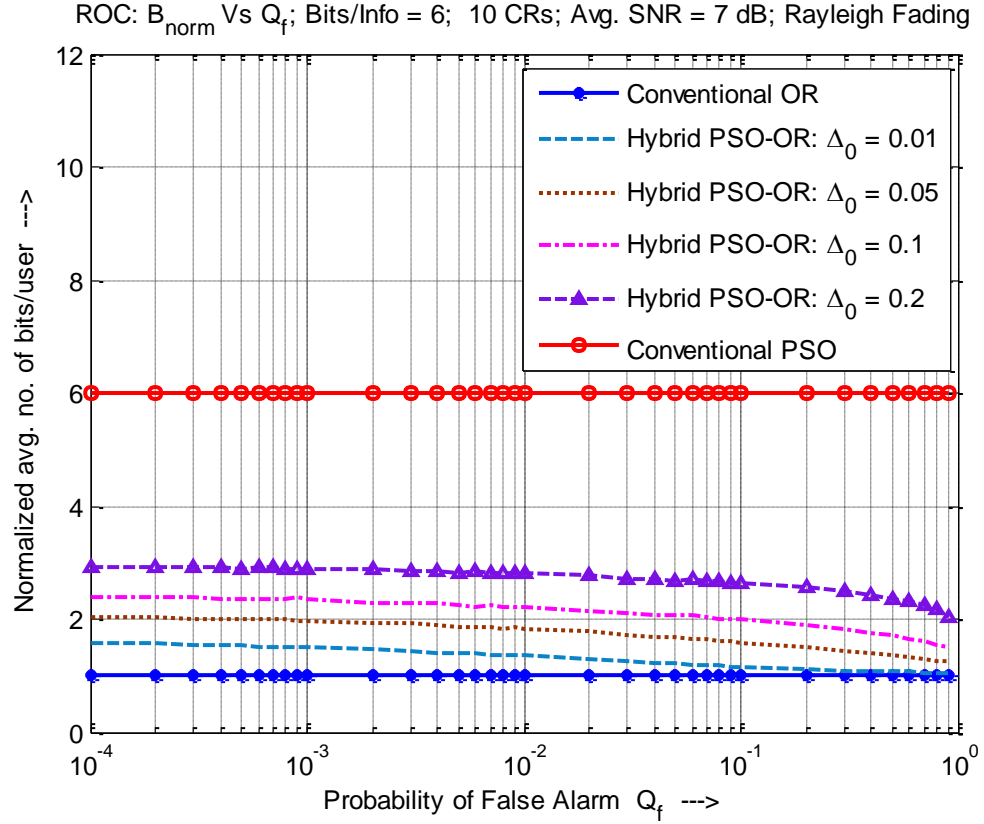


Figure 4.20: Normalized avg. number of bits/user \bar{B} vs. Q_f (10 CRs, Avg. SNR = 7 dB, Rayleigh Fading)

In this case, for $\Delta_0 = 0.1$, the required number of reporting bits reduces to 2.3 bits/CR, with the detection performance close to the conventional PSO technique.

Under Rayleigh fading, for Hybrid EGC-OR technique, cooperating CRs are not required to report the sensing channel gains. Hence, each CR uses 4 bits to report its observed energy value only (i.e. same as AWGN case).

4.6 Summary of Simulation Results

The performance analysis of the proposed Hybrid PSO-OR algorithm under the case of AWGN and Rayleigh fading is summarized in Table 4.1 and Table 4.2 respectively. All the quantitative analysis values mentioned in the tables are for $Q_f = 10^{-3}$.

Table 4.1: Performance analysis summary of the proposed Hybrid PSO-OR algorithm under AWGN

SNR (dB)	Δ_0	Improvement in P_d compared to Hybrid EGC-OR	Savings in \bar{B} compared to Conventional PSO	Loss in P_d compared to Conventional PSO
4	0.01	103.3%	70.4%	64.4%
	0.2	52.1%	46.6%	28.2%
6	0.01	25.7%	66.8%	45.7%
	0.2	8.4%	41.2%	8%

Table 4.2: Performance analysis summary of the proposed Hybrid PSO-OR algorithm under Rayleigh Fading

SNR (dB)	Δ_0	Improvement in P_d compared to Hybrid EGC-OR	Savings in \bar{B} compared to Conventional PSO	Loss in P_d compared to Conventional PSO
5	0.01	15.2%	77.1%	20.2%
	0.1	13.4%	63.5%	10.7%
7	0.01	3.1%	75.0%	9.7%
	0.1	2.9%	61.0%	5.4%

The above tables indicate that at low SNR for a given cooperative false alarm probability and a particular value of Δ_0 , the Hybrid PSO-OR algorithm achieves a much better detection performance compared to the Hybrid EGC-OR algorithm. Under AWGN, for the case of $\Delta_0 = 0.2$, the Hybrid PSO-OR algorithm achieves 46.6% bit savings over the reporting channel with 28.2% loss in detection performance compared to the conventional PSO technique. Under Rayleigh fading, for the case of $\Delta_0 = 0.1$, the Hybrid PSO-OR algorithm achieves 63.5% bit savings with only 10.7% loss in detection performance compared to the conventional PSO technique.

A hybrid, optimal linear cooperative spectrum sensing algorithm (termed as Hybrid PSO-OR algorithm) was developed, using a double threshold energy detector and Particle Swarm Optimization technique. The expressions for the cooperative probabilities, and the normalized average number of bits over the reporting channel are derived for the Hybrid PSO-OR algorithm. The simulation results show that the Hybrid PSO-OR algorithm significantly reduces the normalized average number of reporting bits, while maintaining a detection performance close to that of the conventional single threshold PSO technique. It is shown through simulations that the Hybrid PSO-OR algorithm outperforms the Hybrid EGC-OR algorithm, with a similar communication overhead over the reporting channel.

CHAPTER 5

CONCLUSION AND FUTURE WORK

5.1 Conclusion

Cognitive Radio (CR) has emerged as a promising technology to solve the inefficient usage of licensed spectrum, by opportunistically accessing the under-utilized licensed frequency bands, and without interfering with licensed users. In this thesis, we addressed the spectrum sensing problem in time domain. This thesis proposed a hybrid cooperative spectrum sensing algorithm using a double threshold energy detector and a Particle Swarm Optimization technique. The proposed hybrid algorithm combines decision fusion and data fusion. In the proposed algorithm, the Particle Swarm Optimization technique is used to optimize the performance of the data fusion part. The proposed algorithm was analyzed mathematically, and we derived the expressions for the cooperative probabilities and for the normalized average number of bits over the reporting channel.

The simulation results showed that the proposed algorithm significantly reduces the average number of reporting bits, at the expense of a negligible loss in performance compared to the conventional single threshold data fusion technique using PSO. Thus, the proposed algorithm considerably reduces the communication overhead over the reporting channels. It was also shown that the proposed algorithm outperforms the other hybrid approach, called the Hybrid EGC-OR technique, which uses Equal Gain Combining for its data fusion part. Hence, the proposed algorithm provides a unique flexibility feature to

tradeoff detection performance and the average number of bits over the reporting channel.

5.2 Proposed Future Research Directives

The spectrum sensing problem was addressed in time domain using the double threshold energy detector. As an extension to our work, the double threshold energy detector can be explored further. Some of the recommended research directives are briefly outlined below:

5.2.1 Maximum Eigenvalue Based Detection for Fuzzy CRs

For the CRs falling in the fuzzy region, the received signal samples can be collected to estimate the covariance matrix. The fusion centre can make a soft decision based on the maximum eigenvalue of the covariance matrix. This soft decision can be combined with the other hard decisions from the reliable CRs, to make a final decision on the presence or absence of the primary user.

5.2.2 Cluster-Based Two-Threshold Cooperative Spectrum Sensing

In the proposed algorithm, the reporting channels were assumed to be perfect. However, when the cooperating CRs report their local sensing observations to the fusion centre through fading channels, the sensing performance can seriously degrade. Under such scenarios, cluster based cooperative sensing, proposed in [58], can be used to enhance

sensing performance. Each cooperating CR would use a double threshold energy detector locally. All the cooperating CRs are divided into clusters [98]. For each cluster, a CR with the maximum instantaneous reporting channel gain is selected as the cluster head, whose task is to collect local sensing information from the other CRs in the cluster, then forward it to the fusion centre [58].

Based on the double threshold energy detector, each CR in the cluster either sends its local hard decision or the observed energy value to the cluster head. The cluster head can then use an EGC scheme to combine the received energies and make a soft decision. Finally, the cluster head combines the hard and soft decisions to make a final decision, and reports it to the fusion centre. Hence, this would reduce the reporting errors due to the fading channels [58].

Publications

The publications out of the thesis work are as follows:

- Fahham Mohammed and M. A. Deriche, “A Two-Threshold Cooperative Spectrum Sensing Algorithm using Swarm Intelligence,” in *IEEE Computers, Communications and IT Applications Conference (ComComAp 2013)*, HKUST, Hong Kong, China.
- Fahham Mohammed and M. A. Deriche, “A Two-Threshold Cooperative Spectrum Sensing Algorithm using Swarm Intelligence,” in *The Fourth Scientific Conference for Students of Higher Education in the KSA*, April 2013.
- Fahham Mohammed and M. A. Deriche, “A New Hybrid Cooperative Spectrum Sensing Algorithm using Swarm Intelligence and Double Thresholds,” (submitted to) *Wireless Communications and Mobile Computing Journal*, Wiley, May 2013.

References

- [1] Federal Communications Commission, “Spectrum Policy Task Force Report,” 2002.
- [2] J. Yang, “Spatial Channel Characterization for Cognitive Radios,” UC Berkeley, 2004.
- [3] J. Mitola and G. Q. Maguire, “Cognitive radio: making software radios more personal,” *IEEE Personal Communications*, vol. 6, no. 4, pp. 13–18, 1999.
- [4] C. Stevenson, G. Chouinard, S. Shellhammer, and W. Caldwell, “IEEE 802.22: The first cognitive radio wireless regional area network standard,” *IEEE Communications Magazine*, vol. 47, no. 1, pp. 130–138, Jan. 2009.
- [5] IEEE 802.22, “Working Group on Wireless Regional Area Networks (WRAN).” [Online]. Available: <http://grouper.ieee.org/groups/802/22/>.
- [6] S. Haykin, “Cognitive radio: brain-empowered wireless communications,” *IEEE Journal on Selected Areas in Communications*, vol. 23, no. 2, pp. 201–220, 2005.
- [7] R. W. Thomas, L. A. DaSilva, and A. B. MacKenzie, “Cognitive networks,” in *First IEEE International Symposium on New Frontiers in Dynamic Spectrum Access Networks, 2005. DySPAN 2005.*, pp. 352–360.
- [8] I. F. Akyildiz, W.-Y. Lee, M. C. Vuran, and S. Mohanty, “NeXt generation/dynamic spectrum access/cognitive radio wireless networks: A survey,” *Computer Networks*, vol. 50, no. 13, pp. 2127–2159, Sep. 2006.
- [9] F. K. Jondral, “Software-Defined Radio—Basics and Evolution to Cognitive Radio,” *EURASIP Journal on Wireless Communications and Networking*, vol. 2005, no. 3, p. 652784, 2005.
- [10] FCC, “ET Docket No. 03-222 Notice of proposed rule making and order,” 2003.
- [11] G. Zhao, J. Ma, G. Y. Li, T. Wu, Y. Kwon, A. Soong, and C. Yang, “Spatial spectrum holes for cognitive radio with relay-assisted directional transmission,” *IEEE Transactions on Wireless Communications*, vol. 8, no. 10, pp. 5270–5279, Oct. 2009.
- [12] R. Umar and A. U. H. Sheikh, “Spectrum Access and Sharing for Cognitive Radio,” in *Developments in Wireless Network Prototyping , Design , and Deployment : Future Generations*, pp. 241–271.

- [13] T. Yucek and H. Arslan, "A survey of spectrum sensing algorithms for cognitive radio applications," *IEEE Communications Surveys & Tutorials*, vol. 11, no. 1, pp. 116–130, 2009.
- [14] R. Umar and A. U. H. Sheikh, "A comparative study of spectrum awareness techniques for cognitive radio oriented wireless networks," *Physical Communication*, Aug. 2012.
- [15] P. A. Kumar Acharya, S. Singh, and H. Zheng, "Reliable open spectrum communications through proactive spectrum access," in *Proceedings of the first international workshop on Technology and policy for accessing spectrum - TAPAS '06*, 2006.
- [16] FCC, "ET Docket No. 03-237 Notice of inquiry and notice of proposed Rulemaking," 2003.
- [17] FCC, "ET Docket No. 03-237,07-78 Termination order," 2007.
- [18] S. M. Kay, *Fundamentals of Statistical Signal Processing, Volume II: Detection Theory*. Prentice Hall, New Jersey, 1998.
- [19] H. Urkowitz, "Energy detection of unknown deterministic signals," *Proceedings of the IEEE*, vol. 55, no. 4, pp. 523–531, 1967.
- [20] A. Sahai, N. Hoven, and R. Tandra, "Some Fundamental Limits on Cognitive Radio," in *Allerton Conference on Control, Communications, and Computation*, 2004, pp. 1662–1671.
- [21] J. Ma., G. Y. Li, and Biing Hwang Juang, "Signal Processing in Cognitive Radio," *Proceedings of the IEEE*, vol. 97, no. 5, pp. 805–823, May 2009.
- [22] F. F. Digham, M. S. Alouini, and M. K. Simon, "On the energy detection of unknown signals over fading channels," in *IEEE International Conference on Communications, 2003. ICC '03.*, 2003, vol. 5, pp. 3575–3579.
- [23] J. J. Lehtomaki, M. Juntti, H. Saarnisaari, and S. Koivu, "Threshold setting strategies for a quantized total power radiometer," *IEEE Signal Processing Letters*, vol. 12, no. 11, pp. 796–799, Nov. 2005.
- [24] D. R. Joshi, D. C. Popescu, and O. A. Dobre, "Gradient-Based Threshold Adaptation for Energy Detector in Cognitive Radio Systems," *IEEE Communications Letters*, vol. 15, no. 1, pp. 19–21, Jan. 2011.
- [25] F. F. Digham, M. Alouini, and M. K. Simon, "On the Energy Detection of Unknown Signals Over Fading Channels," *IEEE Transactions on Communications*, vol. 55, no. 1, pp. 21–24, Jan. 2007.

- [26] A. Nuttall, "Some integrals involving the Q_M function (Corresp.)," *IEEE Transactions on Information Theory*, vol. 21, no. 1, pp. 95–96, Jan. 1975.
- [27] Z. Tian and G. B. Giannakis, "A Wavelet Approach to Wideband Spectrum Sensing for Cognitive Radios," in *2006 1st International Conference on Cognitive Radio Oriented Wireless Networks and Communications*, 2006, pp. 1–5.
- [28] H. K. Kathuria, "SPECTRUM SENSING IN TIME AND FREQUENCY DOMAINS," King Fahd University of Petroleum & Minerals, Dhahran, KSA, 2012.
- [29] Z. Tian and G. B. Giannakis, "Compressed Sensing for Wideband Cognitive Radios," in *2007 IEEE International Conference on Acoustics, Speech and Signal Processing - ICASSP '07*, 2007, pp. IV–1357–IV–1360.
- [30] Y. Wang, Z. Tian, and C. Feng, "A Two-Step Compressed Spectrum Sensing Scheme for Wideband Cognitive Radios," in *2010 IEEE Global Telecommunications Conference GLOBECOM 2010*, 2010, pp. 1–5.
- [31] W. A. Gardner, "Exploitation of spectral redundancy in cyclostationary signals," *IEEE Signal Processing Magazine*, vol. 8, no. 2, pp. 14–36, Apr. 1991.
- [32] M. Oner and F. Jondral, "Cyclostationarity-based methods for the extraction of the channel allocation information in a spectrum pooling system," in *Proceedings. 2004 IEEE Radio and Wireless Conference (IEEE Cat. No.04TH8746)*, 2004, no. 1, pp. 279–282.
- [33] M. Ghozzi, F. Marx, M. Dohler, and J. Palicot, "Cyclostationarity-Based Test for Detection of Vacant Frequency Bands," in *2006 1st International Conference on Cognitive Radio Oriented Wireless Networks and Communications*, 2006, no. 1, pp. 1–5.
- [34] A. V. Dandawate and G. B. Giannakis, "Statistical tests for presence of cyclostationarity," *IEEE Transactions on Signal Processing*, vol. 42, no. 9, pp. 2355–2369, 1994.
- [35] R. Tafazolli, "A first-order cyclostationarity based energy detection approach for non-cooperative spectrum sensing," *21st Annual IEEE International Symposium on Personal, Indoor and Mobile Radio Communications*, pp. 554–559, Sep. 2010.
- [36] S. Maleki, A. Pandharipande, and G. Leus, "Two-stage spectrum sensing for cognitive radios," in *2010 IEEE International Conference on Acoustics, Speech and Signal Processing*, 2010, pp. 2946–2949.
- [37] J. G. Proakis, *Digital Communications*, 4th Ed. McGraw-Hill, 2001.

- [38] D. Cabric, S. M. Mishra, and R. W. Brodersen, "Implementation issues in spectrum sensing for cognitive radios," in *Conference Record of the Thirty-Eighth Asilomar Conference on Signals, Systems and Computers, 2004.*, vol. 1, pp. 772–776.
- [39] H. Tang, "Some physical layer issues of wide-band cognitive radio systems," in *First IEEE International Symposium on New Frontiers in Dynamic Spectrum Access Networks, 2005. DySPAN 2005.*, pp. 151–159.
- [40] Y. Zeng, Y.-C. Liang, A. T. Hoang, and R. Zhang, "A Review on Spectrum Sensing for Cognitive Radio: Challenges and Solutions," *EURASIP Journal on Advances in Signal Processing*, vol. 2010, pp. 1–16, 2010.
- [41] Y. Zeng and Y. Liang, "Eigenvalue-based spectrum sensing algorithms for cognitive radio," *IEEE Transactions on Communications*, vol. 57, no. 6, pp. 1784–1793, Jun. 2009.
- [42] Y. Zeng, C. L. Koh, and Y.-C. Liang, "Maximum Eigenvalue Detection: Theory and Application," in *2008 IEEE International Conference on Communications*, 2008, pp. 4160–4164.
- [43] Y. Zeng and Y.-C. Liang, "Covariance Based Signal Detections for Cognitive Radio," in *2007 2nd IEEE International Symposium on New Frontiers in Dynamic Spectrum Access Networks*, 2007, pp. 202–207.
- [44] N. M. Neihart, S. Roy, and D. J. Allstot, "A two-stage sensing technique for dynamic spectrum access," *IEEE Transactions on Wireless Communications*, vol. 8, no. 6, pp. 3028–3037, Jun. 2009.
- [45] A. Ghasemi and E. S. Sousa, "Spectrum sensing in cognitive radio networks: the cooperation-processing tradeoff," *Wireless Communications and Mobile Computing*, vol. 7, no. 9, pp. 1049–1060, Nov. 2007.
- [46] S. Mishra, A. Sahai, and R. Brodersen, "Cooperative Sensing among Cognitive Radios," in *2006 IEEE International Conference on Communications*, 2006, vol. 00, no. c, pp. 1658–1663.
- [47] G. Ganesan and Y. Li, "Cooperative Spectrum Sensing in Cognitive Radio, Part I: Two User Networks," *IEEE Transactions on Wireless Communications*, vol. 6, no. 6, pp. 2204–2213, Jun. 2007.
- [48] G. Ganesan and Y. Li, "Cooperative Spectrum Sensing in Cognitive Radio, Part II: Multiuser Networks," *IEEE Transactions on Wireless Communications*, vol. 6, no. 6, pp. 2214–2222, Jun. 2007.

- [49] G. Ganesan, "Agility improvement through cooperative diversity in cognitive radio," *GLOBECOM '05. IEEE Global Telecommunications Conference, 2005.*, p. 5 pp.–2509, 2005.
- [50] A. Ghasemi and E. S. Sousa, "Collaborative spectrum sensing for opportunistic access in fading environments," in *First IEEE International Symposium on New Frontiers in Dynamic Spectrum Access Networks, 2005. DySPAN 2005.*, pp. 131–136.
- [51] A. Ghasemi and E. S. Sousa, "Opportunistic Spectrum Access in Fading Channels Through Collaborative Sensing," *Journal of Communications*, vol. 2, no. 2, pp. 71–82, Mar. 2007.
- [52] I. F. Akyildiz, B. F. Lo, and R. Balakrishnan, "Cooperative spectrum sensing in cognitive radio networks: A survey," *Physical Communication*, vol. 4, no. 1, pp. 40–62, Mar. 2011.
- [53] R. Tandra and A. Sahai, "SNR Walls for Signal Detection," *IEEE Journal of Selected Topics in Signal Processing*, vol. 2, no. 1, pp. 4–17, Feb. 2008.
- [54] F. Visser, G. J. M. Janssen, and P. Pawelczak, "Multinode Spectrum Sensing Based on Energy Detection for Dynamic Spectrum Access," in *VTC Spring 2008 - IEEE Vehicular Technology Conference, 2008*, vol. 0, pp. 1394–1398.
- [55] Z. Quan, S. Cui, H. Poor, and A. Sayed, "Collaborative wideband sensing for cognitive radios," *IEEE Signal Processing Magazine*, vol. 25, no. 6, pp. 60–73, Nov. 2008.
- [56] Y. Selen, H. Tullberg, and J. Kronander, "Sensor Selection for Cooperative Spectrum Sensing," in *2008 3rd IEEE Symposium on New Frontiers in Dynamic Spectrum Access Networks, 2008*, no. i, pp. 1–11.
- [57] A. W. Min and K. G. Shin, "Impact of mobility on spectrum sensing in cognitive radio networks," in *Proceedings of the 2009 ACM workshop on Cognitive radio networks - CoRoNet '09, 2009*, p. 13.
- [58] C. Sun, W. Zhang, and K. B. Letaief, "Cluster-Based Cooperative Spectrum Sensing in Cognitive Radio Systems," *2007 IEEE International Conference on Communications*, pp. 2511–2515, Jun. 2007.
- [59] C. Sun, W. Zhang, and K. Ben Letaief, "Cooperative Spectrum Sensing for Cognitive Radios under Bandwidth Constraints," *2007 IEEE Wireless Communications and Networking Conference*, pp. 1–5, 2007.
- [60] X. Zhou, G. Y. Li, D. Li, D. Wang, and A. C. K. Soong, "Bandwidth efficient combination for cooperative spectrum sensing in cognitive radio networks," in

2010 IEEE International Conference on Acoustics, Speech and Signal Processing, 2010, pp. 3126–3129.

- [61] X. Zhou, J. Ma, G. Y. Li, Y. H. Kwon, and a. C. K. Soong, “Probability-Based Combination for Cooperative Spectrum Sensing in Cognitive Radio Networks,” in *2009 IEEE International Conference on Communications*, 2009, pp. 1–5.
- [62] E. Visotsky, S. Kuffner, and R. Peterson, “On collaborative detection of TV transmissions in support of dynamic spectrum sharing,” in *First IEEE International Symposium on New Frontiers in Dynamic Spectrum Access Networks, 2005. DySPAN 2005.*, 2005, pp. 338–345.
- [63] J. Zhao, “Distributed coordination in dynamic spectrum allocation networks,” in *First IEEE International Symposium on New Frontiers in Dynamic Spectrum Access Networks, 2005. DySPAN 2005.*, 2005, pp. 259–268.
- [64] A. F. Cattoni, I. Minetti, M. Gandetto, R. Niu, P. K. Varshney, and S. Carlo, “A Spectrum Sensing Algorithm based on distributed cognitive models,” 2006.
- [65] M. Gandetto and C. Regazzoni, “Spectrum sensing: A distributed approach for cognitive terminals,” *IEEE Journal on Selected Areas in Communications*, vol. 25, no. 3, pp. 546–557, Apr. 2007.
- [66] K. Ben Letaief, “Cooperative Communications for Cognitive Radio Networks,” *Proceedings of the IEEE*, vol. 97, no. 5, pp. 878–893, May 2009.
- [67] S. M. Mishra, D. Willkomm, R. Brodersen, and A. Wolisz, “A Cognitive Radio Approach for Usage of Virtual Unlicensed Spectrum.”
- [68] C. Guo, T. Zhang, Z. Zeng, and C. Feng, “Investigation on Spectrum Sharing Technology Based On Cognitive Radio,” in *2006 First International Conference on Communications and Networking in China*, 2006, pp. 1–5.
- [69] P. Pawełczak, C. Guo, R. V. Prasad, and R. Hekmat, “Cluster-Based Spectrum Sensing Architecture for Opportunistic Spectrum Access Networks.”
- [70] L. Musavian and T. Le-Ngoc, “Cross-layer design for cognitive radios with joint AMC and ARQ under delay QoS constraint,” in *2012 8th International Wireless Communications and Mobile Computing Conference (IWCMC)*, 2012, pp. 419–424.
- [71] N. S. Shankar, C. Cordeiro, and K. Challapali, “Spectrum agile radios: utilization and sensing architectures,” in *First IEEE International Symposium on New Frontiers in Dynamic Spectrum Access Networks, 2005. DySPAN 2005.*, 2005, pp. 160–169.

- [72] P. K. Varshney, *Distributed Detection and Data Fusion*. New York: Springer-Verlag, 1997, p. 299.
- [73] D. J. Thomson, "Spectrum estimation and harmonic analysis," *Proceedings of the IEEE*, vol. 70, no. 9, pp. 1055–1096, 1982.
- [74] S. Xu, Y. Shang, and H. Wang, "Eigenvalues based spectrum sensing against untrusted users in cognitive radio networks," in *2009 4th International Conference on Cognitive Radio Oriented Wireless Networks and Communications*, 2009, pp. 1–6.
- [75] J. Ma and Y. G. Li, "Soft Combination and Detection for Cooperative Spectrum Sensing in Cognitive Radio Networks," in *IEEE GLOBECOM 2007-2007 IEEE Global Telecommunications Conference*, 2007, pp. 3139–3143.
- [76] D. G. Brennan, "Linear diversity combining techniques," *Proceedings of the IEEE*, vol. 91, no. 2, pp. 331–356, Feb. 2003.
- [77] S. P. Herath, S. Member, N. Rajatheva, S. Member, and C. Tellambura, "Energy Detection of Unknown Signals in Fading and Diversity Reception," vol. 59, no. 9, pp. 2443–2453, 2011.
- [78] G. Arfken, "Confluent Hypergeometric Functions," in *Mathematical Methods for Physicists*, 3rd Ed., Orlando, FL: Academic Press, 1985, pp. 753–758.
- [79] M. Abramowitz and C. A. (Eds. . Stegun, "Confluent Hypergeometric Functions," in *Handbook of Mathematical Functions with Formulas, Graphs, and Mathematical Tables*, 9th Printi., New York: Dover, 1972, pp. 503–515.
- [80] S. P. Herath and N. Rajatheva, "Analysis of Equal Gain Combining in Energy Detection for Cognitive Radio over Nakagami Channels," in *IEEE GLOBECOM 2008 - 2008 IEEE Global Telecommunications Conference*, 2008, pp. 1–5.
- [81] Q. Wang, D.-W. Yue, and Y. Wang, "Performance Analysis of Spectrum Sensing Using Diversity Technique," in *2009 5th International Conference on Wireless Communications, Networking and Mobile Computing*, 2009, no. 2008, pp. 1–5.
- [82] S. Haghani and N. C. Beaulieu, "On decorrelation in dual-branch diversity systems," *IEEE Transactions on Communications*, vol. 57, no. 7, pp. 2138–2147, Jul. 2009.
- [83] K. T. Hemachandra and N. C. Beaulieu, "Novel Analysis for Performance Evaluation of Energy Detection of Unknown Deterministic Signals Using Dual Diversity," in *2011 IEEE Vehicular Technology Conference (VTC Fall)*, 2011, pp. 1–5.

- [84] N. T. Awon and A. Islam, "Effect of AWGN & Fading (Raleigh & Rician) channels on BER performance of a WiMAX communication System," vol. 10, no. 8, pp. 11–17, 2012.
- [85] J. Kennedy and R. Eberhart, "Particle swarm optimization," in *Proceedings of ICNN'95 - International Conference on Neural Networks*, 1995, vol. 4, pp. 1942–1948.
- [86] S. Luke, et al., *Essentials of Metaheuristics A Set of Undergraduate Lecture Notes by BibTEX*: 2011.
- [87] I. C. Trelea, "The particle swarm optimization algorithm: convergence analysis and parameter selection," *Information Processing Letters*, vol. 85, no. 6, pp. 317–325, Mar. 2003.
- [88] J. Kennedy and R. C. Eberhart, *Swarm Intelligence*. California: Morgan Kauffman Publishers, 2001.
- [89] R. A. Rashid, Y. S. Baguda, N. Fisal, M. A. Sarijari, S. K. S. Yusof, S. H. S. Ariffin, and A. Mohd, "Optimizing Achievable Throughput for Cognitive Radio Network using Swarm Intelligence," no. October, pp. 354–359, 2011.
- [90] R. Eberhart and Y. Shi, "Comparison between genetic algorithms and particle swarm optimization," *Evolutionary Programming VII*, 1998.
- [91] R. C. Eberhart and Y. Shi, "Comparing inertia weights and constriction factors in particle swarm optimization," in *Proceedings of the 2000 Congress on Evolutionary Computation. CEC00 (Cat. No.00TH8512)*, vol. 1, no. 7, pp. 84–88.
- [92] Y. Shi and R. Eberhart, "Parameter selection in particle swarm optimization," *Evolutionary Programming VII*, vol. 160, 1998.
- [93] Y. Shi and R. C. Eberhart, "Empirical study of particle swarm optimization," in *Proceedings of the 1999 Congress on Evolutionary Computation-CEC99 (Cat. No. 99TH8406)*, 1945, pp. 1945–1950.
- [94] S. Gheitanchi, F. Ali, and E. Stipidis, "Particle Swarm Optimization for Resource Allocation in OFDMA," in *2007 15th International Conference on Digital Signal Processing*, 2007, pp. 383–386.
- [95] R. V Kulkarni and G. K. Venayagamoorthy, "Particle Swarm Optimization in Wireless-Sensor Networks: A Brief Survey," *IEEE Transactions on Systems, Man, and Cybernetics, Part C (Applications and Reviews)*, vol. 41, no. 2, pp. 262–267, Mar. 2011.

- [96] Z. Quan, S. Cui, and A. H. Sayed, "Optimal Linear Cooperation for Spectrum Sensing in Cognitive Radio Networks," *IEEE Journal of Selected Topics in Signal Processing*, vol. 2, no. 1, pp. 28–40, Feb. 2008.
- [97] S. Zheng, C. Lou, and X. Yang, "Cooperative spectrum sensing using particle swarm optimisation," *Electronics Letters*, vol. 46, no. 22, p. 1525, 2010.
- [98] O. Younis and S. Fahmy, "Distributed clustering in ad-hoc sensor networks: a hybrid, energy-efficient approach," in *IEEE INFOCOM 2004*, vol. 1, pp. 629–640.

Vitae

Name : Fahham Mohammed

Nationality : Indian

Date of Birth : 09 December 1985

Email : fahham912@hotmail.com

Present Address : KFUPM, P.O. Box 8639, Dhahran 31261, KSA

Permanent Address : 304 A-Tower, Fateh Sagar Complex, Opp. Convent School,
Vadodara 390002, Gujarat, India

Contact Numbers : +966 500416935, +966 3 8943352

Academic Background : B.E. (Electronics and Communication)
Osmania University, Hyderabad, India